Molecular genetic studies of primary open angle and angle closure glaucoma

Tin Aung

A thesis submitted to the University of London for the Degree of Doctor of Philosophy

Department of Molecular Genetics
Institute of Ophthalmology
University College London
Bath Street
London EC1V 9EL

April 2003

ProQuest LLC
789 East Eisenhower Parkway
P.O. Box 1346
Ann Arbor, MI 48106-1346


INSTITUTE O
BATH STREET EC1V 9EL

Statement of Originality

I declare that this thesis, submitted for the degree of Doctor of Philosophy is composed by myself and the work herein is my own, or that the author involved is clearly stated.

Tin Aung

MBBS, M.Med, FRCOphth, FRCS(Ed)

Abstract

Glaucoma, a group of heterogeneous optic neuropathies characterized by progressive visual field loss, is the leading cause of irreversible blindness worldwide. The condition has a substantial heritable basis, as illustrated by the numerous loci and genes identified to date, and the large proportion of patients having a family history. Categorized according to the anatomy of the anterior chamber angle, there are 2 main forms of glaucoma, primary open angle glaucoma (POAG) and primary angle closure glaucoma (PACG). The first half of the thesis describes the molecular genetic study of POAG, while the latter deals with PACG.

Primary open angle glaucoma (POAG) accounts for most glaucoma in Caucasian and Afro-Caribbean populations. The condition is classified according to the presence of elevated intraocular pressure (IOP) into high-tension glaucoma (HTG) or normal tension glaucoma (NTG). *OPA1*, the gene responsible for autosomal dominant optic atrophy represents an excellent candidate gene for POAG (in particular NTG). Single nucleotide polymorphisms on intervening sequence (IVS) 8 of the *OPA1*gene (genotype IVS 8 +4 C/T; +32 T/C) were found to be strongly associated with a fifth of NTG cases and may be a marker for disease association, providing the first evidence of an association between *OPA1* and NTG. However this *OPA1* genotype was not found to be significantly associated with HTG. Further work did not detect a significant difference in a range of phenotypic features in NTG patients with and without these *OPA1* polymorphisms, suggesting that

these specific genetic variations do not underlie any major phenotypic diversity in NTG.

Optineurin (*OPTN*), in the GLC1E interval on chromosome 10p, was recently identified as the second gene underlying POAG, with a common mutation, E50K, being found in 13.5% of families, and a M98K variant identified as a significant risk-associated genetic factor for POAG. However when a large panel of 315 sporadic adult POAG subjects were examined for these 2 *OPTN* sequence variants, the E50K mutation was identified in only 1.5% of NTG subjects, making it an infrequent cause of sporadic NTG. The M98K variant was found to be associated specifically with NTG but not HTG, suggesting allelic heterogeneity between these 2 phenotypes. A characteristic NTG phenotype comprising a young-adult age of onset, advanced visual loss and progressive disease, has been described in individuals carrying the E50K *OPTN* mutation.

Primary angle closure glaucoma (PACG) is the main form of glaucoma in East Asian populations. Two large Singaporean PACG families were examined and the first locus for the disease was identified on chromosome 10 using linkage analysis. The disease interval was refined to 5.0 cM on chromosome 10q11 flanked by the markers D10S225 and D10S568, with the maximum LOD score of 3.4 at θ=.00 for D10S220. Several genes, *GDF10, TIM23, SLC18A3* and *ASAH2* were excluded as candidates for this condition.

This molecular genetic study of both POAG and PACG has contributed to our knowledge of glaucoma.

Acknowledgements

I owe a great deal of thanks to a number people without whom this research would not have been possible. Firstly, let me thank people from back home in Singapore, starting with Paul Chew who first stimulated my interest in research and glaucoma in particular, and has been a constant pillar of support. Paul Foster gave me a lot of confidence and advice; he is a role model in research I aspire to. I am very grateful to Vivian Balakrishnan and Donald Tan, my bosses at Singapore National Eye Centre who were instrumental in persuading me to do a PhD, and getting funding for me, which was generously provided by the National Medical Research Council of Singapore (who kindly awarded me a scholarship), SNEC as well as the Singapore Eye Research Institute. Barry Cullen, Roger Beauman, Steve Seah and Eric Yap were always very encouraging; while Leonard Ang, Wong Tien Yin and Wong Hon Tym are my friends and colleagues who have been extremely helpful over the years.

In London, I am very thankful to Professors Roger Hitchings, Shomi Bhattacharya and Peng Khaw for firstly giving me the opportunity to work here. To my supervisors Shomi Bhattacharya and Roger Hitchings a special thanks for their constant supervision and meticulous guidance. Shomi has given me so much of his precious time- thank you for always being available for advice. Ordan Lehmann has been an invaluable help, particularly for his astute opinions. A very special thanks to Neil Ebenezer, my guru who has taught me almost everything I know in the lab. He is my 'big brother' (in more

ways than one) and is responsible for keeping my weight up with his endless supply of food and snacks. I also owe a lot to Louise Ocaka for her patience and teaching. A large number of individuals have given me lots of sound advice, encouragement and camaraderie during the research period: Suba Poopalasundaram, Reshma Patel, Leen Abu Safieh, Eranga Vithana, Christina Chakarova and Beverly Scott. Many thanks also to Quincy, Zara, Simon, Samantha, Michel, Dawn, Christianne, Alex and Myrto. I must not forget Ashwin Reddy for being a dear friend and for organising regular football and drinks. Finally, I am indebted to my wife and family for being there always, and putting up with me.

I would also like to thank all those with whom I have collaborated: Ted Garway-Heath, Ananth Viswanathan, and Darmalingam Pooinosawmy from Moorfields, Anne Child and Glen Brice from St George's Hospital, Koji Okada from Hiroshima, and Richard Bowman and Andrew Dearlove from HGMP.

I feel extremely fortunate to have spent 3 years at this great department, Institute, Hospital and country. I go home with so many wonderful memories.

Dedication

I dedicate this thesis to my family:

To my wife, Soe Moe, for all your love, encouragement, and understanding, to my children, Eri, Yuri and Miri who have been my inspiration, and to my parents for their endless guidance and support.

Table of Contents

Page

Publications and presentations arising from this research:

Publications:

1. Aung T, Ocaka L, Ebenezer ND, Morris AG, Krawczak M, Thiselton DL, Alexander C, Votruba M, Brice G, Child AH, Francis PJ, Hitchings RA, Lehmann OJ, Bhattacharya SS. A major marker for normal tension glaucoma: Association with polymorphisms in the *OPA1* gene. Hum Genetics 2002; 110: 52-56

2. Aung T, Ocaka L, Ebenezer ND, Morris AG, Brice G, Child AH, Hitchings RA, Lehmann OJ, Bhattacharya SS. Investigating the association between OPA1 polymorphisms and glaucoma: Comparison between normal tension and high tension primary open angle glaucoma. Hum Genetics 2002; 110: 513-514 .

3. Aung T, Okada K, Poinoosawmy D, Membrey L, Brice G, Child AH, , Bhattacharya SS, Lehmann OJ, Garway-Heath DF, Hitchings RA. The phenotype of normal tension glaucoma patients with and without OPA1 polymorphisms. Br J Ophthalmol 2003; 87 149-152

4. Aung T, Ebenezer ND, Brice G, Child AH, Prescott Q, Lehmann OJ, Hitchings RA, Bhattacharya SS. Prevalence of *Optineurin* sequence variants in adult primary open angle glaucoma: Implications for diagnostic testing. J Med Genet 2003; **40**: e101

5. Aung T, Okada K, Viswanathan AC, Child AH, Brice G, White E, Garway-Heath DF, Bhattacharya SS, Lehmann OJ, Sarfarazi M, Hitchings RA. The E50K mutation in the *Optineurin* gene is associated with a severe and progressive normal tension glaucoma phenotype. Submitted to *Ophthalmology.*

Presentations:

1. Aung T, Bowman R, Chew PT, Seah SK, Ang LP, Yap E, Lehmann OJ, Dearlove A, Hitchings RA, Bhattacharya SS. Genome wide linkage scan for primary angle closure glaucoma. Association for Research in Vision and Ophthalmology Annual Meeting, 3-8th, May 2003, Fort Lauderdale, Florida, USA.

2. Aung T, Ebenezer ND, Brice G, Child AH, Prescott Q, Lehmann OJ, Hitchings RA, Bhattacharya SS. Prevalence of *Optineurin* sequence variants in adult primary open angle glaucoma. 4th International Glaucoma Symposium, 19-22 March 2003, Barcelona, Spain.

3. Aung T, Okada K, Poinoosawmy D, Membrey L, Brice G, Child AH, , Bhattacharya SS, Lehmann OJ, Garway-Heath DF, Hitchings RA. The phenotype of normal tension glaucoma patients with and without OPA1 polymorphisms. 52nd Annual Meeting of the American Society of Human Genetics. Oct 15-19 2002, Baltimore, Maryland, USA.

4. Aung T, Ocaka L, Ebenezer ND, Morris AG, Brice G, Child AH, Hitchings RA, Lehmann OJ, Bhattacharya SS. Investigating the association between OPA1 polymorphisms and glaucoma: Comparison between normal tension and high tension primary open angle glaucoma. Association for Research in Vision and Ophthalmology Annual Meeting, 4-10th May 2002, Fort Lauderdale, Florida, USA.

5. Aung T. Investigating the association between the *OPA1* gene and normal tension glaucoma. European Association for vision and eye research (EVER) Annual Meeting, 10-13 Oct 2001, Alicante, Spain

6. Aung T, Chew PT, Seah SK, Ang LP, Ocaka L, Ebenezer ND, Yap E, Lehmann OJ, Hitchings RA, Bhattacharya SS. Genetic exclusion of 2 pedigrees with primary angle closure glaucoma from loci for nanophthalmos and microphthalmia. Association for Research in Vision and Ophthalmology Annual Meeting, 29 April-4th May 2001, Fort Lauderdale, Florida, USA.

List of Figures

List of Tables

Page

CHAPTER 1

INTRODUCTION

1.1. Overview of chapter

The research described in this thesis involves genetic and clinical studies towards the identification of genes involved in primary glaucoma. The following sections review the classification and genetic basis of glaucoma. The human genome project is also discussed with relation to its relevance in the identification of genes involved in ocular diseases, as well as introducing concepts in molecular biology relevant to this thesis.

1.2. The eye

The human eye is the primary receptor organ for light. A typical structure of a mammalian eye is shown in Figure 1.1. Light enters the eye through the cornea and then passes through the pupil (the hole at the centre of the iris), through the aqueous humour, the lens and the vitreous humour before finally reaching the retina. The first step of visual perception requires the focusing of incoming light on to the retina, which contains photoreceptors. The axons of all the photoreceptors converge together to create an oval structure called the optic nerve head or optic disc, which continues as the optic nerve leading to the brain. At the level of the retina, the light energy is converted into electrical signals, which are then transported to the visual cortex in the brain via the

optic nerve.

The production and drainage of aqueous fluid dermines the eye's intraocular pressure (IOP). The intraocular pressure maintains the shape of the eyeball and holds the retina smoothly against the outer layers of the eye. Aqueous humour is produced by the ciliary body of the eye (in the posterior chamber behind the iris) and passes through the pupil into the anterior chamber (Figure 1.2). From there, the fluid travels into the angle, the area in the anterior chamber where the cornea and iris join. The angle is comprised of several structures that make up the eye's drainage system, which include the outermost part of the iris, the front of the ciliary body, the trabecular meshwork, and the Canal of Schlemm. As the aqueous fluid drains out of the eye via the angle, it passes through a filter, the trabecular meshwork then through a tiny channel in the sclera called the Canal of Schlemm. The aqueous finally flows into other tiny channels and eventually into the eye's blood vessels (episcleral venous system). About a fifth of aqueous outflow is via the uveoscleral route, which is primarily through the face of the ciliary body.

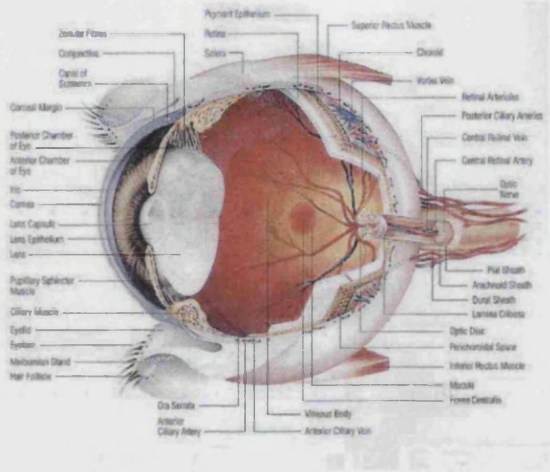

Figure 1.1. Structure of the eye, showing the major anatomical landmarks (Pharmacia Inc).

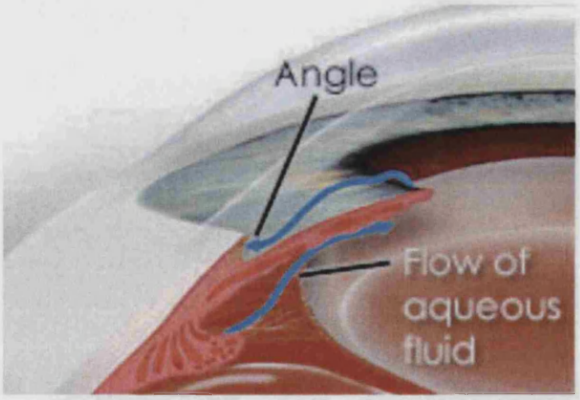

Figure 1.2. Aqueous humor dynamics: Aqueous humour produced by the ciliary body, flows through the pupil and leaves the eye via the trabecular meshwork in the angle.

1.3. Clinical Overview of Glaucoma

The glaucomas are a group of heterogeneous optic neuropathies characterized by progressive loss of axons in the optic nerve. Based on WHOGlobal Data Bank on Blindness, glaucoma accounts for 5.1 million of the estimated 38 million blind in the world (Thylefors *et al.*, 1995). As the number of elderly in the world rapidly increases, glaucoma morbidity will rise causing increased health care costs and economic burden in the future. It has been estimated that glaucoma will be the most common cause of irreversible blindness in the world this century with almost 70 million cases of glaucoma worldwide (Quigley, 1996). This high figure has important public health implications for a condition that is treatable but in which visual loss, at present, cannot be reversed.

The different forms of glaucoma share some common clinical manifestations that include a specific abnormal appearance of the optic nerve head, and progressive loss of visual field (Figure 1.3). The classical change in the optic nerve head is 'cupping' or excavation of the optic disc, with loss of the neuroretinal rim (Figure 1.4).

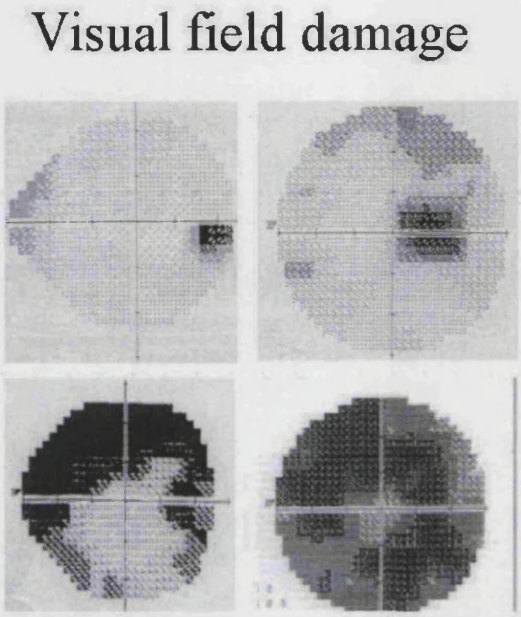

Figure 1.3. Visual field damage in glaucoma. Top left: early nasal loss. Top right: superior hemifield defect. Bottom left: Severe superior defect. Bottom right: End-stage constricted visual field.

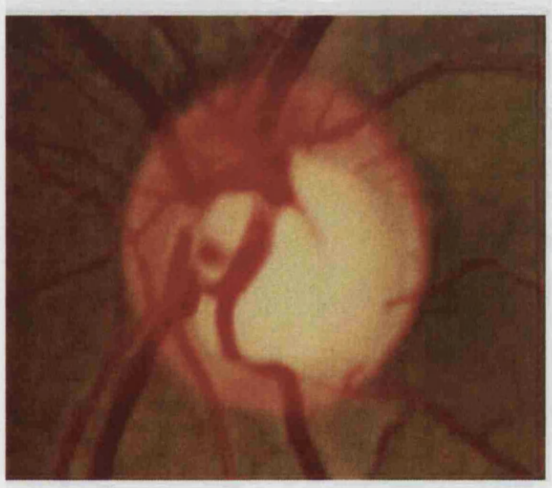

Figure 1.4. Glaucomatous optic disc with increased cup-disc ratio (cupping).

This is accompanied by a characteristic pattern of visual field loss, which usually begins with the loss of peripheral and paracentral vision, with central vision often maintained until the late stages of the disease. Raised intraocular pressure (IOP) used to be synonymous with glaucoma. However, elevation in IOP is not always present. For instance, the IOP may remain in the normal range (10-21mmHg on diurnal testing) in patients with so-called normal tension glaucoma. IOP is now considered to be a major risk factor for the development of glaucoma (Anderson, 1989; Sommer *et al.*, 1991) but is not a criterion for diagnosing the onset or progression of the disease.

1.3.1. Pathophysiology

Visual information from the eye travels as axonal signalling down the optic nerve through approximatlely one million retinal ganglion cells (RGCs) to the brain. In glaucoma, the disease affects primarily the RGCs, though other cell types such as the optic nerve astrocytes and retinal glia may also be involved (Levin, 2003). The primary disease locus is the optic nerve head, either at or near the lamina cribrosa or in the peripapillary retina. The mechanism of damage is not established, it is not known whether it is mechanical compression, ischemic changes, astrocytic reaction (Hernandez, 1997), autoimmune attack (Wax, 2000), or changes due to reactive oxygen species and nitric oxide production (Neufeld *et al*, 1997). One or more of these disease processes occur, which eventually signal RGCs to die via apoptosis (programmed cell death). This is followed by wallerain degeneration of the axon which leads to its loss of function. As RGCs are central nervous system neurons, once they die, RGC loss is irreversible and they are not replaced, leading to the irreversible visual loss seen in glaucoma patients.

1.3.2 Classification of Glaucoma

Glaucoma can be classified in a variety of ways, including: anatomically (open angle versus closed angle), aetiologically (primary versus secondary), chronologically (congenital, juvenile or adult), or on the basis of phenotypic features such as raised IOP (high tension or normal tension glaucoma). The diversity of classifications highlights the paucity of our understanding of the molecular mechanisms responsible for this common disease.

Combining the various forms of classification, the major forms of glaucoma worldwide are primary open-angle glaucoma (POAG) and primary angle-closure or closed angle glaucoma (PACG). These 2 categories are by far the most common forms of glaucoma and account for >90% of all glaucomas. Both forms of glaucoma also affect the elderly, usually above the age of 60 years.

1.3.3. Assessment of the angle

Primary glaucomas are classified according to the configuration of the anterior chamber angle. The angle is assessed by direct visualization using lenses, a technique known as gonioscopy (Figure 1.5 and 1.6). The single most important structure to identify when performing gonioscopy is Schwalbe's line. This can be located at the termination of the peripheral corneal wedge. Lying immediately posterior to this is the trabecular meshwork. It is believed that the posterior half of the trabecular meshwork is responsible for the majority of aqueous drainage via the trabecular route. When assessing the

degree of functional obstruction to drainage, apposition of the iris and posterior trabecular meshwork is of greatest relevance.

There are two widely used schemes for classifying and recording the gonioscopic appearance of the drainage angle. **Scheie's** scheme (Scheie, 1957) describes the angle structures that are visible, and the degree of pigmentation in the angle. The angle width is graded "O" for wide open with the ciliary body visible, and "IV" representing a state where no angle structures are visible. In contrast, the **Shaffer** system (Becker and Shaffer, 1965) attempts to describe the angular width of the irido-corneal recess, and uses Arabic numerals in the reverse order, 0 meaning an angle of 0° (closed angle) and 4 indicating 30-45° (wide open angle). In practice, most ophthalmologists use a combination of these 2 schemes and usually record the findings according to Shaffer's convention in each quadrant (Table 1.1). The angle width is graded '4' for wide open with the ciliary body being visible, and '0' representing a state where no angle structures are visible (Table1.1). Under this convention, angle grades 3 or 4 are considered open, while grade 0 is considered closed.

Description	Shaffer Grade	Angle width	Description
Wide open	4	35-45°	Wide open
Slightly narrower but open	3	20-35°	Open
Angle apex not visible	2	20°	Narrow
Posterior half of trabeculum not visible	1	10°	Extremely narrow
No structures seen	0	0°	Closed

Table 1.1. Clinical grading of the angle.

Another system of grading gonioscopic anatomy was that of Spaeth who described several features of angle configuration, including angular width, the level of insertion of the iris and the iris profile (Spaeth, 1971).

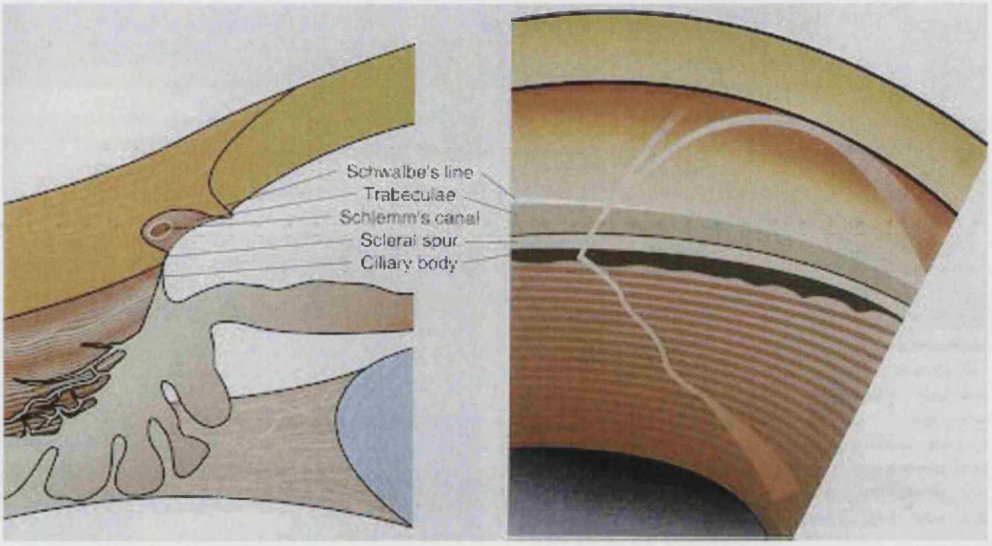

Figure 1.5. Angle structures. Left: In cross section. Right: As seen in gonioscopy (from the front).

Figure 1.6. Gonioscopy. Clinical slide of the view seen during gonioscopy, showing an open angle.

1.3.4. Primary Open Angle Glaucoma (POAG)

POAG accounts for about two thirds of all glaucoma seen in Caucasian populations (Tielsch *et al.*, 1991; Klein *et al.*, 1992; Bonomi *et al.*, 1998) and is also the main form of glaucoma in Afro-Carribeans (Mason el al, 1989). The angle of the anterior chamber appears open but does not function properly in transporting aqueous humour out of the eye in POAG (Figure 1.7). The exact nature of this resistance remains to be elucidated.

The onset of POAG is arbitrarily divided into the juvenile and elderly age groups but with overlapping clinical presentation. Most POAG cases are however found in the elderly, especially those above 60 years. POAG patients present with asymptomatic progressive loss of visual field, accompanied by cupping of the optic disc. In the classical form of the disease, the IOP is raised, usually above 21 mm Hg, and such patients are classified as high tension glaucoma (HTG).

Normal tension glaucoma (NTG) is an important subtype of POAG, in which the IOPs are consistently within the statistically normal population range. NTG accounts for approximately a third (range 20% and 50%) of all POAG cases (Sommer *et al.*, 1991; Shiose *et al.*, 1991; Klein *et al.*, 1992; Bonomi *et al.*, 1998). As the IOP is normal when measured and patients often have good central vision, NTG is under-diagnosed and the condition presents late. The main reason for NTG being under-diagnosed is because the main trigger for case finding is elevated IOP. Without elevated IOP, the index of suspicion falls and as a consequence, glaucomatous cupping may be overlooked. With

NTG, aqueous dynamics are normal, with normal diurnal curves for IOP and normal values for aqueous outflow.

1.3.4.1. Risk Factors Associated With POAG

1. Intraocular Pressure (IOP)

Raised IOP is a major risk factor for POAG (Anderson, 1989; Sommer *et al.*, 1991). The evidence that elevated IOP is the major risk factor for developing glaucoma comes from a series of studies, including the Baltimore survey. This demonstrated that 1.2% of the population with an IOP $\leq$ 21mmHg had glaucoma in comparison to 10.3% population with IOP $\geq$ 22mmHg (Sommer *et al.*, 1991). The IOP level has also been shown to correlate with the relative risk of developing glaucoma and the severity of the field damage at presentation (Sommer *et al.*, 1991; Jay and Murdoch, 1993). Even in NTG patients, the eye with the higher IOP exhibits the more severe degree of field loss (Cartwright and Anderson, 1988). IOP has been found to fluctuate at different times of the day, with nocturnal elevation of IOP and low IOP at the end of the light/wake period (Liu *et al,* 1999). Interestingly, such diurnal fluctuations in IOP have even been reported to affect optic disc morphology, as measured by scanning laser ophthalmoscopy (Lee *et al,*1999).

2. Race

Over the last decade large-scale population studies have shown that individuals from Africa, African Americans and Afro-Caribbeans are at higher

risk of POAG compared to Caucasians (Mason *et al.*, 1989, Sommer *et al.*, 1991, Tielsch *et al.*, 1991).

3. Age and Sex

Population studies have shown that increasing age and male gender is also associated with higher risk for open angle glaucoma (Leske *et al.*, 1995).

4. Family History

A positive family history is a significant risk factor for POAG, the odds ratio of having POAG for those with siblings with the disease being 3.69, parents with the disease 2.17 and for those with children the disease 1.12 (Tielsch *et al.*, 1994). It has been estimated that 20-60% of glaucoma patients have a family history (Wolfs *et al.*, 1998; Nemesure *et al.*, 1996; Nemesure *et al.*, 2001) and under-reporting of a family history has been well documented in glaucoma (McNaught *et al.*, 2000). Twin studies on POAG have reported conflicting results. In a population based twin study from Finland on 108 pairs (29 monozygotic), the heritability of POAG was calculated to be only 13% with a concordance rate of 7.1 (Teikari, 1987). However, in a twin study of 50 twin pairs from Iceland, the concordance of POAG in monozygotic twins was 98% (Gottfredsdottir *et al.*, 1999).

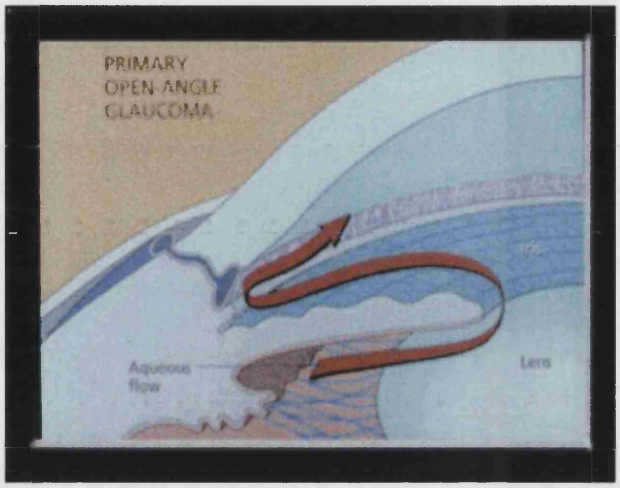

Figure 1.7. Aqueous flow in POAG. Aqueous flows normally from the ciliary body through the pupil into the angle.

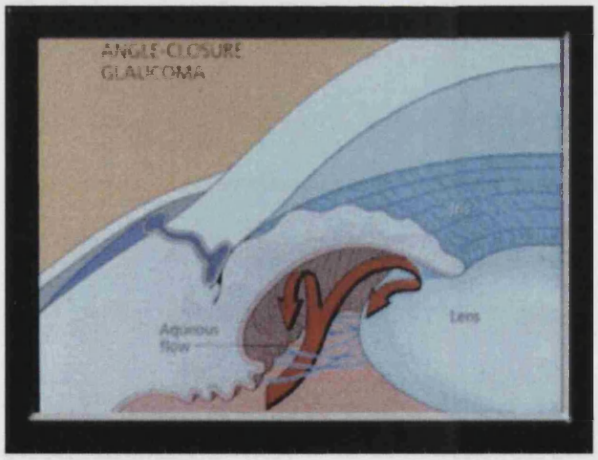

Figure 1.8. Aqueous flow in PACG. Due to the resistance of flow at the pupil (pupil block), pressure builds up in the posterior chamber and bows the iris forwards, obstructing access to the angle.

1.3.5. Primary Angle-Closure Glaucoma (PACG)

Primary angle closure glaucoma (PACG) is the main form of glaucoma in Asia (Hu *et al.*, 1989; Foster and Johnson, 2001), compared to POAG, which is the predominant disease among Caucasians and Africans (Mason *et al.*, 1989; Tielsch *et al.*, 1991; Klein *et al.*, 1992). This is true especially in populations of Chinese and Mongoloid descent, where the prevalence of PACG is between 1-2% in those above 40 (Congdon *et al.*, 1992; Foster *et al.*, 1996; Foster *et al.*, 2000). Recent glaucoma prevalence studies in southern India found that the prevalence of PACG in Indians is also high (Jacob *et al.*, 1998; Dandona *et al.*, 2000), and is close to that reported in Mongolians (Foster *et al.*, 1996). The estimated high prevalence of PACG in China and India make PACG a major form of glaucoma worldwide, possibly as common as POAG. In China itself, it is estimated that PACG afflicts 3.5 million people and 28 million have an occludable drainage angle, which is the anatomical trait predisposing to PACG (Foster and Johnson, 2001).

Primary angle-closure glaucoma is visually destructive. Nearly half of PACG cases were blind in one or both eyes in an Indian study (Dandona, *et al.*, 2000), and PACG accounted for most of the glaucoma blindness in Singapore (Foster *et al.*, 2000). The visual morbidity of the disease may be related to the finding that chronic asymptomatic PACG is the predominant form of the disease (Foster *et al.*, 1996; Foster *et al.*, 2000; Dandona *et al.*, 2000). The absence of symptoms makes the condition difficult to detect, resulting in a large proportion of cases being undiagnosed and untreated. The problem is

compounded by the requirement that the diagnosis of PACG is verified by gonioscopy, but this is not routinely available in many parts of the world.

1.3.5.1. Mechanism of PACG

PACG results from obstruction of the trabecular meshwork to the outflow of aqueous in the angle of the eye, the clinical feature *sine qua non* of the condition. The obstruction to outflow is due to the presence of adherent iris tissue called peripheral anterior synechiae (PAS) overlying the trabecular meshwork in the angle. Pupil block is the main underlying mechanism for PACG (Ritch and Lowe, 1996). In pupil block, there is variable resistance to aqueous flow from the posterior to anterior chamber through the pupil (Figure 1.8). This results in a substantial pressure differential between anterior and posterior chambers causing a flattening of iris contour. As aqueous production continues, posterior chamber pressure rises. The peripheral iris is bowed forward, coming into contact with the trabecular meshwork. This then results in obstruction of aqueous outflow through the trabecular route and a rise in IOP. With time, the iris tissue blocking the angle may adhere to the angle forming PAS.

Other mechanisms that contribute to angle closure include iris crowding with plateau iris type of configuration, and lens factors such as increased thickness and forward lens positioning. It is thought that racial differences seem to play a role in the pathogenesis of angle closure glaucoma. The iris joins the scleral

wall more anteriorly in Asians and more posteriorly in Caucasians (Oh *et al.*, 1994). There is a greater tendency towards plateau iris and anterior lens position without significant lens enlargement in Asia (Congdon *et al.*, 1992; Salmon *et al.*, 1994).

1.3.5.2. New Sub-classification of PACG

The terminology for angle-closure is used inconsistently throughout the literature. Epidemiological studies have used different diagnostic criteria for the definition of angle closure as well as what constitutes an occludable or narrow drainage angle. The clinical classification for angle closure is also not standardized. The current textbook classification of PACG is based principally on symptomatology with PACG traditionally classified as acute or chronic, according to the presence of symptoms. This emphasis may be not be appropriate as it does not consider the degree or consequences of angle obstruction or the presence of optic neuropathy. There is often overlap in the clinical presentation, limiting the use of such a classification. For example, patients with acute angle-closure can develop chronic PACG after the resolution of the acute episode. Similarly, patients with chronic PACG may develop acute angle-closure.

Recently, a new diagnostic classification of PACG has been proposed, which will provide a more uniform definition of the disease and be in line with the classification used in primary open angle glaucoma (Foster and Johnson, 2000; Foster *et al.*, 2002). The focus of the classification is the presence of glaucomatous damage to the optic nerve, as well as damage or obstruction of

the trabecular meshwork. This approach differentiates those with a true disease as opposed to suspects who are at increased risk of disease. The term 'glaucoma' is thus reserved only for people who have suffered injury to the optic nerve as judged by visual field abnormality, combined with enlargement of the cup/disc ratio outside statistical limits for the population studied.

Using this nomenclature, there are thus 3 classes of angle closure:

1. Narrow angle: At the earliest or most basic stage of the condition, eyes have narrow or occludable angles without any other abnormality. The term primary angle-closure suspect is an alternative term for this condition, as these eyes are at increased risk of developing disease.

2. Primary angle-closure (PAC) is said to occur in eyes with angle-closure due to PAS, and/or raised intraocular pressure (IOP) due to closure of the angle, but without the presence of glaucomatous optic neuropathy. Eyes with a history of previous acute angle closure are also classified as PAC.

3. Finally, primary angle-closure glaucoma (PACG) is reserved for cases of primary angle-closure with glaucomatous optic neuropathy.

Symptomatic or acute primary angle closure can occur at any stage of this spectrum of disease. This new classification of PACG is used throughout this thesis.

1.3.5.3. Risk Factors Associated With PACG

1. Race

Prevalence of PACG is race dependent, being least in Caucasians and highest in Inuits, with Asians in between that of Caucasians and Inuits (Congdon *et al.*, 1992; Foster *et al.*, 1996).

2. Age and Sex

The manifestations of ocular damage resulting from primary closure of the drainage angle are rare before the age of 40 years. The prevalence of disease increases from the age of 40 years (Alsbirk, 1976; Shiose *et al.*, 1991; Salmon *et al.*, 1993). Female gender is recognized as a major predisposing factor toward development of PAC (Alsbirk, 1976; Arkell *et al.*, 1987; Shiose *et al.*, 1991; Salmon *et al.*, 1993).

3. Ocular Biometry

The association between a small eye and "acute glaucoma" was first recognised in the 19th century by von Graefe (published in 1857). Lowe reviewed the development of ocular biometry in the study of primary angle-closure and found people suffering angle-closure had shorter axial lengths than did unaffected people (Lowe, 1974). Several studies have since found that a small eye with a shallow anterior chamber is significantly associated with

PACG (Tornquist, 1956; Lowe, 1969; Alsbirk, 1974a; Alsbirk, 1974b; Arkell *et al.*, 1987).

4. Family History

PACG has been found to be more common in first-degree relatives of affected probands than in the general population. (Paterson, 1961; Lowe, 1964; Lowe, 1972; Alsbirk, 1975; Alsbirk, 1976; Leighton, 1976; Lowe, 1988).

1.4. Genetic Basis Of Glaucoma

Glaucoma has a major genetic basis, estimated to account for a third (range 20 - 60%) of all glaucoma cases (Wolfs *et al.*, 1998; Nemesure *et al.*, 1996; Nemesure *et al.*, 2001), although a recent report suggests that this is an underestimate (McNaught *et al.*, 2000). Genetic heterogeneity is illustrated by the more than 15 loci and 7 glaucoma-causing genes identified to date (Craig and Mackey, 1999). These are summarized in Table 1.2. A diverse variety of genetic mechanisms have been found to induce glaucoma and these include coding mutations, particularly in transcription factors (Kozlowski *et al.*, 2000), altered gene dosage (Lehmann *et al.*, 2000; Nishimura *et al.*, 2000) and dominant negative effects (Morissette *et al.*, 1998).

The Human Genome Organisation (HUGO) Genome Database Nomenclature Committee introduced a nomenclature and classification system for glaucoma genetics. The approved gene symbol was GLC1 for all types of primary open angle glaucoma (POAG); the letter A, B, C etc. assigned to each newly

discovered locus. GLC2 was designated to primary angle closure glaucoma and GLC3 to primary congenital glaucomas.

Table 1.2. List of glaucoma-causing genes, loci, chromosomal location and mode of inheritance.

Phenotype	Locus	Position	Inheritance	Gene
JOAG/POAG	GLC1A	1q24.3-q25.2	AD	*MYOC*
POAG	GLC1B	2cen-q13	AD	
POAG	GLC1C	3q21-24	AD	
POAG	GLC1D	8q23	AD	
POAG/NTG	GLC1E	10p15-14	AD	*OPTN*
POAG	GLC1F	7q35q36	AD	
Pigment Dispersion	GPDS1	7q35q36	AD	
Pigment Dispersion	GPDS2	18q11-21	AD	
Axenfeld-Rieger	RIEG1	4q25	AD	*PITX2*
Axenfeld-Rieger	RIEG2	13q14	AD	
Axenfeld-Rieger	IRID1	6p25	AD	*FOXC1*
Axenfeld-Rieger		16q24	AD	
Congenital Glaucoma	GLC3A	2p21	AR	*CYPB1*
Congenital Glaucoma	GLC3B	1p36.2-36.1	AR	
Nail-Patella Syndrome	NPS1	9q34	AD	*LMX1B*
Aniridia	PAX6	11p13	AD	*PAX6*
Nanophthalmos	NNO1	11p	AD	
Micropthalmia		Xp	X	
Micropthalmia	arMi	14q32	AR	
Micropthalmia	CHX10	14q24.3	AR	*CHX10*
Micropthalmia	adCMIC	15q12-15	AD	

1.4.1. Genetics of POAG

The first locus for open angle glaucoma was discovered in 1993, mapped at 1q21-q31 and assigned as GLC1A (Sheffield *et al.*, 1993). The gene at the GLC1A locus was originally referred to as the trabecular meshwork induced glucocorticoid response (TIGR) gene as a candidate cDNA isolated from human trabecular meshwork cells after induction with dexamethasone was found to reside in the candidate interval (Polansky *et al.*, 1996). Independently, other investigators isolated the same cDNA and named it *myocilin*, as they showed its expression in the retina to be localized to the connecting cilium of photoreceptors (Kubota *et al.*, 1997). Families linked to this locus have both juvenile and adult-onset POAG (Stone *et al.*, 1997; Suzuki *et al.*, 1997; Alward *et al.*, 1998; Wiggs *et al.*, 1998; Alward *et al.*, 2002). Mutations have been identified in several populations, including patients from Scotland, France, Japan, Germany and America (Fingert *et al.*, 1999).

It was speculated that the *MYOC* gene product may cause increased intraocular pressure by obstruction of aqueous outflow (Stone *et al.*, 1997). Its expression in trabecular meshwork and ciliary body (structures of the eye involved in the regulation of intraocular pressure) was consistent with this hypothesis. Obstruction of aqueous outflow is, however, not the only mechanism. Because myocilin is expressed in large amounts in various types of muscle, ciliary body, papillary sphincter, skeletal muscle, heart, and other tissues, it is possible that some muscle-related ciliary body mechanism may be

involved in the elevated intraocular pressure. Shepard et al characterized the glucocorticoid responsiveness of the *MYOC* gene in cultured human trabecular meshwork (TM) cells and concluded that *MYOC* is a delayed secondary glucocorticoid-responsive gene (Shepard *et al*, 2001). A recent study reported the generation of mice heterozygous and homozygous for a targeted null mutation in *MYOC*. There was a lack of a discernable phenotype in both *MYOC*-heterozygous and *MYOC*-null mice, suggesting that haploinsufficiency is not a critical mechanism for POAG in individuals with mutations in *MYOC*. Instead, disease-causing mutations in humans are likely to act by gain of function (Kim *et al*, 2001).

There are several other loci for adult onset POAG. The second locus (GLC1B) was assigned to the 2cen-q13 region (Stoilova *et al.*, 1996). The phenotype was less severe than that found in GLC1A linked families. The third locus for adult onset POAG has been described in a single American family, mapping to the 3q21-24 region, GLC1C (Wirtz *et al.*, 1997). The GLC1D locus for mixed normal and high-pressure glaucoma was mapped in one American family (Trifan *et al.*, 1998). A specific locus for normal tension glaucoma (NTG), GLC1E was assigned to 10p14-p15 (Sarfarazi *et al.*, 1998), and a sixth locus for POAG was also mapped to chromosome 7q35 (Wirtz *et al.*, 1999).

Recently, a second POAG gene, *Optineurin* (*OPTN*, MIM 602432) in the GLC1E interval on chromosome 10p was identified (Rezaie *et al.*, 2002), and showed that variations in this gene predominantly resulted in NTG. The most common *OPTN* mutation, $Glu^{50} \rightarrow$ Lys (E50K) was identified in 13.5% of families, 18% of whom had high IOP. A second *OPTN* variant, $Met^{98} \rightarrow$Lys

(M98K) was identified in 13.6% of familial and sporadic POAG cases compared to 2.1% of controls, making it a significant risk-associated genetic factor for glaucoma. Vittitow and Borras studied the effect of glaucomatous insults on the expression of *OPTN* in human eyes maintained in organ culture. Sustained elevated intraocular pressure, TNF-alpha exposure, and prolonged dexamethasone treatment all significantly upregulated *OPTN* expression, indicative of the protective role of *OPTN* in the trabecular meshwork (Vittitow and Borras, 2002).

1.4.2. Genetics of PACG

As the majority of glaucoma research has been centred on populations with a preponderance of POAG, PACG has been a relatively poorly researched condition. There are no studies to date on the genetics of PACG although transmission via a single, dominant gene has been suggested (Tornquist, 1953).

However, there are various published studies on PACG, which suggest a genetic basis for the condition. Firstly, ocular characteristics related to angle closure glaucoma are more common in close relatives of affected patients than in the general population; these characteristics include anterior position of the lens, increased lens thickness and shallow anterior chamber (Tornquist, 1956; Lowe, 1964; Lowe, 1972; Tomlinson and Leighton, 1973; Alsbirk, 1975; Spaeth, 1978; Francois, 1983). Estimates of the prevalence of PACG among first degree relatives in the Caucasian population have ranged from 1-12 %, which is higher than the 0.1% prevalence in the general population (Paterson,

1961; Lowe, 1964; Lowe, 1972; Alsbirk, 1975; Leighton, 1976; Francois, 1983; Lowe, 1988). First-degree relatives of Inuits with PACG have a three and a half times greater risk of developing the disorder compared with the general Inuit population (Alsbirk, 1976). There are also racial differences, with a higher prevalence among Inuits (2 to 8%) and Asians (0.3 to 1.4 %) compared to Caucasians (0.1%), suggesting a genetic predisposition to the disorder (Congdon *et al.*, 1992).

Recently, genetic loci for both nanophthalmos and microphthalmia have been found (Bessant *et al.*, 1998; Othman *et al.*, 1998; Morle *et al.*, 2000; Percin *et al.*, 2000). These cases are characterized by short axial length, high hypermetropia, high lens/eye volume ratio, and a high incidence of prevalence of angle-closure. Intraocular pressure was greatly elevated in many cases. The combination of ocular defects suggested an embryological disorder involving tissues derived from both the neuroectoderm and neural crest. These data provide growing evidence that PACG may have a genetic basis.

1.4.3. Genetics of primary congenital glaucomas

GLC3 is the gene symbol for primary congenital glaucoma. Two loci have been described in pedigrees segregating glaucoma as an autosomal recessive trait, GLC3A at chromosome 2p21 (Tang *et al.*, 1996) and GLC3B at 1p36 (Akarsu *et al.*, 1996). Mutations in the cytochrome P4501B1 (CYP1B1) gene have since been identified in GLC3A linked families (Stoilov I *et al.*, 1997; Bejjani *et al.* 1998).

1.4.4. Genetics of developmental glaucomas

Syndromes of anterior segment dysgenesis such as Axenfeld-Rieger syndrome and iridogoniodysgenesis are frequently accompanied by glaucoma. The usual pattern of inheritance for these conditions is autosomal dominant. Mutations have been identified in the *PITX2* gene, a member of the homeobox family at the RIEG1 locus in patients with Rieger syndrome, iris hypoplasia and iridogoniodysgenesis (Heon *et al.*, 1995; Semina *et al.*, 1996; Kulak *et al.*, 1998). The RIEG2 locus was linked to chromosome 13q14 (Phillips *et al.*, 1996). A number of families with Axenfeld-Rieger syndrome have been linked to chromosome 6p25, and found to have mutations in the *FOXC1* gene. *FOXC1*, was subsequently shown to cause a spectrum of glaucoma-associated developmental phenotypes including Axenfeld anomaly, Rieger syndrome and iris hypoplasia (Nishimura *et al.*, 2001). A large pedigree was reported with a chromosomal duplication encompassing *FOXC1* indicating that gene duplication causes developmental disease in humans and that increased *FOXC1* gene dosage was the probable mechanism responsible for the iris hypoplasia and glaucoma phenotype (Lehmann *et al.*, 2000). Aniridia is also associated with developmental glaucoma. The gene for aniridia (*PAX6)* on chromosome 11p13 is a transcription factor of the paired-box family (Ton *et al.*, 1991).

1.4.5. Monogenic or Polygenic Disease

At present it is unclear whether (genetically-determined) cases of glaucoma are a heterogeneous collection of monogenic disorders or a complex genetic

disorder with multiple genes acting (either alone or in conjunction with environmental factors) to determine an individual's susceptibility to developing glaucoma. In the last two years, evidence for the presence of modifier genes that modulate the penetrance and or severity of certain forms of glaucoma has emerged. The first study, an analysis of Saudi pedigrees with primary congenital glaucoma identified 40 apparently unaffected individuals in 22 pedigrees with *CYP1B1* mutations and haplotypes identical to their affected siblings. This suggested the presence of a dominant modifier locus capable of modulating the severity of the disease (Bejjani *et al.*, 2000). More recently, a single pedigree with autosomal dominant glaucoma was reported in which *CYP1B1* and *MYOC* mutations segregated. The mean age at diagnosis of glaucoma in the *MYOC* mutation carriers was 51 years compared to 27 years in individuals with both mutations, indicating that *MYOC* and *CYP1B1* may interact through a common pathway (Vincent *et al.*, 2002).

1.5. Dominant Optic Atrophy

Autosomal dominant optic atrophy (ADOA) is another condition that is characterized by progressive optic nerve damage (Hoyt, 1980; Votruba *et al.*, 1988; Johnston *et al.*, 1999). This optic neuropathy is attributable to primary degeneration of retinal ganglion cells followed by ascending atrophy of the optic nerve (Johnston *et al.*, 1979; Kjer *et al.*, 1983). Loci for ADOA have been mapped to chromosome 3q28-qter (Eiberg *et al.*, 1994; Jonasdottir *et al.*,

1997) and 18q12.2-q12.3 (Kerrison *et al.*, 1999), and recently, the *OPA1* gene (MIM 165500) was identified (Alexander *et al.*, 2000; Delettre *et al.*, 2000) and shown to be ubiquitously expressed, including in retinal ganglion cells and the optic nerve (Alexander *et al.*, 2000).

Since different mutations in the same gene may cause widely different phenotypes, as illustrated in glaucoma by *FOXC1*, *MYOC*, *PAX6* and *PITX2*, the similarities between glaucoma and ADOA (in terms of the cell type affected and the phenotype) make *OPA1* an excellent candidate gene for glaucoma.

1.6. Strategies to identify genes implicated in human disease

A number of different methods can be employed to identify genes implicated in human disease, ultimately leading to the screening of a candidate gene for mutations. Two major strategies are functional and positional candidate gene approach. The functional approach requires prior knowledge of the protein product, function of the gene, or biochemical understanding of the disease. However, for the majority of inherited human disease, the underlying

biochemical defect is unknown. A positional strategy assumes no functional knowledge and is dependent on the chromosomal location of the disease locus determined by genetic linkage analysis (Figure 1.9). A combination of the two approaches is often used and involves the initial localisation of the disease to a chromosomal region, refinement of the genetic interval using polymorphic markers, and the subsequent selection of candidate genes based on criteria such as gene expression pattern or homology to genes or proteins previously implicated in similar disease processes or pathways. The availability of the sequence of the human genome has greatly facilitated the elucidation of the genetic basis of human disease.

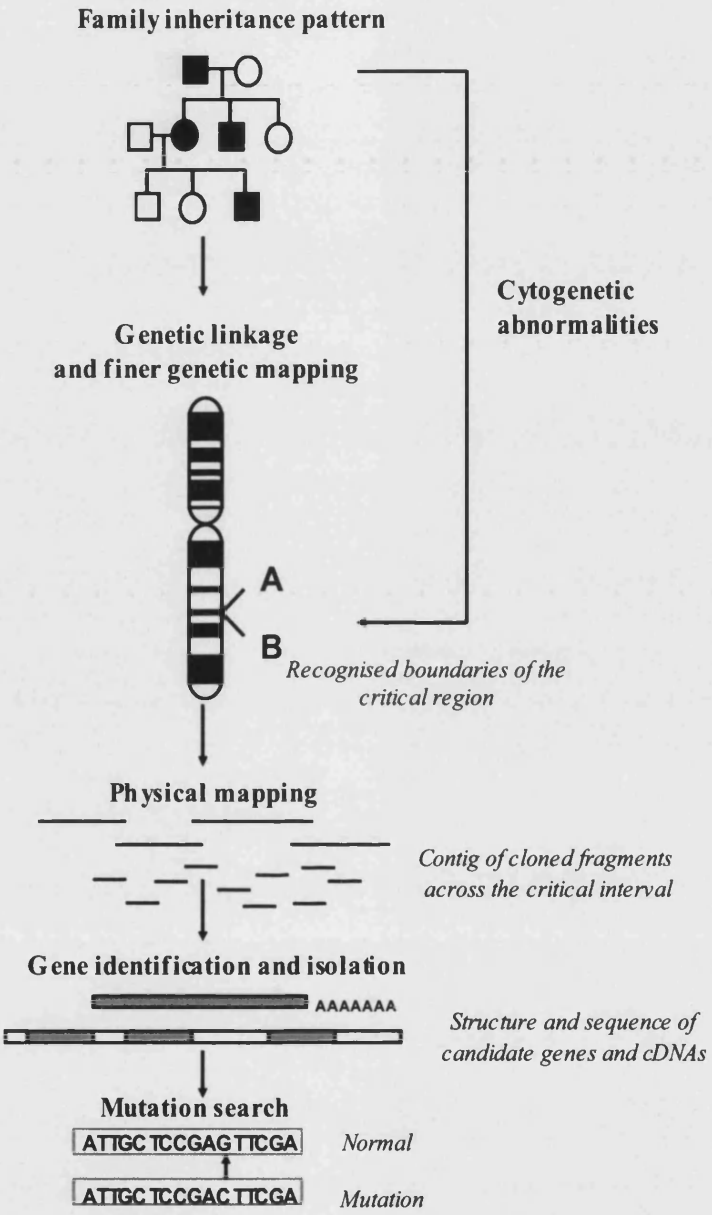

Figure 1.9. Identifying genes in disease: positional approach.

1.7. Principles of genetic mapping

Genetic mapping follows the segregation of alleles at a locus for a genetic marker during meiosis.

1.7.1. Meiotic recombination

Human genomic DNA is distributed between 22 pairs of autosomes and two sex chromosomes. During meiotic cell division, homologous chromosome pairs, each consisting of two chromatids, are aligned together and DNA segments are exchanged between chromatids of homologous chromosomes. This process is referred to as crossing over and results in recombinant chromosomes. These recombination events occur on average at least once on the arm of each chromosome. As a result of these events, a unique chromosome is formed and inherited by the next generation. Loci which lie physically further apart are more likely to recombine while loci which lie closer together on the chromosome are less likely to recombine and can therefore be considered linked to one another.

The frequency of recombination can be calculated by comparing the inherited alleles of offspring to those of their parents. Linkage analysis relies on the frequency of crossovers to infer the distance between genetic markers in a family pedigree. Using linkage analysis, genetic markers can be placed onto genetic maps of chromosomes and the segregation of inherited diseases in a family can be followed. Linkage analysis in family pedigrees expressing a disease phenotype can be used to define a chromosomal locus, leading to the isolation of the causative gene.

1.7.2. Recombination frequency

The number of recombinants expressed as a fraction of the total number of gametes is called the recombination fraction (θ) and it is a measure of the genetic distance between any two loci. The further apart two loci are, the greater the possibility of crossovers being observed and the recombination fraction will then approach 0.5 which indicates independent segregation. Conversely, if two loci lie close together on a chromosome and no crossovers are observed then recombination fraction will be zero.

1.7.3. Genetic map distance

The genetic map distance (in units of Morgans) is defined as the length of chromosomal segment, which on average undergoes one crossover per chromatid strand. The male autosomal map length is estimated to be 26.5 Morgans based on an average occurrence of 53 chiasmata. The recombination rate in females is higher than in males and is estimated to be 39 Morgans. Thus, the sex-averaged autosomal map is 33 Morgans, which implies that the average length of a human chromosome is 1.5 Morgans or that it undergoes 1.5 crossovers per meiosis (Renwick, 1969). However, genetic distance is usually quoted in centimorgans (cM), where two loci are 1 cM apart if they recombine once in 100 meiosis or show a recombination fraction (θ) of 0.01. There is a linear correlation between θ and genetic map distance over short distances however, over longer distances multiple crossovers can occur between two loci and the values of θ are not additive.

1.8. Linkage analysis

Linkage analysis is the method used in families in order to ascertain the location of the disease gene in the human genome. The process involves the use of polymorphic genetic markers of known genomic localisation with the

purpose being to identify co-segregation between the disease locus, represented by the disease phenotype, and an allele of a DNA marker. It relies upon the tendency of genes or DNA sequences at fixed chromosomal positions (loci) to be inherited together due to their physical proximity on the chromosome, and identification of such co-segregation infers linkage between the 2 loci and therefore localises the disease gene to the region where the marker maps. By measuring the frequency of non-random segregation, a statistical value can be calculated for the likelihood that two loci are linked.

1.8.1. Maximum likelihood estimate (MLE)

Linkage analysis utilises the principle of maximum likelihood, which states that the hypothesis with the greatest likelihood is that for which the probability of the observations is maximised. This maximum value is called the maximum likelihood estimate (MLE) or L (θ), and is obtained by finding that value of the recombination frequency (θ) between the disease and the marker that maximises the probability of the data. L (θ) can be calculated for a range of recombination fractions between 0 and 0.5 and the value of θ that produces the highest L(θ) is the MLE. This is often denoted as odds ratios, L(θ)/L(0.5) which expresses the probability of linkage versus non-linkage.

1.8.2. Lod score (Z)

The LOD score (Z) (or logarithm of odds ratio) is a useful mathematical measure of the likelihood of segregation (linked) of a marker to phenotype as opposed to both being unlinked. Crossovers or recombination frequencies will affect the Z value so the LOD score is essentially the ratio that two loci are linked at a given recombination fraction (θ) compared to the same segregation pattern if they are unlinked. This ratio is calculated for a range of recombination values between $\theta=0$ and $\theta=0.5$ (where loci are regarded as independently assorted) (Ott, 1997).

$Z(\theta)=\log10[L(\theta)/L(0.5)]$

where: $L(\theta)$=likelihood if the two loci are linked and have a recombination fraction of θ.

$L(0.5)$=likelihood if the two loci are not linked.

By convention, a LOD score of ≥ 3.0 is regarded as significant evidence that two loci are linked. This is equivalent to a 1:1000 or less likelihood that the observed linkage has occurred by chance. A smaller LOD score is required for

demonstrating linkage in X-linked disorders ($\geq$ 2.0). The presence of a negative LOD score suggests that the two loci are unlinked and, by convention, a LOD score of $\leq$-2.0 is taken as evidence against linkage at the stated recombination fraction.

LOD scores can be calculated with a variety of computer packages including MLINK program (Lathrop and Lalouel, 1984) within Cyrillic 2.1.1 and web based programmes (e.g. Genetic Linkage User Environment (GLUE), Human Genome Mapping Project).

1.8.3. Polymorphic markers used in linkage analysis

Genetic mapping requires markers that are polymorphic, display Mendelian segregation and are distributed at regular interval throughout the genome in order to provide a useful tool for the chromosomal localisation of a disease. A genetic marker defines a particular chromosomal locus and helps in differentiating homologous chromosomes.

1.8.4. Marker characteristics

For linkage analysis, it is necessary to have informative meiosis. However, in order to achieve this, it is necessary for a marker to be polymorphic and informative as increased information content of markers can reduce the number of individuals that need to be typed to genetically map disease genes. The polymorphism information content (PIC) value was used to calculate the informativeness of a marker in a given population and is dependent on the number of alleles in that population (Weber and May, 1989). A PIC value of greater than 70% signifies an extremely polymorphic marker. The formula for PIC is as follows:

$$PIC = 1-\sum p_i^2 -\sum\sum 2p_i^2 p_j^2$$

(where p_i and p_j are the population frequencies of the ith and jth alleles in a diallelic system)

Heterozygosity is defined as the probability that an individual is heterozygous for an allele if picked at random, and is depicted by the formula:

$$H=1-1/a$$

where a is the number of alleles of equal frequency. The greater the number of alleles, the greater the probability of heterozygosity, and if there are a large number of alleles, H approximates PIC.

1.8.5. Types of Markers

1.8.5.1. RFLPs and mini-satellite DNA

The markers used to establish linkage have changed considerably over the last twenty years and have become more informative. Restriction fragment length polymorphisms (RFLPs) exploit the fact the human DNA can be variable and that these variations may result in the alteration of a restriction enzyme site. RFLPs were typed by the hybridisation of Southern blots of restriction digested genomic DNA with a probe tagged with radioisotope and subsequent exposure to autoradiograph film, and were used to provide a marker set spanning the entire genome (Botstein *et al.*, 1980). Most RFLP systems have only two alleles with a maximum heterozygosity of 50%. A major drawback of the use of RFLPs is that it is time consuming and the informativeness of markers is low.

Minisatellite or variable number tandem repeats (VNTRs) are tandemly repeated units of 11-60 bp that can extend up to 1 kb. Polymorphism occurs as

a result of the difference in the number of repeats. As such, VNTRs are more informative than RFLPs and have higher PIC values hence they become more useful for linkage studies. The major limitation of minisatellites is the tendency for clustering around the telomeres and the time consuming method of analysis (Jeffreys *et al.*, 1985).

1.8.5.2. Microsatellite markers (Short Tandem Repeat Polymorphisms)

Microsatellites are simple tandem repeat sequences that can be found at the 5' and 3' untranslated region of genes, as well as within introns and non-coding DNA (Weber and May, 1989).

The use of microsatellites overcame many of the limitations of minisatellite DNA as they are distributed more evenly throughout the genome at approximately 30kb intervals. In addition, the ease of analysis with amplification by PCR, is more efficient (Litt and Luty, 1989). Microsatellites consist of tetra, tri and di-nucleotide repeats with the most common being the dinucleotide CA repeat. A number of genetic maps composed of microsatellite markers have been published, and the final Genethon map in 1996 brought to an end this phase of the human genome project (Dib *et al.*, 1996).

1.8.5.3. Single nucleotide polymorphisms (SNPs)

Single nucleotide polymorphism (SNP) is a bi-allelic system based on a single nucleotide change at the sequence level. SNPs are the most frequently occurring polymorphic markers available estimated at 1 SNP per 100 to 300 bp (http://www.ncbi.nlm.nih.gov/SNP). A genetic map of SNPs was created using a number of microsatellite markers as anchor points and the automation of the analysis was achieved using a genotyping chip that would allow the simultaneous analysis of 500 SNPs (Wang *et al.,* 1998). The SNP database at The National Centre for Biotechnology Information serves as a central repository for both single base nucleotide substitutions and short deletion and insertion polymorphisms. It is estimated that 60,000 SNPs fall within exons and that 85% of exons are within 5 kb of the nearest SNP (Sachidanandam , *et al.*, 2001). As genetic markers, SNPs can be used for conventional linkage analysis. However, due to the availability of high density maps and the improvements in technology that allow for the automation of screening SNPs they are a useful resource for linkage disequillibrium (LD) and association studies.

1.9. Mutation detection

Once a disease gene has been linked to a particular locus on a chromosome the next step is the identification of the gene mutations responsible. A number of different mutation detection methods can be used to detect gene mutations. No method of mutation detection is 100% efficient and if changes are seen in either method they require confirmation by direct sequencing of the DNA product, as direct sequencing of the gene sequence is a more accurate mutation technique.

1.9.1. Heteroduplex analysis

Heteroduplex analysis is a technique that can be routinely used to detect variants in a given sequence. It is based on the fact that two complementary DNA strands, which differ in sequence by even one base pair, will have mismatched positions when base paired. These double stranded heteroduplex molecules tend to show altered mobility in non-denaturing polyacrylamide gels when compared to the homoduplexes of either allele (Keen *et al.,* 1991). Recently, denaturing high-pressure liquid chromatography (DHPLC) technology has been applied to identify mutations such as the Transgenomics Wave machine. DHPLC uses triethylammonium acetate (TEAA), which acts as an ion-pairing reagent that binds to the hydrophobic DNA giving it

hydrophilic characteristics. For the Wave machine (Transgenomics), the TEAA (0.1 M) coats the DNA, which allows it to bind to the divinylbenzene beads on a column. There is a proportional relationship between the association of TEAA and the binding to the DNA separation column. Dissociation of the TEAA-bound DNA from the column is accomplished by an elution gradient comprising 0.1 M TEAA and 25% acetonitrile. The proportions of reagents are changed over time and allow the elution of DNA. Smaller DNA fragments, having less TEAA bound, are eluted before the larger fragments and the technique allows for a sizing application as well as its use for mutation detection. The DNA fragments eluted are detected using a UV detector and visualised as a graph.

1.9.2. Single strand conformation polymorphism (SSCP)

The sequence of interest is amplified by PCR and separated as single-stranded molecules by resolution on native polyacrylamide gels. Sequence variants tend to show a shift in mobility due to changes in the tertiary structure of the single-stranded DNA (Orita *et al.*, 1989).

1.10. Human Genome Project

The Human Genome Project was instigated as an international research initiative to produce detailed genetic and physical maps of each of the human chromosomes. The ultimate goal of the initiative, following the construction of physical maps in large insert clones, is to produce a single continuous sequence for each chromosome and define the positions of all genes. Similar analyses of several other genomes and model organisms were also initiated, and the methods and resources used to determine the significantly smaller genome sequence of the nematode *Caenorhabditis.elegans* (97 million base pairs) greatly aided the planning and execution of the Human Genome Project (approx. 3 billion base pairs). Throughout the progression of the Human Genome Project (HGP), new methods and resources were developed and complimentary approaches used to create, store and analyse the data (Jordan 1994; Haldi *et al.*, 1996; Lander 1996; Schuler *et al.*, 1996).

Major achievements of the HGP include;

1995 – first generation physical map

1996 – comprehensive genetic map

1998 – *C. elegans* genome completed

1999 – sequence of chromosome 22 completed

2001 – complete draft sequence of the human genome

The draft human genome sequence was published in 2001 by the HGP consortium and Celera Genomics (International human genome sequencing consortium 2001; Venter *et al.*, 2001). The HGP project estimates that there are approximately 31,000 genes and Celera estimates an even smaller number of genes, about 26,000. This is in stark contrast to initial estimates of human gene number, which ranged from 50,000 to 100,000, and indicates that the density of genes in the human genome is much lower than for any other genome sequenced so far. Both groups used computational algorithms to model and predict gene sequences, however these methods are known to be inaccurate through over and under prediction. To arrive at a more accurate description of the number of genes in the human genome, reliance will be placed upon individual gene and protein characterisation. Initiatives to characterise full length mRNAs have already highlighted the fact that the current human genome annotation has not detected a significant number of gene sequences (Wiemann *et al.*, 2001). It is also evident that alternative splicing of genes in the human genome is common (over 60% of genes have

alternative transcripts) which would result in a larger number of protein products.

Much work remains to be done to complete the sequence and be assured of its accuracy, but the vast amount of information that has become available through this initiative provides us with basic information on genome evolution and structure, and revolutionises the field of medical genetics.

1.10.1. Bioinformatics and human genome resources

Over the past few decades, major advances in the field of molecular biology, coupled with advances in genomic technologies, have led to an explosive growth in the biological information generated by the scientific community. This deluge of genomic information has, in turn, led to an absolute requirement for computerised databases to store, organize and index the data, and for specialised tools to view and analyse the data. Bioinformatics is the term used to describe the discipline which brings together biology and computer science. The ultimate goal of the field is to enable discovery of new biological insights. Currently the focus on the human genome project has

enabled the analysis and interpretation of various types of data including nucleotide and amino acid sequences, the development of tools that enable efficient access to different types of information, and the development of new algorithms to assess and analyse relationships between data sets.

Alongside the development of new methods for establishing maps of the genome and new sequence strategies a great deal of effort is concentrated on designing databases and programs to accurately represent and analyse the information generated. One major challenge was to collect, store, distribute, analyse and retrieve data created as whole genomes were physically mapped and sequenced. These original databases and programs are constantly evolving and many suites of programs and databases now exist on web sites world wide providing a remarkable resource for the field of molecular genetics.

Genome maps have subsequently integrated clone data and the ultimate map, the genome sequence, is being deposited in these databases in accessible formats for analysis. More recently emphasis has shifted towards the establishment of a SNP map covering the genome. Regional and chromosome

maps can be viewed at many centres, each with their own graphic interface and options to view and analyse.

1.11. Sequence analysis tools

The Basic Alignment Search Tool (BLAST) is the main program used to compare sequence similarity, with algorithms for nucleotide and amino acid sequence analysis. By comparing sequence identity and similarity of a gene or protein with all known sequences (GenBank), function can often be inferred. Gene and protein sequences can also be analysed using suites of programs such as NIX and PIX available at HGMP, which combine many analysis tools in one package. In addition, NIX is a useful tool for analysing genomic sequence which runs gene prediction programmes similar to ACeDB as well as data mining and comparison programs. Many analysis programs have been developed for specific applications, however it is important to note that all bioinformatic tools merely provide a guide for future experimental work. Problems can arise when utilising bioinformatic tools for data analysis. One major draw back is that they all rely on the accuracy of the archived data, as well as our current understanding of gene families, protein function, exon

structure etc. As we learn more about the genome and specific gene/protein functions, the bioinformatic applications will improve.

1.12. Aims of Thesis

The overall aim of this thesis was to investigate the role of genetic factors in the primary glaucomas using genetic and molecular biology techniques.

The specific aims were:

1. To identify the genetic basis of primary angle closure glaucoma with the goal of finding a novel glaucoma-causing gene by linkage analysis of large pedigrees with the condition.

2. To investigate the role of the *OPA1* gene, the gene responsible for dominant optic atrophy, in primary open angle glaucoma, particularly normal tension glaucoma.

3. To determine the significance of the *Optineurin* gene in the causation of primary open angle glaucoma and to characterize the phenotype attributable to mutations in this gene.

CHAPTER 2

MATERIALS AND METHODS

2.1. Patient ascertainment

2.1.1. Patient identification

Pedigrees with primary angle closure glaucoma (PACG) were examined at the glaucoma clinics at Singapore National Eye Centre and the National University Hospital, Singapore. Informed consent was obtained, and the study had the approval of the Singapore National Eye Centre and National University Hospital, Singapore ethics committee.

For primary open angle glaucoma (POAG) studies, all cases and control subjects were from the greater London area. Cases were collected from a cohort of unrelated Caucasian patients who attended tertiary referral glaucoma clinics at Moorfields Eye Hospital, London. Control DNA samples were obtained from unrelated Caucasian individuals randomly recruited from spouses and friends of probands participating in various genetic studies at Moorfields Eye Hospital. Written informed consent was obtained from all participants, and the study had the approval of the Hospital's ethics committee.

2.1.2. Ophthalmic examination

A variety of data were collected from each individual including demographic details, age at diagnosis, and medical or surgical treatment. All glaucoma subjects underwent a detailed eye examination that included assessment of visual acuity, slit lamp examination, and gonioscopy (see below). Intraocular pressure was measured by Goldmann applanation tonometry. The optic disc

and posterior pole were examined using a Volk +78D or +90D lens. The vertical cup-disc ratio was judged by observing disc contour and angulation of blood vessels that crossed the disc rim. Notching (localised neuroretinal tissue loss at the superior or inferior poles) and nerve fibre layer defects were recorded.

2.1.3. Gonioscopy

Gonioscopy was carried out in all subjects using a Goldmann-style 2 mirror gonioscope. A 2% hypromellose solution in saline was used as a coupling medium for the contact lens. The examination was carried out at a low level of ambient illumination. A 1 mm beam of light was reduced to a very narrow slit, and was offset horizontally for assessing superior and inferior angles, and vertically for nasal and temporal angles. Care was taken to avoid light falling on the pupil during gonioscopy. The assessment was carried out at high magnification (x 16 to x 25). Slight tilting to gain a view over the convexity of the iris was permitted, but further manipulation of the lens or redirection of gaze was avoided because of the possibility of exerting pressure on the cornea and artificially widening the angle. The drainage angle was graded according to Shaffer's convention in each quadrant (as detailed in Section 1.3.2.). The total gonioscopic angle width was also calculated by adding the Shaffer grade in each of 4 quadrants.

Manipulative or indentation gonioscopy using a Zeiss or Sussman lens was used (unless the angle was wide open) to detect peripheral anterior synechiae

(PAS), graded as present or absent in each quadrant, and the number of clock hours of PAS was also recorded.

2.1.4. Biometry

Probands with PACG as well as unaffected family members underwent biometry, specifically measurement of the anterior chamber depth (ACD) and the axial length (AXL) of the eyeball. After anaesthetising the eye to be examined with a drop of local anaesthetic, measurement of ACD and AXL was performed by A-mode applanation ultrasonography (Sonomed A2500, Haag-Streit, Koniz, Switzerland). Special care was taken in aligning the transducer beam probe along the optical axis and to exert minimal corneal pressure. Measurements were performed until 5 consecutive readings with a standard deviation of ≤ 0.05 were obtained for each variable.

2.1.5. Visual field testing

Patients underwent automated white-on-white threshold perimetry (program 24-2, model 750, Humphrey Instruments, San Leandro, California, USA). The first visual field test for all subjects was discarded from the analyses to allow for learning effects, and the subsequent first reliable visual field was used as the baseline. A reliable visual field test was defined as one with less than 25% false-positive response, 30% false-negative response, and 30% fixation loses. The global indices such as mean deviation (MD) and corrected pattern standard deviation (CPSD) of the baseline visual fields were recorded for all cases.

The visual fields of some subjects who had at least 5 years of follow-up with at least 10 visual field tests performed during this time were also analysed for progression. Pointwise linear regression analysis was applied to the field series of each of these subjects using PROGRESSOR for Windows software (Fitzke FW *et al.*, 1996). Progression was defined as the presence of a significant regression slope ($p<0.01$) showing 1 dB per year or more of sensitivity loss at the same test location with the addition of two out of three successive field tests to the series starting with the first three. The mean number of progressing points per subject, the mean slope for the progressing points as well as the mean slope of the whole visual field per year was evaluated.

2.1.6. Optic Disc Imaging

A scanning laser ophthalmoscope, the Heidelberg retina tomograph (HRT, Heidelberg Engineering, Heidelberg, Germany) was used to image the optic disc in POAG subjects (Figure 2.1). The mean topography of three images was generated in the 10×10 degree frame and the disc edge delineated on the mean image by a trained observer, using a drawn contour line. Images with significant movement artefact were rejected. Global and segmental disc and cup areas were analysed directly by means of HRT software (version 2.01b) using the standard reference plane. Rim area was calculated by subtracting the cup area from the disc area. Six predefined segments were used (0 degrees always temporal, 90 degrees always superior): temporal quadrant (-45 to +45 degrees), temporal superior octant (+45 to +90 degrees), temporal inferior octant (-90 to –45 degrees), nasal quadrant (+135 to +225 degrees), nasal

superior octant (+45 to +90 degrees), and nasal inferior octant (-135 to –90 degrees).

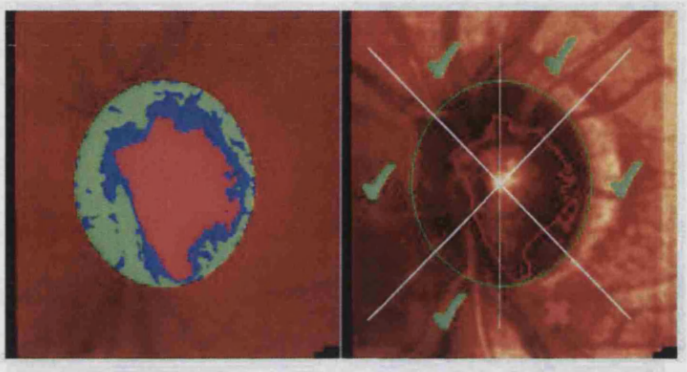

Figure 2.1. HRT image of an optic disc showing overall disc topography (left) and segment analysis (right).

2.2. Diagnostic Criteria

2.2.1. Angle closure

The minimum criteria for the diagnosis of angle closure was the presence of a narrow or occludable angle. This was defined as the presence of at least 180 degrees of angle in which the posterior trabecular meshwork was not visible on indentation gonioscopy (Shaffer Grade 0 or 1).

Eyes with a narrow angle with raised IOP (>21 mm Hg) and/or PAS in the angle were termed to have primary angle closure (PAC).

Primary angle closure glaucoma was defined as the presence of glaucomatous optic neuropathy with compatible visual field loss, in association with a narrow angle on indentation gonioscopy.

Cases of secondary angle closure such as neovascularisation of the iris, uveitis, trauma, lens intumescence or subluxation were excluded.

2.2.2. Open angle glaucoma

POAG cases were defined by the following strict criteria: the presence of glaucomatous optic neuropathy with compatible visual field loss; open drainage angles on gonioscopy, and absence of a secondary cause for glaucomatous optic neuropathy such as a previously raised IOP following trauma, a period of steroid administration or uveitis. Patients also did not have evidence of high myopia or congenital abnormality, and had no other cause for their visual loss.

Among POAG subjects, IOP was used to subdivide the cases into normal tension glaucoma (NTG) and high tension glaucoma (HTG). NTG patients had mean IOP without treatment that was consistently ≤ 21 mm Hg on diurnal testing, while HTG patients had IOP consistently > 21 mm Hg.

2.3. Sample collection

Two 10 ml EDTA impregnated vials of venous blood were collected from each adult using Vacuette vacutainer blood collection system. One vial of blood underwent DNA extraction and the other vial of the blood from the same patient was stored at -20^0 C. The latter vial was stored for future reference and in case there was an error with the DNA extraction from the first vial.

2.3.1. DNA Isolation

Genomic DNA was extracted from EDTA-sequestered blood samples using the Nucleon II DNA extraction kit (Scotland Bioscience). Initially, blood collected in sodium EDTA tubes were thawed, inverted a couple of times and then transferred in a 50 ml tapered falcon tube that contained 37 ml of Reagent A for erythrocyte lysis. The tapered tubes containing the solutions were then centrifuged at 3500 rpm for 6 minutes. Supernatant from the tapered tubes was discarded, retaining a pellet of white blood cells. 2 ml of reagent B was added to the pellet for leucocyte lysis and deproteination. The pellets were broken up and transferred to a 5 ml polypropylene centrifuge tube containing sodium perchlorate and mixed thoroughly. For the DNA extraction, 1.5 ml of chloroform was added to each tube and again mixed thoroughly before the addition of 300 µl nucleon^{TM} resin without re-mixing the phases. The tubes were placed in a centrifuge for a final spin again at 3500 rpm for 4 minutes. After the spin, DNA-containing upper phase of the spin was removed without disturbing the nucleon resin and added in a 15 ml tapered tube containing 6 ml of 100% ethanol and shaken slowly. The pellet of DNA was then spooled out with disposable spool and placed in a labelled 1.5 ml eppendorf and left to air dry. Upon drying, 400 µl of fresh autoclaved distilled water was added to the dried pellet and left in a fridge to dissolve overnight. 20 µl of the stock DNA was taken and dissolved in 180 µl distilled water and used as working solution.

2.4. Polymerase Chain Reaction (PCR)

PCR has become one of the most valuable *in vitro* techniques in molecular biology by allowing the synthesis of microgram amounts of specific nucleic acid sequences from any part of the genome. To permit selective amplification, some prior DNA sequence information from the target sequences is required. This enables the construction of two oligonucleotide primer sequences (often 15-30 nucleotides long) which derive opposite strands of the template DNA to be amplified with their 3' termini face each other. The two primers, when added to genomic DNA are denatured at a high temperature, before it binds specifically to complementary DNA sequences immediately flanking the desired target region at an appropriate annealing temperature. In the presence of a suitably heat-stable DNA polymerase enzyme (*Taq* polymerase), DNA precursors (the four dinucleotide triphosphates; dATP, dCTP, dGTP, dTTP) and the target DNA, the reaction is subjected to an optimal temperature for elongation and synthesis of new DNA strands. These are complementary to their individual DNA strands of the target DNA segment, and overlap each other.

The newly synthesised DNA strands act as templates for further DNA synthesis in subsequent cycles. After approximately 30-35 cycles of DNA synthesis, the products of PCR will include, in addition to the starting DNA, approximately 10^5 copies of the original specific target sequence.

The reaction involves cycles composed of three steps: denaturation, annealing and extension. A typical temperature of these steps are stated below:

I) *Denaturation* - this occurs typically at about 93-95°C for human genomic DNA;

II) *Annealing* - at temperatures usually from about 50-70°C, depending on T_m of the expected primer/target DNA duplex (the annealing temperature is typically about 5^0C below the calculated T_m).

III) *Extension (DNA synthesis)* - DNA synthesis occurs typically at 70-75°C.

PCR was carried out using a $(NH_4)_2$ SO_4 reaction buffer or KCL, with *Taq* (*Thermus aquaticus*) polymerase in a 50ul volume. A typical 50 ul volume PCR mix contained:

5 ul of 1 X concentration reaction buffer (NH_4)

5 ul of dNTPs (2 mM each of dATP, dCTP, dGTP and dTTP)

2 ul of each oligonucleotide primer

1.5 ul of $MgCl_2$ (50 mM)

0.1 ul of *Taq* polymerase

1.5µl of DNA in solution to be amplified (100ng)

(Or no DNA, for negative control)

37 ul of dH_20.

PCR conditions varied to take in account of annealing temperature of the primers and the expected length of the amplified product. Average conditions were as follows; an initial denaturation step of 5 min at 95^0C, which followed by 35 cycles of 3 steps of denaturation at 95^0C for 1 min, a primer annealing

step for 1 min and an extension step at 72^0C for 1 min. A final extension step at 72^0C for a minimum of 5 minutes was also added. Occasionally, extra $MgCl_2$ was added to the reaction buffer to optimise specificity of primer annealing.

Great care was taken to prevent cross contamination of DNA samples and minimise the potential for errors. Separate tip was used for each sample of patient DNA. Frequently, a separate work area, pipettes for pre-and post-amplification steps, and aerosol resistant tips were used for pipetting.

2.4.1. Primer design

PCR primers were designed, whose 5' end lay more than 30 nucleotides from the coding start (forward) and end (reverse) of an exon and which would yield an end product of between 200-400 base pairs to enable amplification of the entire coding region.

The following default parameters were used:

a) Primer lengths were designed to be unique for the human genome and varied from 17mer to 24mer, according to the formula:

$2N(O.25)^n = 1$

where for any given nucleic acid sequence of length, N, containing only the four normal nucleotides, the segment length, n, is necessary to define a unique sequence.

b) to avoid 3' pentamer instability, false priming, dimerisation and secondary structure formation, the pentamer ▲G was set below -8.5kCaJ/mol.

c) Primers with discrete 3' 7mer were preferred to avoid false priming.

d) The melting temperature T_m is determined by the nucleotide sequence of the primer, and calculated according to the equation $T_m = 4(G+C) + 2(A+T)$
Ideally, primer pairs were designed with similar Tm values. An annealing temperature 5°C below the estimated Tm was used as a starting point.

Online human genome databases (NCBI Genbank) were consulted to obtain the complete intron and exon sequences for each gene of interest. Where this was not readily available or only partially published, exons were reconstructed from full length mRNA and intron boundaries characterised by utilising BLAST sequence comparison software to identify human clones localised to the genomic region of interest.

2.4.2. Reverse transcription PCR (RT-PCR)

Leukocytes were isolated from whole blood by Ficoll-Paque density-gradient centrifugation following manufacturer's instructions (Amersham Pharmacia Biotech, Little Chalfont, UK) and total RNA extracted with Trizol reagent (Invitrogen Life Technologies, Groningen, The Netherlands). Oligo(dT)-primed total leukocyte RNA was reverse transcribed into single-stranded cDNA using Ready-To-Go You-Prime First-Strand Beads (Amersham

Pharmacia Biotech). Primers were then used to amplify cDNA segments by PCR.

2.5. Cloning of PCR product fragments into plasmid vectors

The plasmid vector used for cloning of PCR products was pGEM®-T Easy (Promega), which is a pUC-derived vector and contains dT overhangs at the cloning site in order to generate a sticky end. The sticky end is compatible with the terminal dA overhangs produced on any PCR product due to the template-independent action of certain Taq polymerases. These dA overhangs greatly improve the efficiency of PCR product ligation into the plasmid. Insertional activation of the alpha-peptide allows recombinant clones to be directly identified by colour screening on indicator plates (LB agar plus X-gal, IPTG and ampicillin).

2.5.1. Ligations

Ligation takes advantage of the template-independent addition of a single adenosine (A) to the 3' end of PCR products by certain thermostable polymerases. 50 ng of vector was ligated to an appropriate amount of purified PCR product such that the ratio of molar ends of vector to PCR product was 1:1 to 1:3. Ligations were incubated at room temperature for 1 hour. Reactions were stored at –20 °C following withdrawal of an aliquot for transformation of competent E.Coli. Appropriate controls were also set up as per manufacturer's instructions.

2.5.2. Transformations

JM109 competent cells (Promega) were used and transformed according to the manufacturer's recommendations. Briefly, 2 ul of the ligation reaction was mixed with 50ul of competent cells and incubated on ice for 30 minutes. The reactions were heat shocked at 42 ° C for 50 seconds and then replaced on ice for 2 minutes. 300 ul of Super Optimal Catabolite (S.O.C.) medium was added to the reaction, which was then incubated with agitation at 37 ° C for 90 minutes to allow expansion of the plasmid. 150 ul aliquots of transformation reactions were plated onto to LB-ampicillin-Xgal-IPTG agar plates enabling for colour selection (white for positive, blue for negative).

2.5.3. Colony PCR

Twelve to 24 positive colonies were picked with sterile picks or disposable pipette tips and mixed in a PCR tube. This was used for PCR using pTAG primers with 50 °C annealing temperature. The products were then run on an agarose gel to see which clones contain inserts of the correct size. The colonies of positive clones were then inoculated into LB media containing ampicillin and incubated overnight at 37 ° C.

2.5.4. Extraction of Plasmid DNA

To extract DNA from the plasmids, QIAprep Spin Miniprep kits were used. The kits act by lysing the host bacterial cells, releasing the DNA and protein, the protein is then precipitated and the DNA eluted out to be subsequently sequenced.

2.6. Restriction enzyme digests

Restriction digestion was used to confirm changes found in sequence data. Gene Work, a computer programme was used to identify restriction sites in both the wild type sequence and the mutated sequence. Restriction mixtures (10 µl PCR product, 1 µl of desired enzyme and buffer) were incubated at 37°C in a water bath for 3-4 hours. Products were compared with undigested PCR product and digested unaffected patient controls run on agarose gel.

2.7. Fractionation of DNA by electrophoresis

Electrophoresis is the most commonly used method for separating DNA. This method of fractionation separates molecules in an electric field according to their charge, size and shape. If a mixture of linear DNA molecules is placed in a well cut into an agarose gel, and the well is placed near the cation (-ve) of an electric field, the molecules will move through the gel to the anode (+ve), at speed dependent on their size (molecular weight). The bands can be visualised by staining the DNA with ethidium bromide, which causes the DNA to fluoresce in ultraviolet (UV) light.

2.7.1. Agarose Gel Electrophoresis

This was the method of choice for fractionation of DNA fragments between 0.5 - 25 kb and was used routinely for visualising PCR generated products. The appropriate agarose concentrations used for separating DNA fragments of various sizes are listed below.

Agarose (%)	Range Of Resolution Of Linear DNA (kb)
0.3	5.0 –60
0.6	1.0 –20
1.0	0.5-10
1.5	0.2-6.0
2.0	0.1-2.0
3.0	0.05-<0.1

Table 2.1. Agarose concentrations for separating DNA fragments.

The gel was prepared by melting electrophoresis grade agarose (Biorad) in 1 x TAE in a microwave oven. The mixture was heated at a high temperature until the agarose had completely dissolved in the solution. The mixture was cooled under cold running tap water and a drop of 10 mg/ml ethidium bromide was added using a pipette, swirled, and poured into a sealed casting electrophoresis tray containing a 10ul well-forming comb and left to polymerise for 30 minutes.

After PCR amplification had completed, samples were prepared with an appropriate amount of 10x loading dye. For example, 10 µl of each PCR product was placed in a mixing plate and 5 µl of Ficoll orange G dye was added in each of the samples. An appropriate DNA molecular weight size marker was always included. The most commonly used markers to size DNA were ϕX174/HaeIII or 1kb ladder (see below). Once the gel had polymerised, the samples were loaded with the molecular weight marker in the wells. The gel was then placed within an electrophoresis tank containing sufficient 1X TAE buffer. Electrophoresis was carried out at 80 volts for 1 hour or until the required resolution was achieved (rule of thumb: 5 V/cm gel). Gels were photographed on a UV transilluminator using polaroid MP4 camera with a orange/red filter and Kodak plus-X film.

ϕX174/haeIII	*λ/HindIII*	*1 kb ladder*
1.358	23.130	10,000
1.078	9.416	8,000
0.872	6.682	6,000
0.602	4.361	5.000
0.310	2.322	4,000
0.281/0.271	2.027	3,000
0.234	0.564	2,500
0.194	0.125	2,000
0.118		1,500
0.072		1,000
		750
		500
		250

Table 2.2. Size of DNA markers (Kb) used for DNA electrophoresis and heteroduplex analysis.

2.8. Mutation Detection

2.8.1. Heteroduplex Analysis

The PCR products formed of normal and mutant alleles are separated from other homo-allelic products using non-denaturing gel electrophoresis. Resolution is based upon detecting conformational differences that occur in the DNA molecule as a result of the mutant allele annealing with the wild type allele, which can be a result of insertions, deletions or base pair mismatches. Heteroduplex DNA is generated by standard PCR amplification and amplification occurs between homologous DNA segments as well as across the segment containing the mutant allele. By denaturing these samples and allowing them to cool to room temperature, double stranded DNA is formed between the identical complementary strands (homoduplexes) and also between strands of the 2 different amplified segments (heteroduplexes). The heteroduplexes migrate at a slower rate on acrylamide than the corresponding homoduplexes. Overall the technique is around 80 -85% effective in picking up mutations.

2.8.2. Procedure for Heteroduplex Analysis

MDE gels were used routinely used for the detection of heteroduplexes. The size range of PCR products in this study ranged from 100 - 300 bp in size

(within the optimal size range for resolution). The electrophoresis apparatus (using 40-cm X 20-cm glass plates) was vertically assembled according to manufacturer's instructions (J.T.Baker, USA) and clamped within the casting tray.

A typical 100 ml gel solution was prepared by addition of 50 ml MDE gel solution; (Sequagel^{TM}) for mutation detection containing acrylamide, 15g of urea which acts as a denaturing agent, 40 ml distilled water, and 10x TBE (6ml). The gel was polymerised with 450 µl 10 % Ammonium persulphate (APS) and 45 µl TEMED. Prior to addition of APS and TEMED, 2 ml was removed to which 30 µl and 12 µl TEMED added, and gently poured between the plates to form a seal at the base. On setting, the remaining gel was mixed and poured between the plates avoiding the formation of air bubbles. On insertion of an appropriate comb, the gel was allowed to polymerise for an hour following which the comb was removed and 1X TBE made-up buffer added to the upper and lower buffer reservoirs. On rinsing the wells with syringe and needle, 10 µl samples containing 100-200 ng PCR product in 5 µl sucrose loading buffer (containing xylene cyanol and bromophenol blue) was loaded into each well. A DNA marker was used in each lane. Electrophoresis was allowed to occur for ~ 16 hours at 180 volts with the xylene cyanol and bromophenol blue being indicator of resolution as they run at 180 - 200 bp and 50 - 60 bp respectively. The gel were run at 150-180 volts for 14-18 hours, and then stained with ethidium bromide and photographed under UV illumination.

Factors affecting the resolution of heteroduplex DNA in MDE gel include DNA size (100 to 400 base pairs is optimal, up to 900 base pairs is possible), position of mismatch within DNA segment (central mismatch optimal) and type and context of mismatch.

2.8.3. Mutation detection by Denaturing High-Performance Liquid Chromatography (DHPLC)

PCR products were analysed using the WAVE^{R} nucleic acid fragment analysis system (Trangenomic). The buffers used for DHPLC consist of Buffer A (0.1 M triethylammonium acetate (TEAA) and buffer B (0.1 M TEAA with 25% acetonitrile). DNA fragment elution profiles were captured online and visually displayed using the Transgenomic WAVEMAKER^{TM} software. Chromatograms were compared with those of normal controls to detect samples with altered elution profiles.

2.8.4. Minisequencing

This method is used to characterize known mutations or single nucleotide polymorphisms (SNPs). Briefly, this protocol relies on the extension of a primer that ends exactly one base short of a polymorphic site with fluorescent-labelled dideoxynucleotides, which are complementarily incorporated according to the sequence of the amplified target. The minisequencing reactions were carried out in a total volume of 6 ul containing 2.5 ul of SNaPshot Multiplex Ready Reaction reagent (Applied Biosystems, Foster City, CA, USA), 2.5 ul of primer mixture (5 pmol of each primer, see Table 1) and 1 ul of purified PCR product. The SNaPshot Multiplex Ready Reaction

reagent set contains AmpliTaq DNA polymerase, fluorescently labelled dideoxynucloetide triphosphates, and reaction buffer. The minisequencing was performed as follows: 25 cycles at 96 ° C for 10 seconds, 50 ° C for 5 seconds, and 60 ° C for 30 seconds. After extension, the samples were treated with shrimp alkaline phosphatase according to the manufacturer's protocol. The samples were then electrophoresed on an automated ABI PRISM 3100 Genetic Analyzer (Applied Biosystems) and analysed with the ABI GeneScan 3.1 analysis software. Size determinations were performed using the GeneScan-120 LIZ size calibrator using the GeneScan 3.1 software.

2.9. DNA Sequencing

Prior to DNA sequencing, PCR products underwent the following procedures:

1. PCR purification
2. Cycle-sequencing
3. Ethanol precipitation

2.9.1. Purification of PCR products by QIAquick™ spin columns

Double stranded DNA products from PCR products were purified using QIAquick™ PCR purification kit. Fragments ranging from 100 bp to 10 kb were purified using QIAquick spin columns in a microcentrifuge. Firstly, 5 volumes of buffer PB were added to 1 volume of the PCR reaction mix. The provided QIAquick spin columns were placed in 2 ml collection tubes and the PCR product samples were applied to the QIAquick column and centrifuged at 13,000 rpm for 1 minute. The supernatant flow-through was discarded after the first spin, before the QIAquick columns were placed back into the same tube. To wash the fragments from PCR, 0.75 ml of buffer PE was added to the columns and centrifuged for 1 minute. Again the flow-through was discarded

and the QIAquick columns were placed back in the same tube. The columns were centrifuged for an additional minute at maximum speed. After the spin, the QIAquick columns were placed in a clean 1.5-ml microcentrifuge tube. To elute the DNA, 50 ul of buffer EB (10 mM Tris.CL, pH 8.5) was added to the centre of the QIAquick membrane and the columns were centrifuged for 1 minute.

2.9.2. Cycle sequencing

Cycle sequencing was performed on a Perkin-Elmer Cetus 2400 machine. Cycle sequencing reactions consisted of 10 µl volumes containing 4µl ABI reaction mix (from ABI PRISM^{TM} Big Dye terminator cycle sequencing kit with Amplitaq^{R} DNA polymerase FS), 0.5 µl of 3.2 µM sequencing primer, 3.0 µl of sterile distilled water and 2.5 µl of purified DNA. The temperature cycling profiles consisted of 26 cycles of denaturation at 96°C for 10 seconds, annealing at 50°C for 5 minutes and extension at 60°C for 4 minutes. Upon completion, the resultant products were transferred to sterile 0.5 ml eppendorf tubes and purified to remove unincorporated fluorescent dyes by ethanol precipitation.

2.9.3. Ethanol precipitation

After completion of the sequencing reaction, the extension products were brought to a final volume of 20µl with deionized water, and transferred to 1.5 ml microcentrifuge tubes. An additional 16 µl of deionized water and 64 µl of non-denatured 95% ethanol at room temperature was added to the extension product. The tubes were then capped and vortexed briefly. The tubes were then left at room temperature for 15 minutes to precipitate the extension

products. After 15 minutes, the capped tubes were placed in the microcentrifuge and the orientation of the tubes were marked. The samples were then spun at 13.000 rpm for 20 minutes. Upon completion, the ethanol was pipetted out carefully and discarded. The pellet of DNA was washed with 250µl of 70% ethanol, capped and briefly vortexed. Samples were centrifuged again for a further 10 minutes at the same speed. The supernatant was carefully aspirated with a pipette and discarded. The DNA pellet was either air dried or placed to dry in a vacuum centrifuge for approximately 10-15 minutes. The samples were either stored in this state at -20°C or resuspended in ABI loading buffer and sequenced on the ABI automated sequencer.

2.9.4. Direct Sequencing

Sequencing procedures generally use primers or dideoxynuleotides to which are attached *flourophores* (chemical groups capable to fluorescing). During electrophoresis, a monitor detects and records the fluorescence signal as the DNA passes through a fixed point in the gel. The use of different fluorophores in the four base-specific reactions means that, unlike conventional DNA sequencing, only one lane on the denaturing gel per reaction is required, as unique fluorescent labels can distinguish individual labelled nucleotides. The output of the DNA sequence when printed can be seen as a profile of the different coloured fluorophores, but the information is simultaneously stored electronically and can be seen immediately in a computer analysis file.

The resultant pellet after ethanol precipitation was suspended in a 5 µl of ABI loading buffer and the sample was denatured in a PCR block at 95°C for 5

minutes before loading onto the denaturing acrylamide gel. The sequencing gel consists of 40 ml Sequagel 6 (National Diagnostics), 10 ml Sequagel buffer reagent and 0.04 g Ammonium persulphate (APS). Automated sequencing was performed on an ABI 373A DNA sequencer (Perkin Elmer). The gel was generally run for 8-12 hours overnight. The data was converted to a text file and an analysis file on a computer.

Many samples were also loaded onto 96-well microtitre plates and sequenced on the ABI 3100 Genetic Analyser. This more automated process involves samples being electrophoretically injected into fused silica capillaries that are filled with polymer. DNA fragments migrate towards the other end of the capillaries, with the shorter fragments moving faster than the longer fragments. The fragments enter a detection cell and move through a laser beam in turn. The laser light causes excitation of the fluorescent dye on the fragments, which is captured by a CCD camera and converted into electronic information., which is in turn transferred to the computer workstation for processing by the 3100 Data Collection Software. The data is presented in 2 formats, text and a sequence analysis file. The latter type of file incorporates the electropherogram data and constitutes the original sequence data.

The important differences between the gel and capillary electrophoresis systems used in these instruments are the structure of the fragment-sieving component, the method of sample loading and overall speed and throughput of sample analysis.

2.10. Linkage Analysis

2.10.1. Polyacrylamide Gel Electrophoresis

This was used for genetic linkage analysis. A non-denaturing 6% polyacrylamide sequencing gel was used in 50cm x 38 cm gel plates (Sequi-GenII, Bio-Rad Laboratories Ltd., Hertfordshire), washed with warm water immediately prior to use. The inner inspects of the glass plates were cleaned with ethanol and the back of the plate coated with a siliconising agent-dichlorodimethylsilane (Sigmacote, Sigma Chemicals, Co., St. Louis), to ensure that during separation of the rig the gel adhered to the front glass plate. The apparatus were assembled with 0.75 mm spacers, clamped together in a 40 cm casting tray.

A 6% non-denaturing polyacrylamide sequencing gel was made up as follows:

40 ml acrylamide (Protogel:EC890, National Diagnostics)

20 ml 10 x TBE

140 ml dH_2O

700 µl 25% ammonium per sulphate

70 µl tetramethylethylenediamine (TEMED, Sigma Chemicals Co., St. Louis)

The above solution was then syringed using a 120 ml volume syringe from the base of the rig in a slow manner to prevent air bubbles. Soon afterwards a 64 well comb was inserted into place and the gel was left to set for approximately 30 minutes.

The set polyacrylamide gel was placed vertically and fixed in a continuous electrophoresis tank. The tank and buffer reservoir of the sequencing rig were filled with 1.5 litres of 1 x TBE buffer and pre-run for 30 minutes at 110 watts to pre-heat the gel to 55^0C. Then the comb was removed and the wells were flushed clean.

Once set and pre-run, samples were loaded. Microsatellite PCR samples containing 3 μl of 15% ficoll loading dye were then loaded onto the pre-warmed 6% non-denaturing polyacrylamide gel. Electrophoresis was then performed out at a constant power of 100 watts for an appropriate length of time to achieve maximum resolution in the size required; approximately 2-5 hours for microsatellites depending upon the expected allele sizes. Product size recognition was aided by the use of ladders. Upon completion of electrophoresis, the gel was then cut and stained with ethidium bromide and photographed with UV illumination using polaroid MP4 camera with a orange/red filter and Kodak plus-X film.

2.10.2. Automated Genotyping

PCR reactions were carried out for each marker individually in a 5 ul reaction volume, containing 25 ng DNA, 15 mM Tris-HCL, 50 mM KCl, 2.5 mM MgCl2, 250 uM each dNTP, 1.25 pmol primer (fluorescently labelled) and 0.25U Taq polymerase. Reactions were performed on a Perkin Elmer 9600 thermocycler with a standard thermocycling profile for all markers. This

consisted of an initial denaturation for 12 minutes immediately followed by 10 cycles at 95°C for 15 seconds, 55'C for 15 seconds and 72'C for 30 seconds and then by 20 cycles of 89'C for 15 seconds, 55'C for 15 seconds and 72'C for 30 seconds with a single final extension step for 72'C for 10 minutes. PCR products for selected sets of markers were pooled, diluted and denatured in formamide and size-fractionated using an ABI 3100 Genetic Analyser. PCR products were automatically sized by the ABI 3100 *Data Collection Software* version 10.1 program using ROX-500 (Applied Biosystems) as the size standard, and scored using the *GeneMapper* version 2.0 program.

A total genome scan was undertaken utilizing markers from version 2.0 of the ABI MD-10 (Applied Biosystems). These allow approximately 10 cM resolution of the human genome and consist of fluorescently labelled PCR primer pairs for highly polymorphic dinucleotide-repeat microsatellite markers chosen from the Genethon human linkage map. Subsequently, and where appropriate, markers from the HD-5 Linkage Mapping set which allow 5 cM resolution of the genome were used. Most of the initial total genome scan was carried out using facilities at the Medical Research Council's Human Genome Mapping Project Resource Centre (HGMP-RC). This unit offers a number of services to aid researchers in genetic analysis, and the facilities available may be also used by the client themselves to carry out the work. More than half the markers were genotyped by staff at HGMP-RC. Other markers were genotyped at the Institute of Ophthalmology.

2.10.3. Linkage LOD score calculation

Pedigree data was collated and checked using the software programme Cyrillic 2.1.3 (Cherwell Scientific Publishing Limited, Oxford), and the Pedcheck program (O'Connell and Weeks, 1998). Two point LOD scores were calculated using the program MLINK of the LINKAGE package (version 5.1) via the HGMP Genetic Linkage User Environment (GLUE: www.hgmp.co.uk). A fully penetrant dominant model with a disease frequency of 0.0001 (1 in 10,000) was assumed. Marker allele frequencies were assumed to occur at equal frequencies since population allele frequencies were not available.

When a significant positive Lod score for a marker was obtained, haplotype reconstruction using genotype information from the markers surrounding this positive marker(s) was carried out. Haplotypes were compiled by assuming minimal number of cross-overs and by forming haplotypes from different starting points within the pedigree to achieve a 'best fit.' This enabled examination of the segregation of the disease haplotype in the family and allowed identification of any cross-overs that might serve to limit the defined disease interval.

2.11. Computational analysis

The analysis of nucleic acid sequences *in silico* was essential to this research. ENSEMBL was used extensively for identifying genes within genetic

intervals, contig assessment and Single Nucleotide Polymorphism (SNP) analysis. Additional web-based programs included the NCBI homepage for BLAST (Basic Alignment Search Tool) and the generation of nucleotide sequences.

The Marshfield map was used extensively in order to estimate genetic distances between microsatellite markers. A web-based nomenclature system was also used for describing sequence variants. The following online databases were used:

Online Mendelian Inheritance in Man	http://www3.ncbi.nlm.nih.gov/Omim/
Human Genome Mapping Project	http://www.hgmp.mrc.ac.uk/
National Centre for Biological Information	http://www.ncbi.nlm.nih.gov/
NCBI-UniGene	http://www.ncbi.nlm.nih.gov/UniGene/
The Genome Database	http://gdbwww.gdb.org/
Genbank	http://www.ncbi.nlm.nih.gov/Genbank
European Cell Culture collection	http://www.ecacc.org.uk/
Whitehead Institute for Genome Research	http://www-genome.wi.mit.edu/
ENSEMBL	http://www.ensembl.org/
Human Gene Mutation Database	http://uwcm.ac.uk/uwcm/mg/hgmd0.html
SWISS-PROT	http://www.expasy.ch/sprot/sprottop.html
SNP database	http://www.ncbi.nlm.nih.gov/SNP/
Primer 3	http://www-genome.wi.mit.edu/cgi-in/primer/primer3_www.cgi
Marshfield	http://research.marshfieldclinic.org/
Glue analysis	http://www.hgmp.mrc.ac.uk/
Nomenclature for sequence variants	http://archive.uwcm.ac.uk/uwcm/mg/

2.12. Buffers and reagents

Buffers

♦ TAE (Tris acetate EDTA)	♦ TBE (Tris borate EDTA)
4 mM Tris acetate	1 M Trizna Base
0.1 mM EDTA	0.83 M Boric Acid
pH 8	10 mM EDTA

♦ **Ficoll Loading Dye for Agarose Gels**

30% (v/v) Ficoll 400.

0.25% (w/v) Bromophenol blue

0.25% (w/v) Xylene cyanol FF

1% (v/v) Tris-EDTA

♦ **Heteroduplex loading dye (stock)**

40 g sucrose

250 mg orange G

250 mg xylene cyanol

250 mg bromophenol blue

100 ml sterile distilled water

♦ **ABI loading buffer**

5:1 (v/v) formamide

50 mM EDTA with 50mg/ml dextran blue

♦ **PCR buffer (10x)**

NH4 buffer

500 mM KCl

50 mM $MgCl_2$.

Solutions for Human Genomic DNA Isolation

♦ **Reagent A (5 x lysis buffer)**

320 mM sucrose

10 mM Tris HCl (pH 7.5)

5 mM MgCl2 (adjust to pH 8.0 with NaOH)

autoclaved and 1% (v/v) Triton X-100 added.

♦ **Reagent B**

400 mM Tris-HCl (pH7.5)

60 mM EDTA

150 mM NaCl (adjusted to pH 8.0 with 5 mM NaOH)

CHAPTER 3

INVESTIGATING THE ASSOCIATION BETWEEN PRIMARY OPEN ANGLE GLAUCOMA AND THE *OPA1* GENE

3.1. Introduction

Glaucoma is characterised by progressive loss of optic nerve axons and visual field damage. The majority of glaucoma in Caucasian and Afro-Caribbean populations is of the primary open angle glaucoma (POAG) type, where elevated intraocular pressure (IOP) is a major feature. Normal tension glaucoma (NTG) is an important subtype of POAG, in which the IOPs are consistently within the statistically normal population range, and accounts for approximately a third (range 20% and 50%) of all POAG cases. As the IOP is normal when measured and patients often have good central vision, NTG is under-diagnosed and the condition presents late.

Autosomal dominant optic atrophy (ADOA) is another condition that is characterised by progressive optic nerve damage. This optic neuropathy is attributable to primary degeneration of retinal ganglion cells followed by ascending atrophy of the optic nerve (Johnston *et al.*, 1979; Kjer *et al.*, 1983). Loci for ADOA have been mapped to chromosome 3q28-qter (Eiberg *et al.*, 1994; Jonasdottir *et al.*, 1997) and 18q12.2-q12.3 (Kerrison *et al.*, 1999), and recently, the *OPA1* gene (MIM 165500) was identified (Alexander *et al.*,

2000; Delettre *et al.*, 2000) and shown to be ubiquitously expressed, including in retinal ganglion cells and the optic nerve (Alexander *et al.*, 2000).

Since different mutations in the same gene may cause widely different phenotypes, as illustrated in glaucoma by *FOXC1*, *MYOC*, *PAX6* and *PITX2*, the similarities between glaucoma and ADOA (in terms of the cell type affected and the phenotype- Figure 3.1) made *OPA1* an excellent candidate to examine in glaucoma patients. It was hypothesised that NTG would be the most promising glaucoma subset to study due to the manifestation of optic neuropathy in the absence of raised IOP.

3.2. Aim

To investigate whether an association existed between *OPA1* and NTG.

Figure 3.1: Genomic structure of the OPA1 gene. Exons are numbered in boxes.

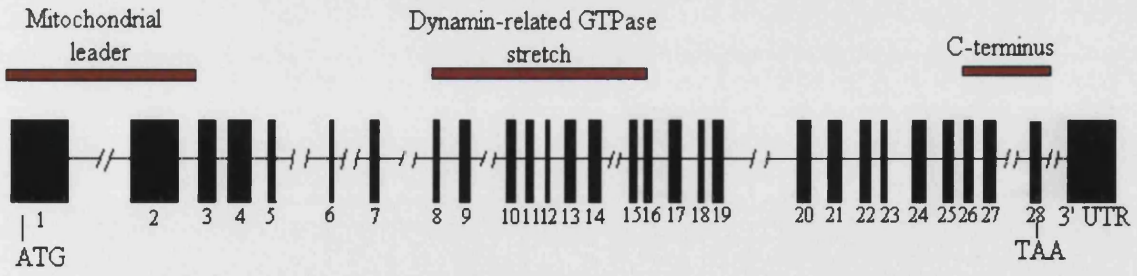

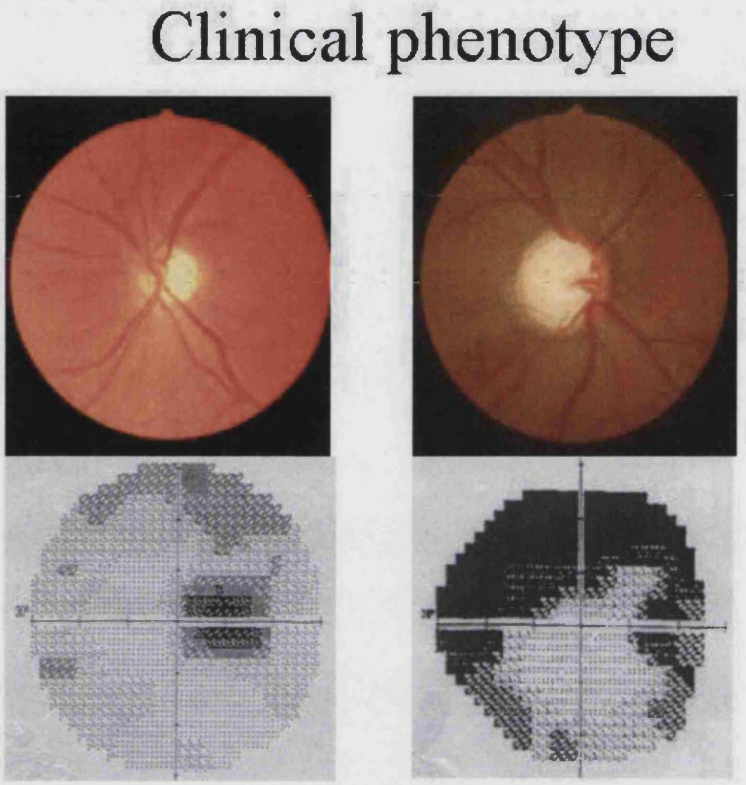

(a) (b)

Figure 3.2. Similarities in the phenotype between NTG and DOA.

(a) Top**:** Left eye of an individual affected with DOA showing pallor of the optic disc especially over the temporal half of the disc.

Bottom: Right visual field of a patient with ADOA showing a superior centrocaecal scotoma.

(b) Top: A markedly cupped optic disc of a patient with NTG

Bottom: Visual field of a patient with NTG showing a superior hemifield arcuate defect.

3.3. Methods

3.3.1. Study subjects

All cases and control subjects were from the greater London area. Written informed consent was obtained from all participants, and the study had the approval of the Hospital's ethics committee and was performed in accordance with the Helsinki Declaration [as last revised in Edinburgh in October, 2000). NTG cases were collected from a cohort of unrelated Caucasian NTG patients who attended a tertiary referral NTG clinic at Moorfields Eye Hospital, London, and were defined by the following strict criteria (Kamal and Hitchings, 1998) (Section 2.2.2.): the presence of typical glaucomatous optic neuropathy with compatible visual field loss; mean IOP without treatment that was consistently equal to or less than 21 mm Hg on diurnal testing, open drainage angles on gonioscopy, and absence of a secondary cause for glaucomatous optic neuropathy such as a previously raised IOP following trauma, a period of steroid administration or uveitis. Patients also did not have evidence of high myopia or congenital abnormality, and had no other cause for their visual loss.

Control DNA samples were obtained from unrelated Caucasian individuals randomly recruited from spouses and friends of probands participating in various genetic studies at Moorfields Eye Hospital.

3.3.2. Screening for mutations in the *OPA1* gene

Genomic DNA, extracted from venous blood using the Nucleon II extraction kit (Scotlab Inc., Shelton, CT, USA), was subjected to 35 cycles of PCR amplification using oligonucleotide primers (Pesch *et al.*, 2001, Table 3.1) in 50 ul reaction volumes (20 ng genomic DNA, 10 pmol of each primer, 200 mM dNTPs, 1.5 mM MgCl and 2 units of Taq DNA Polymerase (Promega, Madison, USA)). Amplified exons were analyzed by heteroduplex gel electrophoresis on MDE Flowgen gels run at 180 V for 14-18 hours on

Hoeffer 600S apparatus. PCR products that demonstrated a heteroduplex pattern were purified with QIAquick columns (Qiagen, UK) and then sequenced bidirectionally with fluorescent dideoxynucleotides (PE Biosystems, Foster City, USA) on an ABI 373 automated sequencer (Applied Biosystems, Foster City, CA, USA) using standard conditions. Exons found to be altered in NTG subjects (exons 8, 10, 17 and 20) were subsequently examined for variations in 100 population controls by the same methodology.

Genotype frequencies among cases and controls, or for different polymorphisms, were tested for significant differences using either standard χ^2 analysis or Fisher's exact test, depending upon cell counts. Differences between odds ratios were tested for statistical significance using a Breslow-Day test as implemented in the FREQ procedure of version 8.02 of the SAS software package (SAS Institute, Cary NC).

Table 3.1. *OPA1* primers used in mutation analysis.

Exon	Forward primer (5'→3')	Reverse primer (5'→3')
1	ACT TCC TGG GTC ATT CCT GG	TCT GGG AAT TCT CCA ACT GC
2	TGC TCT TTT AAT GCC ATT TCC	CAT CCA ATT GTA TTC CAC TAC ACA A
3	AAT TTT TCT TTA CAT GTT TAT TTG GC	TTT CTC TTT CCT CGA GAT GAC C
4	TTT TGT AGT GGT TGT CAT GAG G	AAA AAT GTC CTG TTT TTC ATT GG
5	TGG AGA ATG TAA AGG GCT GC	TCT TTC AAG ACT ACC TAC ATG AAC AA
6	AAA AAT TTA ACT TGC TGT ACA TTC TG	CAC CTT CCA AAT TTT GCT CTG
7	ACT ATT TGA TAA CCA TCT TTT GC	CAG CTC CTT AGA AAC TGG TAC TGA
8	CCG TTT TAG TTT TTA CGA TGA AGA	TTT TTG CTA GTT GGC AAG TTC A
9	AGA GCA GCA TTA CAA ATA GGT TTT	CAG GTT TCC CTG AAG CAG TT
10 + 11	CTG TCT AGA CCA CAT ACG GGC	CCA TAA AAC GTC ACT GAA ATG AA
12 + 13	AAA TTC TTG ACA AAT TCC CCC	CGA AGA GAA GGC AAA AAT GC
14	TTG CTA TAA TGT AGA CAC AGG GG	TAT CAC AGC TGA GCT TTT ACA
15 + 16	AGC ATT ATT TTG CTT TCT AAA TTG T	TGA AAA CAG TTC AAT TTA AGC TAC TC
17	CTG TTA GCA AGC ACA TTC GC	TAT GGA TGC CAA AGA TTG CC
18	ACA TCT GGA AAG AAG GAG GG	CCC ACT AAA TTA CAG GAA TAC ACG
19	CAG CCT AGT CAA AAA CCT CCC	CAA GGC AAC AAT AAA TCA CTG C
20	TCT AAA ATT CAC AGC TCC TAC TCC	TGA CTG GTG CGA TTT ACA GG
21	TTT GGC TTG AGC TCG TGT TA	CCT ATG AAA AAG TAT CAA TTT GAG AAG
22	TTT TTC CAT ATT TAC TAA GCT GTC AA	GAC TCC TTC ACC ACT GTG AAC TC
23	TTT TTC CTT TAT TTC AAC TGC C	TGG TCT AGA GCC ACA AAA AGG
24	TTG AGA CTG TTT TTC AAG CAC C	CAC GTG ACA AAA GTC AAA TTA AGC
25	TTT TTG TAC AAC TTC TCA GTG TGG	TTT CCC CAG ATG ATC AAA GG
26	ATG CTG AAT TTC ATG GCT CC	TGG GAA GTA TTT TGG CAT CC
27	TTC ATT TAT AAA AAC GAT GCT CC	GAT TAC AAG CGT GAG CCA CC
28	CCT CCT GAT TTG TGA TAC CTT TG	CAA GCA GGA TGT AAA TGA AGC A

3.4. Results

3.4.1. Sequence variants identified in the *OPA1* gene

Of the 83 NTG patients in the first cohort, 65 (78%) were females. Overall, 50 instances of 6 different sequence variations were identified in *OPA1* in the first cohort of NTG patients (summarized in Table 3.2). All variations found were synonymous nucleotide changes, with none resulting in an altered amino acid. The most frequent sequence alterations detected were located in intron 8 (intervening sequence [IVS] 8) with two particular single nucleotide polymorphisms (SNPs) identified: +32 T/C and +4 C/T (positions in base pairs (bp) relative to beginning of IVS 8).

To test for association of the overall genetic variation in IVS 8 with disease, the frequency distribution of the combined genotypes of the two SNPs in the NTG group was compared to that in population controls by using a 2 x 4 χ^2 test with the CLUMP program. The genetic variation in IVS 8 was found to be associated with disease (χ^2=13.92, p= 0.002). Nearly 20% of NTG subjects carry the double heterozygote in IVS 8 corresponding to +4 C/T together with +32 T/C, compared to only 3% of controls (Table 3.2). We tested this genotype to see if it could underlie the overall association previously obtained, then corrected for multiple comparisons of the 4 genotypes detected. The 17% difference in frequencies was indeed found to be significant (χ^2 =12.91, p=0.002) showing that an association exists between +4 C/T, +32 T/C in IVS 8 and NTG.

Table 3.2. Sequence variations detected in first cohort of patients and controls.

Exon and nucleotide change	NTG panel (n=83) (%) (95% CI)	Controls (n=100) (%) (95% CI)	P-value	Odds Ratio (95%CI)
8: IVS 8 +32 T→C	20 (24.1%) (14.5-33.5%)	25 (25%) (15.5-34.5)	0.89	0.95 (0.5-1.9)
8: IVS 8 +4 C→T	10 (12.0%) (4.0-18.0%)	11 (11%) (4.0-18.0%)	0.83	1.1 (0.4-2.8)
8: IVS 8 +4 C→T; +32 T→C	16 (19.3%) (11.0-29.0)	3 (3%) (0-6.5%)	<0.001	7.7 (2.1-27.5)
10: IVS10 +77 A→C	2 (2%) (0-5.0%)	0 (0%) (0-3.0%)	*	N/A
17: 1609A→C	1 (1%) (0-3.5%)	4 (4%) (0-8.5%)	*	N/A
20: 1894A→G	1 (1%) (0-3.5%)	1 (1%) (0-3.0%)	*	N/A

* frequencies too small for evaluation

3.4.2. Confirming the association between NTG with Intron 8 *OPA1* polymorphisms

In order to determine whether the initial findings could be replicated, a separately ascertained second cohort of Caucasian NTG subjects (n=80) and controls (n=86) was analyzed by bidirectional sequencing (Figure 3.2), for variations in intervening sequence (IVS) 8 found to be more prevalent in the first cohort of NTG cases.

In the second cohort of 80 NTG patients and 86 controls, genetic variation in IVS8 was again found to be associated with disease (χ^2=11.49, p= 0.008). Twenty percent of these NTG subjects are double heterozygotes with +4 C/T and +32 T/C in IVS 8, compared to 4.7% in controls (Table 3.3). After correcting for multiple testing for 4 genotypes, this difference was significant (χ^2 =9.21, p=0.01), confirming that an association existed between this variant and disease. The genotype frequencies found in the second cohort of patients were in fact markedly similar to that obtained in the first cohort. Statistical comparison of the controls from each cohort showed that their genotype frequency distributions are not significantly different (χ^2 =2.5, p=0.48) and the same holds for the patient groups from each panel (χ^2 =0.6, p=0.89). Therefore, these samples appear to have been drawn from the same population and may be pooled. Finally, the genotype frequency distribution of the pooled patient group was compared to that of the pooled control group. The difference in frequency distribution was found to be highly significant (χ^2 =24.87, p= $1x10^{-5}$). The association of the IVS 8 +4 C/T, +32 T/C genotype with disease was then tested and found to be very strongly associated with the occurrence of NTG in the pooled sample (χ^2 =22.04, p= $8x10^{-6}$ after correcting for testing four genotypes). Although the frequency of female patients is significantly larger than that of male patients when compared to controls in the pooled sample, stratification by gender showed that the association is maintained in both sexes. This indicates that the association of the IVS 8 +4 C/T, +32 T/C genotype with disease is still valid.

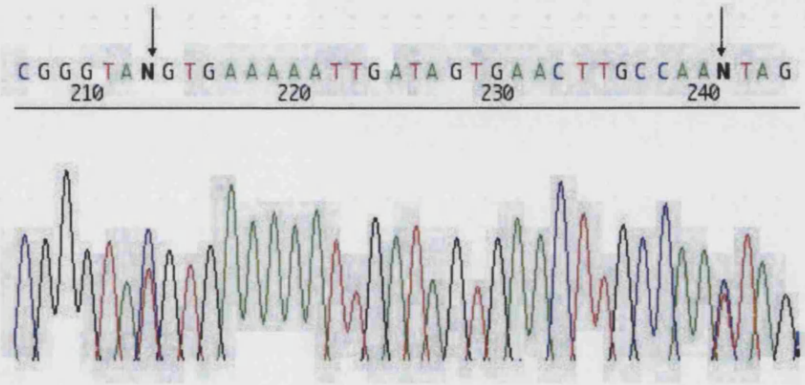

Figure 3.3. Electropherogram section showing SNPs at IVS 8 +4 C/T (left arrow) and IVS 8 +32 T/C (right arrow).

Table 3.3. Genotypes in intron 8: comparison of the 2 cohorts of patients.

GENOTYPE		*FIRST COHORT*		*SECOND COHORT*	
IVS8 +4	IVS8 +32	NTG Patients (n=83)	Controls (n=100)	NTG Patients (n=80)	Controls (n=86)
C/C	T/C	20 (24.1%)	25 (25%)	23 (28.8%)	27 (31.4%)
C/T	T/T	10 (12%)	11 (11%)	8 (10%)	5 (5.8%)
C/T	T/C	16 (19.3%)	3 (3%)	16 (20%)	4 (4.7%)
C/C or T/T	C/C or T/T	37* (44.6%)	61* (61%)	33 (41.3%)	50 (58.1%)
Combined genotype association with disease		χ^2=13.92, p=0.0019		χ^2=11.49, p=0.0079	
C/T-T/C genotype association with disease		χ^2=12.91, p=0.002		χ^2= 9.21, p=0.013	

*Only Cohort 1 subjects with heteroduplexes were sequenced, so it was not possible to ascertain the genotype of homozygotes.

The IVS 8 SNPs from patient and control samples of cohort 2 were sequenced and found to be in Hardy-Weinberg equilibrium (χ^2 = 0.83, df=1, p < 0.5 and χ^2 = 0.025, df=1, p<0.9 respectively), demonstrating that the alleles in these 2 samples appear to be behaving like normal Mendelian traits in a randomly mating population.

Finally, the allele frequencies at the two common IVS8 SNPs were compared to that of controls by applying the χ^2 test using CLUMP. The frequency of the T allele at IVS8 +4 was found to be significantly associated with disease (χ^2=10.66, p=0.002), but this did not apply to alleles at IVS8+32 (χ^2=0.003, p=1.0). The T allele at IVS8+4 confers a relative risk of 3.5 (95% CI: 1.4-8.8) and when considered with the IVS8 +32 site, the relative risk is increased to 6.2 (95% CI: 2.7-14.6).

3.4.3. Matching of groups

To confirm that affected and control populations were matched, the frequencies of 2 SNPs in 2 other genes unrelated to glaucoma were assessed in the affected and control populations. The first SNP was 261C/A in the *Tyrp-1* (Tyrosine related protein-1) gene located on chromosome 9p23, and the second SNP was IVS7 +46T/C in the *BIGH3* (transforming growth factor) gene on chromosome 5q31.

The first SNP, 261C/A in the *Tyrp-1* gene was found in 7.5% of the affected panel and 9% in controls (χ^2=0.09, p=0.76) (See Figure 3.3) and the second SNP, IVS7 +46T/C in the *BIGH3* gene was found in 94.5% and 92% respectively (χ^2=0.27, p=0.60). This confirmed that affected and control populations were matched and that there was no skew in the population polymorphisms.

3.4.4. Effect on splicing: RT-PCR

The SNP IVS8+4 C/T is adjacent to the splice donor site of Intron 8. In order to establish if there was any molecular consequence at the RNA level such as an effect on splicing, RT-PCR was performed in an affected NTG patient compared to an unaffected control.

Leukocytes were isolated from whole blood by density-gradient centrifugation (Ficoll-Paque) according to the manufacturer's instructions (Amersham Pharmacia Biotech, Little Chalfont, UK) and total RNA extracted (Trizol reagent; Invitrogen Life Technologies, Groningen, The Netherlands). Oligo(dT)-primed total leukocyte RNA was reverse transcribed into single-stranded cDNA using Ready-To-Go You-Prime First-Strand Beads (Amersham Pharmacia Biotech) and used to amplify cDNA segments encompassing the 2 SNPs IVS8+4 C/T and +32 T/C (cDNA PCR primers exon c6F: 5'-TGTCAGACAAAGAGAAAATTGAC-3', and exon c10R: 5'-ATCAAACTCCCGAGAACTATC-3'). RT-PCR products were separated on a 2% low-melting-point agarose gel.

The RT-PCR amplification products are shown in Figure 3.4. There was no difference in the product size between the affected patient and control, indicating that the SNPs did not exert a major effect on splicing or result in alternate splicing.

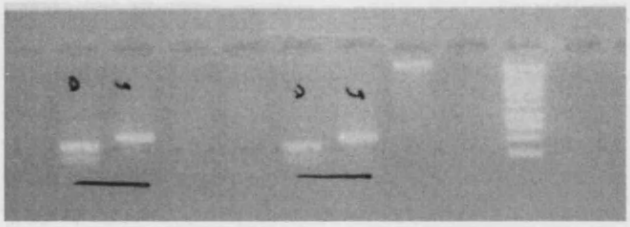

Figure 3.4. Restriction digest of the SNP, 261C/A in the *Tyrp-1* gene. The 2 bands indicate digested and 1 band undigested product.

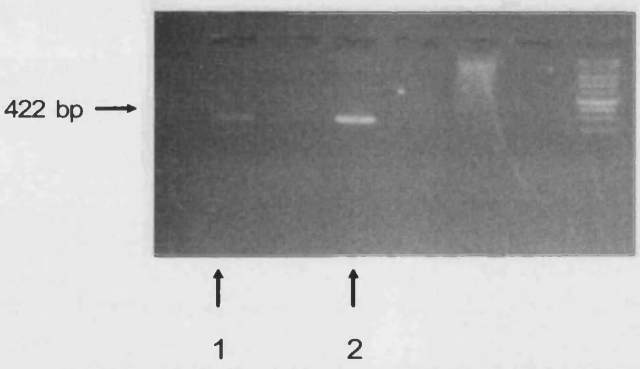

Figure 3.5. RT-PCR products of an affected subject with the *OPA1* SNPs, IVS 8 +4 C/T and +32 T/C (Lane 1) and an unaffected individual (Lane 2) showing identical product size (422 bp).

3.4.5. Determining the phase of the 2 SNPs and haplotype construction

In order to determine to phase of the alleles of the 2 SNPs, PCR products were cloned into pGEM®-T Easy (Promega) plasmid vector system (as detailed in section 2.5). Colony PCR was performed to identify those plasmids that contained the inserts. Colonies containing ligated plasmid were selected and cultured overnight in 5 ml of LB culture medium with antibiotic selection. DNA was extracted from the cultured cells by use of a QIAGEN DNA Miniprep kit according to the manufacturer's protocol (Section 2.3.1.). Inserts were subsequently sequenced using pTAG vector primers and sequenced on an ABI 3100 Genetic Analyzer (Section 2.9.4.).

A total of 7 affected subjects with the 2 SNPs IVS 8 +4 C/T, +32 T/C were used for the above experiment. The haplotype of 5 subjects showed a C-T, T-C trans phase, while in 2 subjects, there was a C-C, T-T cis phase. The results showed that there was no consistent haplotype for individuals with the *OPA1* SNPs IVS 8 +4 C/T, +32 T/C and that the alleles were not in linkage disequilibrium with each other.

3.4.6. Comparison between high-tension glaucoma (HTG) and NTG

Although NTG is a major subtype of glaucoma, the majority of glaucoma cases in Caucasian and Afro-Caribbean populations are of the high-tension glaucoma (HTG) type with elevated intraocular pressure (IOP). In order to investigate whether a similar association existed between *OPA1* and HTG, a cohort of 90 unselected HTG patients was screened for the at-risk *OPA1*

genotype IVS8+4C/T;+32T/C by PCR amplification and bi-directional sequencing. Of the 90 HTG subjects, five subjects (5.6%; 95% CI 1.8-12.5) were found to carry the genotype, IVS8+4C/T;+32T/C on the *OPA1* gene, this frequency being similar to 7/186 (3.8%; 95% CI 1.5-7.6) in control subjects (χ^2=0.47, p=0.49, OR 1.5 [95% CI 0.5 to 4.9]). In contrast, 32/163 (19.6%; 95% CI 13.8-26.6) NTG subjects carried this genotype (χ^2= 9.2, p= 0.002, OR 4.1 [95% CI 1.6 to 11.1]). This is summarised in Table 3.4.

Table 3.4. Comparison between NTG, HTG and controls.

Comparison between NTG, HTG and controls	NTG **(n=163)**	HTG (n=90)	Controls (n=186)
Frequency of the genotype IVS8+4C/T;+32T/C (%) (95% CI)	32 (19.6%) (13.8-26.6)	5 (5.6%) (1.8-12.5)	7 (3.8%) (1.5-7.6)
χ^2 test Odds Ratio (95%CI)	χ^2= 9.2, p= 0.002 OR 4.1 (1.6 to 11.1)		
χ^2 test Odds Ratio (95%CI)		χ^2=0.47, p=0.49 OR 1.5 (0.5 to 4.9)	

The genotypes at IVS8+4 and IVS8+32 for NTG subjects and controls of Cohort 2 and HTG subjects are summarized in Table 3.5.

Table 3.5. Genotypes at IVS8+4 and IVS8+32 for NTG subjects and controls of Cohort 2 and HTG subjects.

Genotype				
IVS8+4	**IVS8+32**	**Cohort 2 NTG subjects (n=80)**	**Cohort 2 control subjects (n=86)**	**HTG subjects (n=90)**
CT	TC	16	4	5
CC	TC	23	27	19
CT	TT	8	5	11
CC	TT	17	26	34
CC	CC	16	24	21

3.5. Discussion

Our results provide the first evidence of an association between *OPA1* and NTG, a major form of glaucoma. Two *OPA1* SNPs, IVS 8 +4 C/T and +32 T/C have been previously identified in other studies (Pesch *et al.*, 2001; Toomes *et al.*, 2001) but these polymorphisms were now found to be associated with the NTG disease phenotype, and may be a marker for disease association. This is an interesting observation as polymorphisms are associated with a variety of diseases including Alzheimer's dementia (Bullido *et al.*, 1998), age-related macular degeneration (Allikmets, 2000), diabetes mellitus (Horikawa *et al.*, 2000) and schizophrenia (Wei and Hemmings, 2000). The results highlight the possibility that the SNPs are in linkage disequilibrium with another sequence variation nearby that may be have a major role in NTG, possibly in non-coding regions of *OPA1*.

Although this study demonstrates an association between *OPA1* and NTG, it

does not prove causation and the molecular mechanisms mediating NTG remain unknown. A number of possibilities can be proposed to explain the observed association, including subtle alterations in RNA splicing, protein function or the gene product of *OPA1*, which is thought to affect mitochondrial integrity (Alexander *et al.*, 2000). Alternatively, indirect mechanisms may be present, possibly by conferring susceptibility in patients to other factor(s) that mediate NTG. The CT genotype at IVS8+4, identified as being associated with disease, is adjacent to the splice donor site, but RT-PCR failed to show any major effect on splicing. However, minor effects on splicing cannot be excluded. It appears that IVS8+32, although not a strong risk factor for NTG on its own, may serve to modify the disease risk conferred by IVS8+4 T. Compound heterozygotes comprised of such SNPs have been reported in a range of conditions and species including the level of alcohol dehydrogenase expression in *Drosophila melanogaster* (Stam and Laurie, 1996) as well as in complex human diseases such as diabetes mellitus (Horikawa *et al.*, 2000) and schizophrenia (Sivagnanansundaram *et al.*, 2000).

One limitation of this study was the use of a single screening modality to detect mutations, namely heteroduplex analysis. This may not be expected to identify all disease-causing sequence variations, and may be prone to masking of sequence alterations by mutations or SNPs (Orban *et al.*, 2000). Another limitation was that while the NTG population studied was well-characterized using strict diagnostic criteria and is considered typical of NTG patients, control individuals were not subjected to identical clinical examination. Although we could not be certain that controls subjects did not have NTG, it is unlikely that this would have significantly altered the results.

The results also indicate that unlike NTG, the *OPA1* genotype IVS 8 +4 C/T, +32 T/C is not significantly associated with high-tension primary open angle glaucoma. Some reports have noted optic disc and visual field differences between NTG and HTG patients, implying different mechanisms of optic nerve damage (Kamal and Hitchings, 1998). The results raise the possibility of genetic differences between the conditions, as the *OPA1* genotype IVS8+4C/T;32T/C, associated with NTG, was not found to be associated with HTG. Such genetic differences may be particularly significant in NTG, possibly by affecting susceptibility to factor(s) that mediate glaucoma. The possibility that some HTG patients may harbour other mutations or sequence changes in *OPA1* cannot be excluded.

CHAPTER 4

THE PHENOTYPE OF NORMAL TENSION GLAUCOMA PATIENTS WITH AND WITHOUT *OPA1* POLYMORPHISMS

4.1. Introduction

Work described in Chapter 3 found that approximately a fifth of NTG subjects were found to carry two single nucleotide polymorphisms (SNPs) on intervening sequence (IVS) 8 of the *OPA1* gene (IVS 8 +4 C/T; +32 T/C), compared to only 3.7% of control subjects (χ^2 =22.04, p= 0.00001), indicating that the genotype IVS 8 +4 C/T, +32 T/C was strongly associated with the occurrence of disease, and may be a marker for disease association. This association raises the possibility that there exist different subgroups of NTG, distinguished by genetic variations in *OPA1*.

4.2. Aim

The aim of this study was to compare the presenting clinical features of NTG patients with and without such polymorphisms in order to identify any possible phenotypic differences that may occur in such patients.

4.3. Methods

4.3.1. Ascertainment of subjects

A retrospective analysis was performed of 108 well-characterized NTG patients who had been genotyped for *OPA1* variations, and who had previously undergone automated perimetry and Heidelberg retina tomography (HRT). The diagnostic criteria for NTG have been described in Section 2.2.2. There were 25 NTG patients (Group 1) with, and 83 NTG patients (Group 2) without the at-risk *OPA1* genotype IVS 8 +4 C/T; +32 T/C. Only one eye from each patient was included. For bilateral cases, the right eye was analysed. The study had the approval of the Moorfields Eye Hospital ethics committee and was performed in accordance with the Helsinki Declaration.

Differences between groups were sought in a wide range of structural, psychophysical and demographic factors. These included gender, age at diagnosis, family history of glaucoma, history of ischaemic risk factors and vasospasm, laterality of glaucoma, presenting and highest diurnal intraocular pressure (IOP), initial cup-disc (CD) ratio, baseline visual field global indices (Section 2.1.5.), and optic disc parameters as measured by HRT (Section 2.1.6.). For a subgroup of patients with at least 5 years of follow-up and 10 visual field tests, pointwise linear regression analysis (PROGRESSOR for Windows software) was applied to the visual field series. Progression was defined as the presence of a significant regression slope ($p<0.01$) showing 1 dB per year or more of sensitivity loss at the same test location with the

addition of two out of three successive field tests to the series starting with the first three.

4.3.2. Statistics

Statistical analysis was carried out using Statistical Package for Social Sciences version 9.0 (SPSS Inc, Chicago, Illinois). Parametric and non-parametric tests of significance were carried out where appropriate. Comparisons between groups were done with Mann-Whitney U tests for continuous variables that were not normally distributed. Chi-square analysis was used for comparison of proportions. Statistical significance was assumed at the $p < 5\%$ level.

4.4. Results

4.4.1. Demographics and history

There was no significant difference in the 2 groups with respect to demographic factors such as gender and age at diagnosis. There was also no significant difference with respect to family history of glaucoma, history of ischaemic risk factors, history of vasospasm or laterality of glaucoma (Table 4.1).

Table 4.1. Demographic features and systemic history of study subjects.

		Group 1 (n=25)	Group 2 (n=83)	P value
Sex	Male	8	21	0.51
	Female	17	62	
Age of onset	<60 years	11	31	0.67
	>60 years	14	52	
Family history of glaucoma	Positive	7	28	0.59
	Negative	18	55	
Ischaemic risk factors	Positive	12	33	0.46
	Negative	13	50	
Vasospasm	Positive	7	17	0.41
	Negative	18	67	
Laterality	Bilateral	19	65	0.81
	Unilateral	6	18	

4.4.2. Glaucoma status: IOP, visual field and optic disc

The comparison of IOP, CD ratio and visual field global indices, MD and CPSD in the 2 groups is summarized in Table 4.2. There was no significant difference found although the difference in mean highest diurnal IOP between the two groups approached significance ($p = 0.06$). The mean HRT parameters are summarized in Table 4.3. There were no differences in the mean values for any parameter analysed. The optic disc photograph and HRT of an NTG subject with the *OPA1* genotype IVS 8 +4 C/T; +32 T/C is shown in Figure 4.1 and 4.2.

Table 4.2. Presenting clinical features.

	Group 1 (n=25)	Group 2 (n=83)	P value
Mean presenting IOP (mmHg)	16.2 ± 1.8	17.0 ± 2.8	0.11
Mean highest diurnal IOP (mmHg)	17.9 ± 2.3	18.9 ± 2.6	0.06
Mean presenting cup disc ratio	0.75 ± 0.1	0.76 ± 0.1	0.93
Mean presenting MD (dB)	-8.7 ± 8.4	-8.0 ± 6.5	0.96
Mean presenting CPSD (dB)	8.5 ± 4.8	8.0 ± 4.3	0.60

IOP: intraocular pressure
MD: mean deviation
CPSD: corrected pattern standard deviation

Table 4.3. Presenting optic disc parameters, as measured by HRT.

	Group 1 (n=25)	Group 2 (n=83)	P value
Disc area (mm^2)	2.04 ± 0.41	2.11 ± 0.45	0.77
Global rim area (mm^2)	0.90 ± 0.31	0.89 ± 0.31	0.88
Temporal rim area (mm^2)	0.13 ± 0.07	0.14 ± 0.07	0.57
Temporal superior rim area (mm^2)	0.10 ± 0.04	0.10 ± 0.05	0.80
Temporal inferior rim area (mm^2)	0.10 ± 0.08	0.08 ± 0.06	0.36
Nasal rim area (mm^2)	0.29 ± 0.12	0.30 ± 0.11	0.49
Nasal superior rim area (mm^2)	0.13 ± 0.06	0.14 ± 0.05	0.63
Nasal inferior rim area (mm^2)	0.16 ± 0.06	0.13 ± 0.06	0.14

Figure 4.1. Right optic disc of a patient with the *OPA1* genotype IVS 8 +4 C/T; +32 T/C.

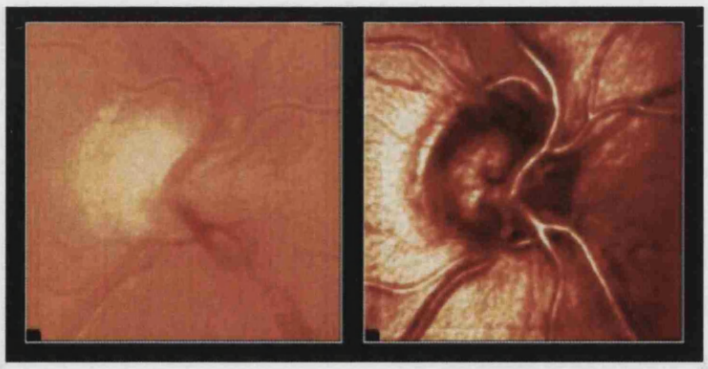

Figure 4.2. HRT scan of the right optic disc of the same patient.

4.4.3. Visual field progression

Comparing the visual fields of the subgroup of 88 subjects (18 from Group 1 and 70 from Group 2) who had at least 5 years of follow-up (with at least 10 visual field tests performed during this time) revealed no difference in the number of patients with progressing locations, the mean number of progressing locations per subject, the mean slope of the progressing locations or the mean slope for whole visual field (Table 4.4).

Table 4.4. Visual Field progression of subjects with at least 5 years of follow-up and at least 10 visual fields performed during this time.

	Sub-Group 1 (n=18)	Sub-Group 2 (n=70)	P value
Number of patients with progressing locations	16 (88.9%)	54 (77.1%)	0.98
Mean number of progressing locations per subject	7.89 ± 14.67	7.28 ± 7.77	0.46
Mean slope of progressing locations per year (dB/year)	-0.51 ± 0.91	-0.37 ± 0.56	0.91
Mean slope for whole visual field per year (dB/year)	-1.99 ± 1.62	-1.92 ± 1.13	0.39

4.5. Discussion

This study did not detect a significant difference in a range of phenotypic features in normal tension glaucoma patients with and without the *OPA1* polymorphisms IVS 8 +4 C/T; +32 T/C. This suggests that these specific genetic variations in *OPA1* do not underlie any major phenotypic diversity in NTG, although the possibility of more subtle phenotypic differences, such as variable rates of response to treatment cannot be excluded. The mean presenting IOP and the highest diurnal IOP appeared to be lower in NTG patients with the *OPA1* polymorphisms (almost reaching significance for the latter), which may indicate that the glaucoma in such patients is less IOP dependent. If this were to be the case, it would suggest that NTG patients have different IOP thresholds for glaucomatous damage to occur, and that those with *OPA1* polymorphisms may be at risk of glaucoma at lower IOP levels.

Polymorphisms are associated with a variety of other diseases including Alzheimer's dementia (Bullido *et al.*, 1998), age-related macular degeneration (Allikmets, 2000), diabetes mellitus (Horikawa *et al.*, 2000) and schizophrenia (Wei and Hemmings, 2000). Although intronic polymorphisms, of which *OPA1* (IVS 8 +4 C/T and +32 T/C) is an example, are associated with conditions like intracerebral haemorrhages and cerebral aneurysms (Takenaka *et al.*, 1999), little is known about how intronic polymorphisms influence disease phenotype. Possible mechanisms include regulation of transcription (Cruts *et al.*, 1996; Bailly *et al.*, 1996), effects on protein function or indirectly by conferring susceptibility in patients to other factor(s) that mediate disease. The biochemical mechanisms by which *OPA1* may influence NTG remain

obscure. The pathogenic characteristics of *OPA1* resemble those of Leber hereditary optic neuropathy, which results from a defect of the mitochondrion. Alexander et al hypothesized that mutations in the *OPA1* gene affect mitochondrial integrity, resulting in an impairment of energy supply (Alexander *et al.*, 2000). Occurring in the highly energy-demanding neurons of the optic nerve, notably the papillomacular bundle, this would presumably lead to damage of retinal ganglion cells and visual loss.

A variety of factors may contribute to the development of optic neuropathy in glaucoma. In the apparent absence of elevated IOP, which is the main risk factor identified for glaucoma, non-IOP related factors are advocated to predominate in eyes with NTG including abnormal blood flow (Drance *et al.*, 1973; Phelps *et al.*, 1985; Drance *et al.*, 1988), systemic hypotension (Hayreh *et al.*, 1994; Graham *et al.*, 1995; Meyer *et al.*, 1996) and an abnormal coagulability profile (Drance, 1972; Carter *et al.*, 1990; Hamard *et al.*, 1994; O'Brien *et al.*, 1997). A strong genetic component is likely to be significant in NTG (Bennett *et al.*, 1989; Stoilova *et al.*, 1996; Sarfarazi *et al.*, 1998; Rezaie *et al.*, 2002). It is hypothesized that several interacting genes contribute to the development of disease, with the putative role of each polymorphic sequence variation influenced by an individual's genetic and environmental background. However the number and identity of genes contributing to NTG has yet to be fully determined. Much remains to be learned about the phenotypic effects of specific genes and alleles in this condition.

CHAPTER 5

PREVALENCE OF *OPTINEURIN* SEQUENCE VARIANTS IN ADULT PRIMARY OPEN ANGLE GLAUCOMA

5.1. Introduction

The majority of primary open angle glaucoma (POAG) in Caucasian and Afro-Caribbean populations is of the high-tension glaucoma (HTG) type, with elevated intraocular pressure (IOP) being a major contributory factor for visual loss (Mason *et al.*, 1989, Sommer *et al.*, 1991; Klein *et al.*, 1992). Normal tension glaucoma (NTG) is another important subtype of POAG in which typical glaucomatous cupping of the optic nerve head and visual field loss are present, but IOPs are consistently within the statistically normal population range.

In 1997, *Myocilin* (*MYOC*, MIM 601652) was the first POAG gene to be characterized and found to be mutated in patients with juvenile and adult onset POAG (Stone *et al.*, 1997). Subsequent studies found that *MYOC* mutations account for fewer than 5% of cases of adult POAG (Stone *et al.*, 1997; Suzuki *et al.*, 1997; Alward *et al.*, 1998; Fingert *et al.*, 1999; Alward *et al.*, 2002). Recently, a second POAG gene, *Optineurin* (*OPTN*, MIM 602432) in the GLC1E interval on chromosome 10p was identified (Rezaie *et al.*, 2002), and variations in this gene were shown to predominantly result in NTG. The most

common *OPTN* mutation, $Glu^{50} \rightarrow$ Lys (E50K) was identified in 13.5% of families, 18% of whom had high IOP. A second *OPTN* variant, $Met^{98} \rightarrow$Lys (M98K) was identified in 13.6% of familial and sporadic POAG cases compared to 2.1% of controls, making it a significant risk-associated genetic factor for glaucoma. Such high prevalence levels suggest that the E50K/M98K variants may be more frequent than the Gln368Stop *MYOC* mutation, the most common mutation found in POAG, identified in 1.6% of unrelated glaucoma probands (Fingert *et al.*, 1999).

5.2. Aim

The purpose of this study was to determine the prevalence of these 2 *OPTN* sequence variants in a large cohort of unrelated British patients with adult-onset POAG in order to assess the feasibility of developing diagnostic testing for these variants in glaucoma subjects.

5.3. Methods

5.3.1. Ascertainment of patients

Written informed consent was obtained from all subjects and the study had been approved by the Moorfields Eye Hospital ethics committee and was performed in accordance with the Helsinki Declaration. The patients comprised an unselected cohort of 315 unrelated Caucasian individuals with adult onset POAG that included 186 women with ages ranging from 52 to 81 years. All were from the greater London area and were attending tertiary referral glaucoma clinics at Moorfields Eye Hospital. The diagnostic criteria and definitions have been described earlier in Section 2.2.2.

5.3.2. Molecular genetic studies

Genomic DNA, extracted from venous blood using the Nucleon II extraction kit (Scotlab Inc., Shelton, CT, USA), was subjected to 35 cycles of PCR amplification using oligonucleotide primers in 50 ul reaction volumes (20 ng genomic DNA, 10 pmol of each primer, 200 mM dNTPs, 1.5 mM MgCl and 2 units of Taq DNA Polymerase (Promega, Madison, USA)). To detect the E50K mutation, exon IV of the *OPTN* gene was amplified using the primers (5' CAGGTGACTTTTCCACAGGA3') and

(5'GATTTAGCATTTGGCAAGGC3'), and amplified exons purified with QuickStep columns (Edge Biosystems, Gaithersburg, MD, USA), then sequenced bidirectionally with fluorescent dideoxynucleotides (PE Biosystems, Foster City, USA) on an ABI 3100 automated sequencer (Applied Biosystems, Foster City, CA, USA) using standard conditions (as detailed in Section 2.9.4.). A section of the electropherogram showing the *OPTN* E50K mutation is shown in Figure 5.1.

To detect the M98K sequence variant, exon V of the *OPTN* gene was amplified using the primers (5' TCCACTTTCCTGGTGTGTGA3') and (5'CAGACCGATCCATTGTGATG 3'). The 273 base pair polymerase chain amplification product was then digested with 1.0 U of *Stu I* restriction enzyme (Promega, Corporation, Madison, WI, USA). The M98K nucleotide change resulted in the gain of the *Stu I* restriction site with the production of two fragments of 98 bp and 175 bp in size. For individuals heterozygous for this change, three bands were produced (the third band being the 273-bp fragment) (Figure 5.2).

5.3.3. Haplotype Analysis: Single nucleotide polymorphism (SNP) characterisation

In order to establish whether individuals with the E50K and M98K variants share a common ancestral haplotype or represent independent mutation events, 4 single nucleotide polymorphisms (SNPs) located within the *OPTN* gene were typed. The SNPs flanked E50K/M98K and were located within a 12 kb interval (Figure 5.3). There were 3 non-coding SNPs with the respective reference dbSNP (http://www.ncbi.nlm.nih.gov/entrez/query.fcgi?db=Snp) numbers (660592, 577910 and 545734) and 1 coding SNP (2234968).

The SNPs were characterized by minisequencing reactions. Briefly, this relies on extension of a primer that ends one base short of a polymorphic site, with fluorescent-labelled dideoxynucleotides, which are complementarily incorporated according to the sequence of the amplified target. The minisequencing reaction (5 ul of SNaPshot Multiplex Ready Reaction reagent [Applied Biosystems, Foster City, CA, USA], 5 pmol of each primer and 3 ul of purified PCR product) was performed as follows: 25 cycles at 96 degrees C for 10 seconds, 50 degrees C for 5 seconds, and 60 degrees C for 30 seconds.

E50K

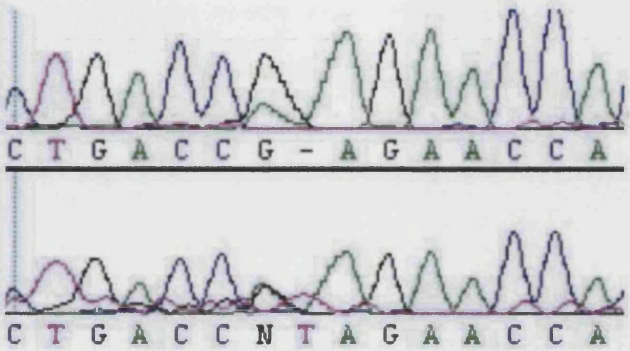

Figure 5.1. Section of the electropherogram showing the *OPTN* E50K mutation.

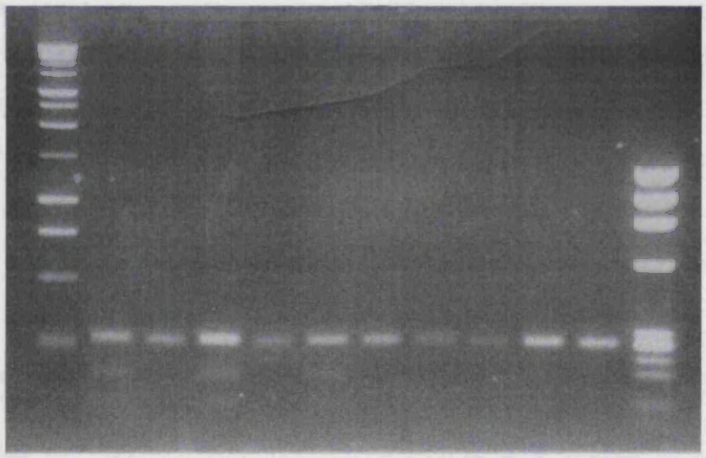

Figure 5.2. *Stu I* restriction enzyme digest: In the presence of the M98K nucleotide change, three bands were produced. Single band indicates undigested product.

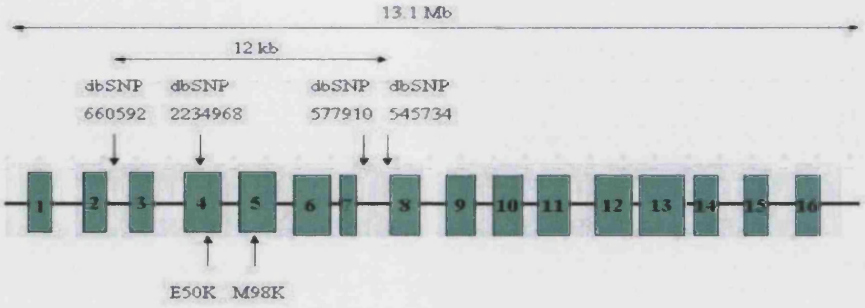

Figure 5.3. *Optineurin* gene: Position of SNPs genotyped in relation to E50K and M98 variants (not to scale). Exons are numbered in boxes.

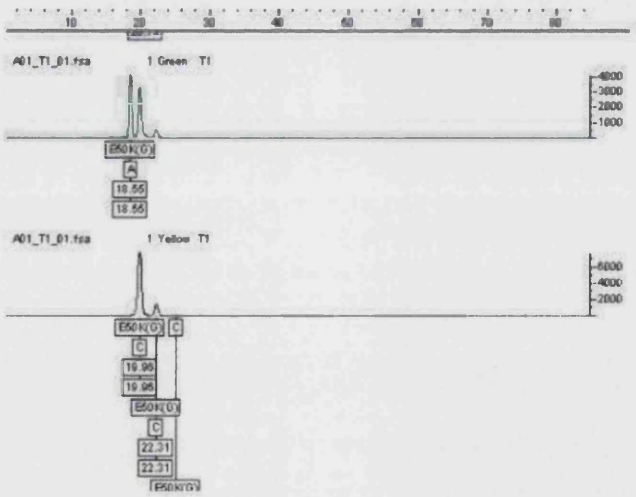

Figure 5.4. SNaPshot minisequencing reaction.

After extension, the samples were treated with shrimp alkaline phosphatase according to the manufacturer's protocol. The samples were electrophoresed on an automated ABI PRISM 3100 Genetic Analyzer and analysed with the ABI GeneScan 3.1 analysis software (Applied Biosystems) (Figure 5.4). Size determinations were performed using the GeneScan-120 LIZ size calibrator with the Genotyper Version 2 data collection software.

5.3.4. Statistical Analysis

Genotype frequencies among cases and controls were tested for significant differences using standard χ^2analysis. Differences between odds ratios were tested for statistical significance using a Breslow-Day test (version 8.02, SAS software package, SAS Institute, Cary, NC, USA).

5.4. Results

5.4.1. Prevalence of E50K and M98K

A total of 315 POAG subjects (consisting of 132 NTG and 183 HTG subjects) and 95 control subjects were examined. Overall the E50K change was found in 2 out of 315 POAG subjects (0.6%; 95% CI 0.08-2.3) and none out of 95 control subjects (χ^2= 0.61, p= 1.0). The M98K variant was found in 22 out of 315 POAG subjects (7.0%; 95% CI 4.4-10.4) and 3 out of 95 (3.2%; 95% CI 0.7-9.0) control subjects (χ^2= 1.87, p= 0.17). This is summarized in Table 5.1.

Table 5.1. Overall prevalence of E50K and M98K in glaucoma and control subjects.

Frequency (%) (95% CI)	**Glaucoma Subjects** (n=315)	**Controls** (n=95)	χ^2 test Odds Ratio (95%CI)
E50K	2 (0.6%) (0.08 – 2.3)	0 (0%) (0 – 3.8)	χ^2=0.606, p= 1.0 RR = 1.01 (0.998 to 1.02)
M98K	22 (7.0%) (4.4 – 10.4)	3 (3.2%) (0.7 – 9.0)	χ^2=1.87, p= 0.172 OR = 2.3 (0.67 to 7.9)

Looking at the subgroups (Table 5.2), the prevalence of the E50K change was 2/132 (1.5%; 95% CI 0.2-5.4) in NTG subjects and 0/183 (0%; 95% CI 0-2) in HTG subjects. The M98K variant was present in 14 /132 (10.6%, 95%CI 5.9 – 17.2) NTG subjects, compared to 8/183 (4.4%, 95%CI 1.9 – 8.4) HTG subjects (χ^2= 4.6, p= 0.03, OR=2.6 [95% CI 1.1 to 6.4]) and 3/95 (3.2%, 95%CI 0.7 – 9.0) control subjects (χ^2= 4.4, p= 0.04, OR= 3.6 [95% CI 1.02 to 13.0]). The difference in frequency of M98K between HTG and control subjects was not significant (χ^2= 0.17, p= 1.0, OR = 1.3 [95%CI 0.34 to 5.1]).

Table 5.2. Prevalence of E50K and M98K by subgroup.

	E50K	χ^2 test Odds Ratio (95%CI)	**M98K**	χ^2 test Odds Ratio (95%CI)
HTG (n=183)	0 (0%) (0 – 2.0)	χ^2=2.8, p=0.18 RR = 1.02 (0.99 to 1.04)	8 (4.4%) (1.9 – 8.4)	χ^2=4.6, p=0.03 OR =2.6 (1.1 to 6.4)
NTG **(n=132)**	2 (1.5%) (0.2 – 5.4)	χ^2=1.5, p= 0.51 RR = 1.02 (0.99 to 1.04)	14 (10.6%) (5.9 – 17.2)	χ^2=4.4, p=0.04 OR = 3.6 (1.02 to 13.0)
Controls (n=95)	0 (0%) (0 – 3.8)		3 (3.2%) (0.7 – 9.0)	

5.4.2. Haplotype

Haplotype analysis of a 12 Kb region within the *OPTN* gene revealed that no common haplotype between patients with either the E50K or M98K variants (Table 3).

Table 5.3. Haplotypes of subjects with E50K and M98K variants.

SNP	**Alleles segregating with E50K change**		**Alleles segregating with M98K change**		
660592	G/G	G/G	G/G	T/T	T/G
2234968	A/G	G/G	G/G	G/G	G/G
577910	G/G	A/A	G/G	A/A	A/A
545734	G/G	G/G	G/G	G/G	G/G

5.5. Discussion

Our data indicate that the E50K mutation is an infrequent cause of sporadic NTG accounting for 1.5% of cases, and it is not associated with HTG in the UK population. Based on these results, as only a small proportion of NTG subjects (95% CI 0.2-5.4%) would be expected to have the E50K change, diagnostic testing of sporadic NTG cases for E50K is not at present indicated in the UK population. Similarly pre-symptomatic screening in the general population would be expected to yield an exceedingly low detection rate, as an abnormal test result would be rare and a normal test result would be meaningless. Commercially available kits such as the OcuGene test (InSite Vision), which screen for *MYOC* variations, have also been found to have low sensitivity for detecting glaucoma-causing mutations (Alward *et al.*, 2002), and illustrate the current limitations of genetic testing in glaucoma.

Our results contrast with the findings of Rezaie and co-workers who identified E50K in 7 out of 52 POAG families (13.5%), most of whom had NTG (Rezaie *et al.*, 2002). The ten-fold higher prevalence of E50K mutations in familial compared to sporadic cases highlights the enrichment in inherited cases that is associated with a family history. Such a high difference in prevalence between familial and sporadic cases supports the introduction of targeted diagnostic testing in individuals with a family history of NTG, although not at present in sporadic cases. As the cost of screening for known mutations declines with the continuing rapid advances in mutation detection techniques, it seems likely

that the cost/benefit considerations of screening singleton NTG patients for common mutations such as E50K may become more favourable in the future.

The second sequence change studied, M98K, has previously been reported to be an attributable risk factor for POAG, present in 13.6% of both familial and sporadic POAG cases compared to 2.1% of controls (Rezaie *et al.*, 2002). However our study did not identify an overall difference in prevalence between POAG cases and controls, but that the M98K variant was associated specifically with NTG but not HTG. About 10% of NTG subjects were found to have this variant, compared to 4% of HTG and 3% of controls. The difference in results between the 2 studies may be attributable to the panel of patients in the earlier study consisting of predominantly NTG subjects (only 13% of the POAG subjects used in that comparison actually had IOP values above normal). The association of M98K with NTG but not HTG suggests genetic and/or allelic heterogeneity between these 2 phenotypes. Such genetic differences may imply different mechanisms of optic nerve damage, possibly by affecting susceptibility to factor(s) that mediate glaucoma.

In view of the high prevalence of M98K and that reported for E50K (Rezaie *et al.*, 2002), we investigated whether this was caused by a founder effect. Using intragenic SNPs spanning a 12 kb interval of the *OPTN* gene (Figure 1), we identified three different M98K and two E50K haplotypes, indicating that these sequence changes arose independently.

Our study was based at a tertiary referral centre, which raises the possibility of selection bias related to severity of disease, as subjects with more complex problems may be over-represented. We cannot exclude the possibility that

these POAG patients may harbour other mutations or sequence changes in *OPTN*. Complete sequencing of the *OPTN* gene may reveal further mutations, and other differences between these groups.

CHAPTER 6

THE PHENOTYPE OF PATIENTS WITH THE E50K MUTATION IN THE *OPTINEURIN* GENE

6.1. Introduction

A second gene for primary open angle glaucoma (POAG), *Optineurin* (*OPTN*, MIM 602432) in the GLC1E interval on chromosome 10p, was recently identified, and variations in this gene were shown to result predominantly in normal tension glaucoma (NTG), a major subtype of POAG in which IOPs are within the statistically normal population range (Rezaie *et al.*, 2002). The most common *OPTN* mutation, $Glu^{50} \rightarrow$ Lys (E50K) was found to be a significant cause of glaucoma identified in 13.5% of families studied.

Knowledge of the clinical behavior of specific mutations is helpful in disease management by providing patients with useful information regarding the course and prognosis of their disease. This is illustrated in POAG with the finding that the Ile477Asn and Tyr437His mutations in the *MYOC* gene are associated with a more severe form of glaucoma with an early age of onset, high IOP and resistance to medical treatment (Alward *et al.*, 1998; Richards *et al.*, 1998) while the Gln368STOP *MYOC* mutation causes a less virulent form of disease that is similar to usual cases of adult onset POAG (Alward *et al.*, 1998; Allingham *et al.*, 1998; Angius *et al.*, 2000; Craig *et al.*, 2001).

6.2. Aim

The aim of this study was to investigate the clinical features of subjects carrying the E50K *OPTN* mutation in order to determine if this mutation imparts a characteristic phenotype in glaucoma patients. The onset, severity and clinical course of these patients were then compared with a group of POAG patients without the E50K *OPTN* mutation.

6.3. Methods

6.3.1. Ascertainment of subjects

A retrospective analysis was performed of all patients attending glaucoma clinics at Moorfields Eye Hospital, London who were identified to have the E50K mutation in the *OPTN* gene. The study had the approval of the Moorfields Eye Hospital ethics committee and was performed in accordance with the Helsinki Declaration. These subjects had been previously identified in 2 separate studies; in the first study, families with glaucoma were investigated for OPTN mutations (Rezaie *et al.*, 2002), while the second study has been described in chapter 5.

The diagnostic criteria and definitions for POAG, NTG and HTG have been described earlier (Section 2.2.2.).

Patients' hospital records were reviewed and the following data collected: demographic characteristics including gender and age at diagnosis; family history of glaucoma; history of ischaemic risk factors such as hypertension, diabetes mellitus, ischaemic heart disease and smoking; history of vasospasm such as migraine and cold hands and feet; the presenting and highest recorded diurnal intraocular pressure (IOP) as measured by applanation tonometry; cup-disc (CD) ratio at presentation and interocular symmetry of glaucoma. The treatment administered including the type and number of medications, the history of filtering surgery was also recorded.

Subjects underwent static automated white-on-white threshold perimetry (program 24-2, model 640, Humphrey Instruments, Dublin, California, USA) (Section 2.1.5.). The first 2 visual field tests for all subjects were discarded from the analyses to allow for learning effects, and the subsequent first reliable visual field was used as the baseline. The visual fields of a subgroup of subjects who had at least 5 years of follow-up were also analyzed for progression. Pointwise linear regression analysis was applied to the field series of each of these subjects using PROGRESSOR for Windows software (Fitzke *et al.*, 1996). Progression was defined as the presence of a significant regression slope ($p<0.01$) showing 1 dB per year or more of sensitivity loss at the same test location with the addition of two out of three successive field tests to the series starting with the first three. The Heidelberg retina tomograph (HRT, Heidelberg Engineering, Heidelberg, Germany) was used to image the optic disc and the baseline optic disc parameters were analyzed (Section 2.1.6.).

6.3.2. Control Group

From 315 unrelated POAG subjects, a control group of subjects of the same glaucoma category (NTG or HTG) but without the *OPTN* E50K mutation was selected for comparison, using identical study methodology and data collection. Only those that had undergone repeated automated perimetry (with at least 5 years of follow-up), as well as imaging of the optic disc with the HRT were eligible for selection as controls.

6.3.3. Statistical analysis

Only one eye from each patient was analyzed. This was randomly selected in bilateral cases, and the affected eye in unilateral cases. Statistical analysis was carried out using Statistical Package for Social Sciences version 9.0 (SPSS Inc, Chicago, Illinois). Parametric and non-parametric tests of significance were carried out where appropriate. Comparisons between groups were done with Mann-Whitney U tests for continuous variables that were not normally distributed. Chi-square analysis was used for comparison of proportions. Statistical significance was assumed at the $p < 5\%$ level, and significant statistical associations were corrected by the Bonferroni test for multiple comparisons (20 comparisons made).

6.4. Results

6.4.1. Affected subjects

A total of 19 Caucasian subjects were found to have the E50K *OPTN* mutation. This comprised 13 POAG-affected subjects, all of whom were classified as having NTG, and 6 asymptomatic mutation carriers. Eight of the glaucoma subjects and 2 asymptomatic mutation carriers were from one family (Pedigree 1-Figure 6.1a), and 3 glaucoma subjects and 4 asymptomatic carriers were from another family (Pedigree 2-Figure 6.1b). Two unrelated sporadic NTG cases were also identified with the mutation. The glaucoma phenotype in both pedigrees segregated as an autosomal dominant condition, and every glaucoma-affected case in the families carried the E50K mutation. Two of the NTG subjects (individuals II:3 and III:9), with the E50K mutation from Pedigree 1 were excluded from the results as they were not examined at this hospital.

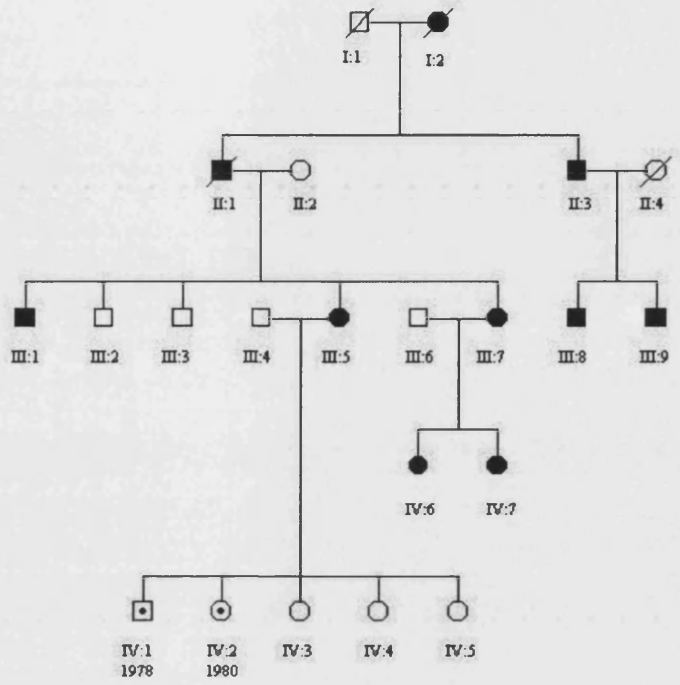

Figure 6.1. Pedigrees with the E50K *OPTN* mutation. **A**. Pedigree 1. **B.** Pedigree 2. Phenotype information is included on the pedigrees: Primary open angle glaucoma with E50K mutation (filled symbol), asymptomatic mutation carriers (dotted symbol), normal individuals without mutation (unfilled symbol). Individuals' pedigree number and year of birth (only for asymptomatic mutation carriers) is displayed.

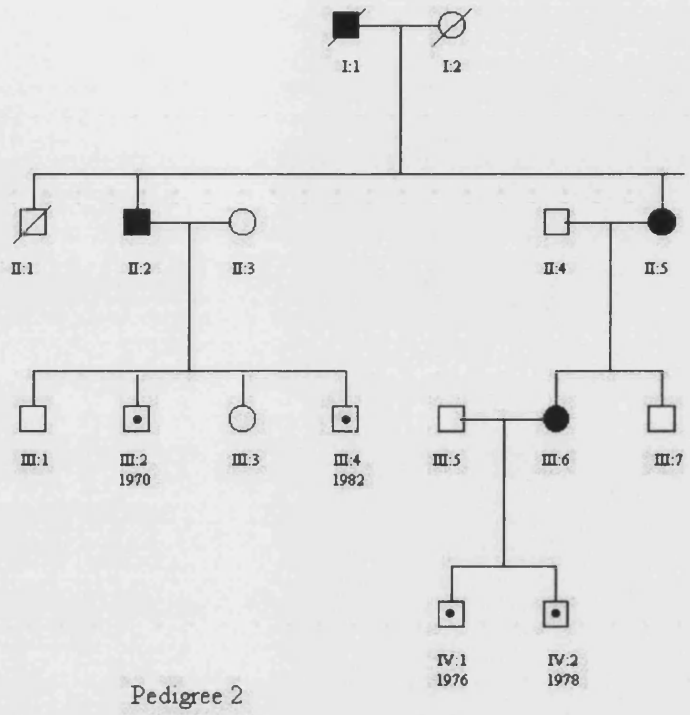

Figure 6.1B

6.4.2. Glaucoma status of affected subjects

Table 6.1 lists the age, sex, age at diagnosis, laterality, presenting CD ratio, presenting MD and CPSD, and surgical treatment of the 11 remaining NTG patients with the E50K *OPTN* mutation. These subjects had presenting and highest IOP (on diurnal testing) of 15.3 ± 3.0 mm Hg (mean ± SD) (range: 12-20 mm Hg) and 16.5 ± 2.5 mm Hg (range: 12-21 mm Hg) respectively. The mean corneal thickness (measured in 8 individuals) was 543 ± 10.6 (range:

533-558 um). The mean age at diagnosis was 40.8 ± 11.0 years (range 24-59 years) with only 2/11 subjects being diagnosed when older than 50 years. All but one subject had bilateral disease. This 56-year old had glaucomatous cupping (cup-disc ratio 0.8) and visual field defect in one eye, but the other eye had a cup-disc ratio of 0.6 with normal visual field and HRT tests. Interestingly, the glaucomatous eye had a few signs of pigment dispersion, such as deposition of iris pigment on the corneal endothelium, pigmentation of the trabecular meshwork and iris transillumination defects. However, IOP was consistently within the normal range.

Most of the subjects with NTG presented with relatively advanced disease: the mean CD ratio at the time of diagnosis was 0.86 ± 0.1, and all but one subject had CD ratio ≥ 0.8. Visual field status was also quite severe at the time of diagnosis: 8/11 subjects had presenting MD < -15.0 dB, and 7/11 subjects had presenting CPSD >10.0 dB. The visual field defects consisted of paracentral nerve fiber bundle type defects in all cases except for one subject who had a nasal step. One subject was already blind at the time of diagnosis with bilateral central visual fields of less than 20 degrees. Eight of the 11 glaucoma subjects had undergone filtering surgery for progressive visual field loss.

Table 6.1. Clinical features of glaucoma patients affected with the E50K *OPTN* mutation.

Pedigree	Patient Number	Sex	Age	Age at diagnosis	Presenting IOP	Highest IOP recorded on diurnal testing	Laterality	Presenting Cup-Disc ratio	Presenting MD (dB) on Humphrey perimetry	Presenting CPSD (dB) on Humphrey perimetry	Filtering Surgery
1	III:1	Male	56	50	18	18	Unilateral	0.8	-8.1	13.5	+
1	III:5	Female	53	38	12	14	Bilateral	0.9	-15.6	14.5	+
1	III:7	Female	64	52	12	14	Bilateral	0.9	-19.6	14.7	+
1	III:8	Male	60	43	17	19	Bilateral	0.7	-6.5	4.4	+
1	IV:6	Female	33	31	16	17	Bilateral	0.8	-1.2	2.0	Nil
1	IV:7	Female	31	24	13	12	Bilateral	0.9	-16.7	16.6	Nil
2	II:2	Male	63	42	15	15	Bilateral	0.95	-23.5	11.6	+
2	II:5	Female	82	45	18	16	Bilateral	0.9	-32.2	3.4	+
2	III:6	Female	60	25	14	18	Bilateral	0.9	-25.1	10.6	+
Sporadic	1	Female	59	40	12	18	Bilateral	0.8	-21.4	11.8	+
Sporadic	2	Female	71	59	20	21	Bilateral	0.9	-22.3	8.3	Nil
(Mean $\pm$ SD)			57.0 $\pm$ 15.0	40.8 $\pm$ 15	15.3 $\pm$ 3.0	16.5 $\pm$ 2.5		0.86 $\pm$ 0.1	-16.0 $\pm$ 9.5	9.7 $\pm$ 4.7	

6.4.3. Asymptomatic mutation carriers

Six E50K mutation-carrying individuals had normal optic discs and visual fields and as yet show no signs of glaucoma. Their ages ranged from 22 to 32 years (year of birth shown under subject symbols in Figure 1).

6.4.4. Comparison with control group

The clinical features of the 11 NTG subjects with the *OPTN* E50K mutation were compared with that of 87 NTG subjects without the mutation who had undergone repeated automated perimetry (with at least 5 years of follow-up) and imaging of the optic disc with HRT.

There was no significant difference in the 2 groups with respect to gender, history of ischaemic risk factors, history of vasospasm or laterality of glaucoma (Table 6.2). NTG patients with the *OPTN* E50K mutation however were younger when first diagnosed (p=0.0001, Bonferroni adjusted p=0.002). The comparison of IOP, CD ratio, visual field global indices, MD and CPSD and rate of surgery in the 2 groups is summarized in Table 6.3. NTG patients with the *OPTN* E50K mutation had lower mean peak IOP on diurnal testing (p=0.01 Bonferroni adjusted p=0.2), and lower mean presenting IOP, which approached significance (p =0.06). These patients also had worse initial cup-disc ratio (p=0.001 Bonferroni adjusted p=0.02) and higher mean presenting MD of initial visual fields (p=0.006 Bonferroni adjusted p=0.12). However there was no significant difference in the initial CPSD. Eight patients (72.7%) with the *OPTN* E50K mutation underwent filtering surgery for progression of visual field loss, compared to 22/87 (25.3%) patients without the mutation (p<0.0001 Bonferroni adjusted p=0.002).

The presenting optic disc parameters (as measured by HRT) are summarized in Table 6.4. There was no difference in the mean optic disc area. However optic discs of the 9 patients with the *OPTN* E50K mutation (HRT scans of 2 subjects were not interpretable due to poor quality of images) had smaller neuroretinal rim areas (global, nasal and temporal). The difference was more marked in the nasal neuroretinal rim, for both superior and inferior nasal rim areas. Comparing the visual fields of the subgroup of subjects who had at least 5 years of follow-up, all 8 subjects (100%) with the *OPTN* E50K mutation were found to have progressing locations, as compared to 71/87 (81.6%) of those without the mutation (p=0.0001 Bonferroni adjusted p=0.002). However, there was no difference in the mean number of progressing locations per subject, the mean slope of the progressing locations or the mean slope for whole visual field (Table 6.5).

Table 6.2. Comparison between NTG patients with and without the E50K *OPTN* mutation: Demographic features and systemic history.

		Group 1 (n=11)	Group 2 (n=87)	P value	Corrected p value
Sex	Male	3 (27.3%)	23 (26.4%)	1.0	
	Female	8 (72.7%)	64 (73.6%)		
Age at diagnosis	<60 years	11 (100%)	33 (37.9%)	0.0003	0.006
	≥60 years	0 (0%)	54 (62.1%)		
Mean age at diagnosis (years)		40.8 ± 11.0	61.7 ± 10.1	0.0001	0.002
Ischaemic risk factors	Positive	3 (27.3%)	33 (37.9)	0.74	
	Negative	8 (72.7%)	54 (62.1%)		
Vasospasm	Positive	4 (36.4%)	17 (19.5%)	0.24	
	Negative	7 (63.6%)	70 (80.5%)		
Laterality	Bilateral	10 (90.9%)	70 (80.5%)	0.68	
	Unilateral	1 (9.1%)	17 (19.5%)		

Table 6.3. Comparison of clinical features between NTG patients with and without the E50K *OPTN* mutation.

	Group 1 (n=11)	Group 2 (n=87)	P value	Corrected p value
Mean presenting IOP (mmHg)	15.3 ± 3.0	17.0 ± 2.7	0.06	
Mean highest diurnal IOP (mmHg)	16.5 ± 2.5	18.8 ± 2.6	0.01	0.2
Mean presenting cup disc ratio	0.86 ± 0.1	0.76 ± 0.1	0.001	0.02
Mean presenting MD (dB)	-16.0 ± 9.5	-7.8 ± 6.8	0.006	0.12
Mean presenting CPSD (dB)	9.7 ± 4.7	8.1 ± 4.4	0.25	

Table 6.4. Comparison between NTG patients with and without the E50K *OPTN* mutation: Presenting optic disc parameters, as measured by HRT.

	Group 1 (n=9)	Group 2 (n=87)	P value	Corrected p value
Disc area (mm^2)	1.95 ± 0.53	2.09 ± 0.47	0.26	
Global neuroretinal rim area (mm^2)	0.50 ± 0.28	0.89 ± 0.31	0.001	0.02
Temporal rim area (mm^2)	0.08 ± 0.04	0.13 ± 0.08	0.02	0.40
Temporal superior rim area (mm^2)	0.07 ± 0.05	0.10 ± 0.05	0.09	
Temporal inferior rim area (mm^2)	0.05 ± 0.03	0.08 ± 0.07	0.13	
Nasal rim area (mm^2)	0.14 ± 0.11	0.30 ± 0.11	0.0004	0.008
Nasal superior rim area (mm^2)	0.08 ± 0.04	0.14 ± 0.06	0.006	
Nasal inferior rim area (mm^2)	0.08 ± 0.06	0.14 ± 0.06	0.01	

Table 6.5. Comparison between NTG patients with and without the E50K *OPTN* mutation: Visual Field progression of subjects with at least 5 years of follow-up.

	Sub-Group 1 (n=8)	Sub-Group 2 (n=87)	P value
Number of patients with progressing locations	8 (100%)	71 (81.6%)	0.34
Mean number of progressing locations per subject	8.63 ± 8.68	7.95 ± 9.6	0.66
Mean slope of progressing locations per year (dB/year)	-2.02 ± 0.75	-1.97 ± 1.22	0.4498
Mean slope for whole visual field per year (dB/year)	-0.57 ± 0.36	-0.43 ± 0.66	0.15

6.4.5. Further Subgroup Analysis

In order to reduce bias due to having a younger age of diagnosis, those with E50K were compared with a subgroup of 13 control subjects all of whom were diagnosed below the age of 50 years (mean 45.2 $\pm$ 4.5 years, p=0.28). The global, temporal and nasal neuroretinal rim areas of those with E50K at the time of diagnosis were still smaller than in controls (0.91±0.21 mm^2 [p=0.005], 0.13±0.05 mm^2 [p=0.01] and 0.28±0.09 mm^2 [p=0.004] respectively), and there were a higher percentage of E50K patients with progressing locations in the visual fields (100% vs 76.9%, p=0.39). In another subgroup analysis, the 11 subjects with the E50K mutation were matched by initial MD with 22 subjects without E50K (2 subjects without the mutation matched with each subject with E50K) in order to correct for severity of glaucoma. Subjects with E50K were found to be diagnosed at a younger age ($p<0.0001$) but there was no significant difference for the other comparisons made.

6.5. Discussion

This study has shown that the E50K mutation in the *OPTN* gene causes a distinctive glaucoma phenotype with fairly homogeneous characteristics. All subjects with this mutation were found to develop normal tension glaucoma, with IOP usually in the mid teens (mean 15.3 mm Hg). The highest measured IOP on diurnal testing was found to be significantly lower (mean of 16.5 mm Hg) than a control group of other NTG subjects without the mutation. Although IOP is a major risk factor for visual damage in glaucoma (Anderson, 1989, Sommer *et al.*, 1991), the disease caused by E50K thus appears to be less IOP dependent than other forms of glaucoma. Interestingly, the corneal thickness in these individuals was in the normal range (533-558 um), which suggests that IOP was not influenced by an abnormal corneal thickness, and

contrasts with the finding of thinner corneas in other NTG subjects (Wolfs *et al.*, 1997; Morad *et al.*, 1998; Copt *et al.*, 1999; Lee *et al.*, 2002).

As patients are usually asymptomatic and the condition is difficult to diagnose, NTG patients often have marked irreversible visual damage at the time of diagnosis. Subjects with the E50K mutation were found to have a particularly severe glaucoma phenotype, as evidenced by the advanced optic disc cupping, neuroretinal rim thinning and visual field damage when first examined. The degree of glaucomatous damage at the time of diagnosis exceeded that of other NTG subjects without the mutation, despite some of the subjects in the 2 pedigrees being screened for glaucoma at a younger age due to a positive family history. These findings emphasize the importance of early detection of glaucoma in individuals at risk, such as those with a family member affected by this mutation. The glaucomatous disease process caused by E50K is also characterized by a progressive course with visual field progression detected in all subjects over 5 years (example shown in Figure 6.2a and b), as opposed to 81% of NTG controls, and 77% in a previously reported series of NTG subjects (Membrey *et al.*, 2000). Filtering surgery for visual field progression was performed in 70% of NTG cases with E50K, compared to only 25% in those without the mutation. The therapeutic implications of such an aggressive form of disease are that close monitoring and earlier intervention may be necessary in these subjects in order to minimize visual loss. Treatment should involve lowering of IOP by 20% or more, as this has been found to favorably alter the course of visual field progression in some NTG patients (Wilson *et al.*, 1991; Hitchings *et al.*, 1995; Bhandari *et al.*, 1997; Koseki *et al.*, 1997; Collaborative Normal-Tension Glaucoma Study Group 1998; Membrey *et al.*, 2001). However with starting IOPs in the 12-18 mm Hg range, this may be difficult to achieve except by means of filtering surgery, possibly augmented by antiproliferative drugs.

The E50K mutation seems to predispose individuals to an early age of onset in young adulthood (mean age at diagnosis 40 years), which is about 2 decades

earlier than most NTG subjects, and all subjects (including the 2 sporadic cases) were diagnosed before the age of 60. However, there is likely to be selection bias towards earlier diagnosis due to positive family history, resulting in individuals from the pedigrees being examined systematically for glaucoma at a young age. There was some variation in the age of onset of disease. There were 2 individuals with the mutation who were diagnosed in the 20s, while others were diagnosed in the 50s. It was not possible to ascertain the penetrance of E50K as most asymptomatic carriers were below the age of 30, and may still develop glaucoma by the time they reach the ages of the affected individuals in the study in the future.

The mechanism by which the E50K mutation causes disease is unknown. Vittitow and Borras studied the effect of glaucomatous insults on the expression of *OPTN* in human eyes maintained in organ culture (Vittitow and Borras, 2002). Sustained elevated IOP, TNF-alpha exposure, and prolonged dexamethasone treatment all significantly upregulated *OPTN* expression, suggesting a protective role of OPTN in the trabecular meshwork. The recurrent E50K mutation is located within a putative bZIP motif, conserved in the mouse, bovine, and macaque genomes, and it was hypothesized that visual loss and optic neuropathy may be the result of a dominant-negative effect (Rezaie *et al.*, 2002). It remains to be seen if there are other molecular mechanisms or modifying factors mediating NTG which interact with this gene.

Our study was based at a tertiary referral center, which raises the possibility of selection bias related to severity of disease, as subjects with more complex problems may be over-represented. It was not possible to ascertain the effect of treatment or surgery on disease progression due to the retrospective design of the study and the small sample size of subjects with E50K. The preponderance of familial cases among those with E50K may also have limited some of the comparisons made between the 2 groups, and it is possible that the severity of the phenotype may be related to other factor(s) common in

these families. The possibility that the control NTG subjects may harbor other mutations or sequence changes in *OPTN* cannot be excluded. It remains to be seen if other specific features distinguishing those with and without the mutation will become apparent, as may be the case when more patients are diagnosed with the mutation.

Figure 6.2. Visual fields of individual III:8 (Pedigree 1) showing progressive visual field damage. **A.** Initial visual field of left eye **B.** Visual field of left eye after 5 years.

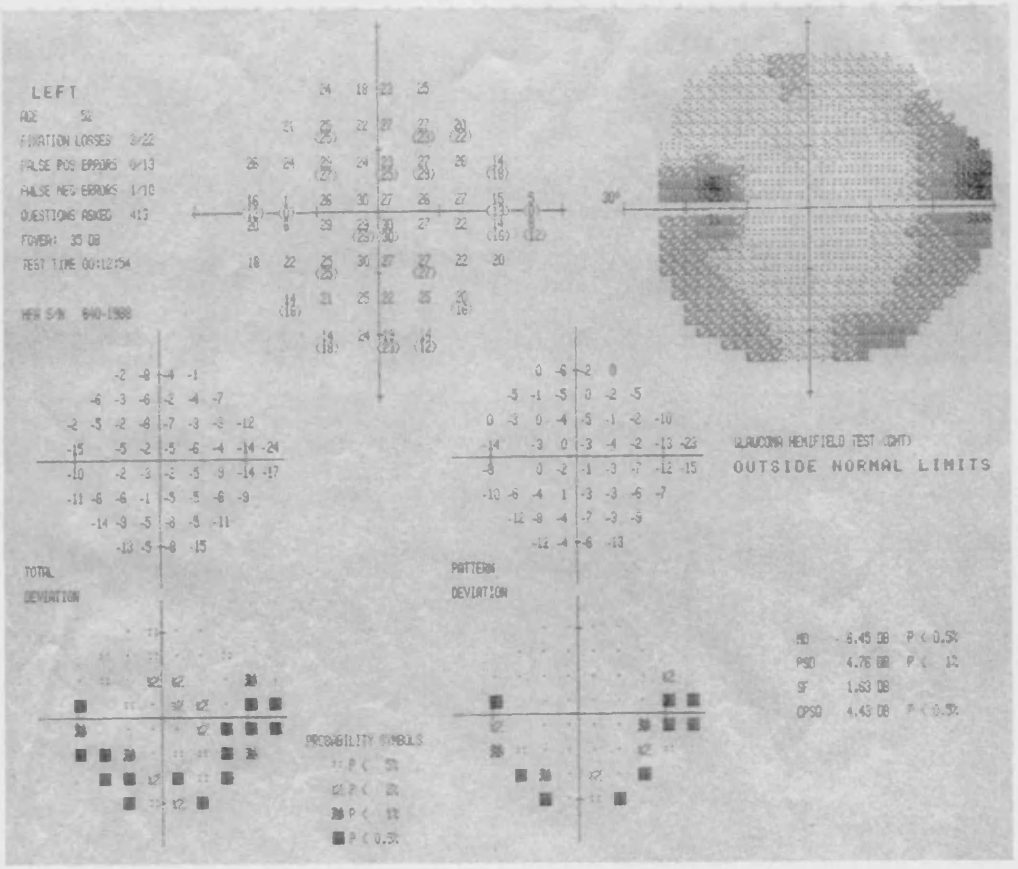

Figure 6.2A

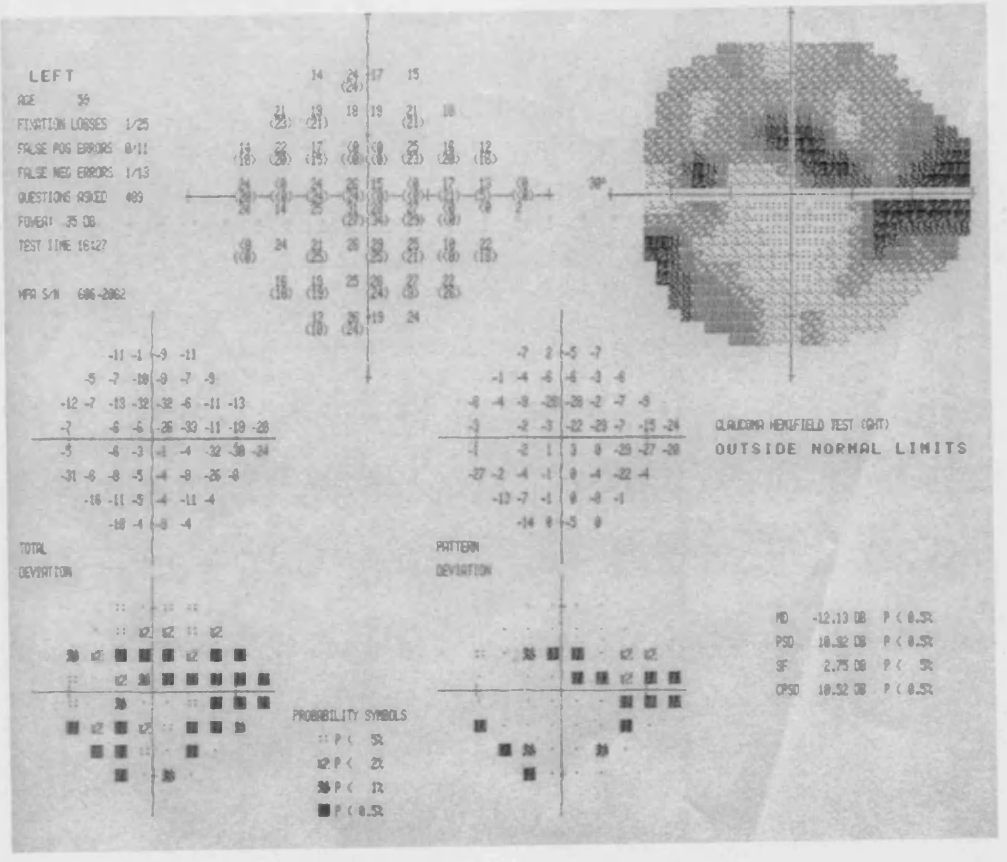
LEFT
AGE 39
FIXATION LOSSES 1/25
FALSE POS ERRORS 0/11
FALSE NEG ERRORS 1/13
QUESTIONS ASKED 409
POWER 35 DB
TEST TIME 16:27
HFA S/N 686-2862
TOTAL DEVIATION
PATTERN DEVIATION
PROBABILITY SYMBOLS
:: P < 5%
P < 2%
P < 1%
P < 0.5%
CLAUCOMA HEMIFIELD TEST (OHT)
OUTSIDE NORMAL LIMITS
MD -12.13 DB P < 0.5%
PSD 10.32 DB P < 0.5%
SF 2.75 DB P < 5%
CPSD 10.32 DB P < 0.5%

Figure 6.2B

CHAPTER 7

PHENOTYPE OF PRIMARY ANGLE CLOSURE GLAUCOMA PEDIGREES

7.1. Introduction

Although primary angle closure glaucoma (PACG) is the leading cause of glaucoma in East Asia, no pedigrees with the condition have been described in the literature. Two large Chinese families with PACG were identified in Singapore, and underwent detailed characterization for subsequent molecular genetic studies. The clinical phenotype of the families ascertained will be described in this chapter.

7.2. Methods

7.2.1. Identification of pedigrees

Pedigrees with primary angle closure glaucoma were identified through a national press campaign in Singapore that included publicity in newspapers, television news and radio. Families who responded were examined at the Glaucoma clinics of Singapore National Eye Centre and the National University Hospital, Singapore. Informed consent for genetic studies in adherence to the Declaration of Helsinki was obtained from all participants, and the study had the approval of the ethics committees of the Singapore National Eye Centre and the National University Hospital, Singapore.

7.2.2. Examination

Only subjects older than 40 years of age were included. The subjects were asked about a history of glaucoma including age at diagnosis, previous acute angle closure episodes and glaucoma treatment (if any), as well as the visual and glaucoma status of deceased ancestors. All participants then underwent a detailed eye examination, which involved slit lamp examination, Goldmann applanation tonometry, optic disc assessment (measurement of vertical cup: disc [CD] ratio and neuro-retinal rim width), and indentation gonioscopy. The gonioscopic method and diagnostic criteria used are discussed in Section 2.1.3 and 2.2.1 respectively. The drainage angle was graded according to Shaffer's convention in each quadrant (as detailed in Section 1.3.2.). The total gonioscopic angle width was also calculated by adding the Shaffer grade in each of 4 quadrants. Eyes were also assessed for the presence of peripheral anterior synechiae (PAS). All subjects with narrow angles also underwent visual field testing (see Section 2.1.5.). In addition to the clinical examination, subjects underwent refraction, and biometric measurement of the anterior chamber depth and axial length of the eyeball by A-scan ultrasound (described in Section 2.1.4.).

7.2.3. Diagnostic criteria

The diagnostic criteria for angle closure has been described previously in Section 2.2.1, and will be briefly summarized as follows. The minimum criteria for the diagnosis of angle closure was the presence of a narrow or occludable angle. This was defined as the presence of at least 180 degrees of angle in which the trabecular meshwork was not visible on indentation gonioscopy. Eyes with a narrow angle with raised IOP (>21 mm Hg) and/or PAS in the angle, or with a history of a previous acute angle closure episode, were termed to have primary angle closure (PAC). Primary angle closure glaucoma was defined as the presence of glaucomatous optic neuropathy with

compatible visual field loss, in association with a narrow angle on indentation gonioscopy.

7.2.4. Statistical analysis

Only one randomly selected eye from each patient was analysed. Comparisons between groups were done with Mann-Whitney U tests for continuous variables that were not normally distributed. Chi-square analysis was used for comparison of proportions. Statistical analysis was carried out using Statistical Package for Social Sciences version 9.0 (SPSS Inc, Chicago, Illinois), and statistical significance was assumed at the $p < 5\%$ level.

7.3. Results

Twelve families with angle closure were ascertained. However, only the 2 largest families will be described, as these were particularly suitable for linkage analysis (> 10 meioses). All subsequent linkage studies described in Chapter 8 were also limited to these 2 pedigrees.

7.3.1. Mode of inheritance

The angle closure phenotype in both pedigrees segregated as an autosomal dominant condition (Figure 7.1 and 7.2).

7.3.2. Ocular features of Pedigree 1

In Pedigree 1, there were 8 living affected subjects and 7 unaffected subjects (Figure 7.1).

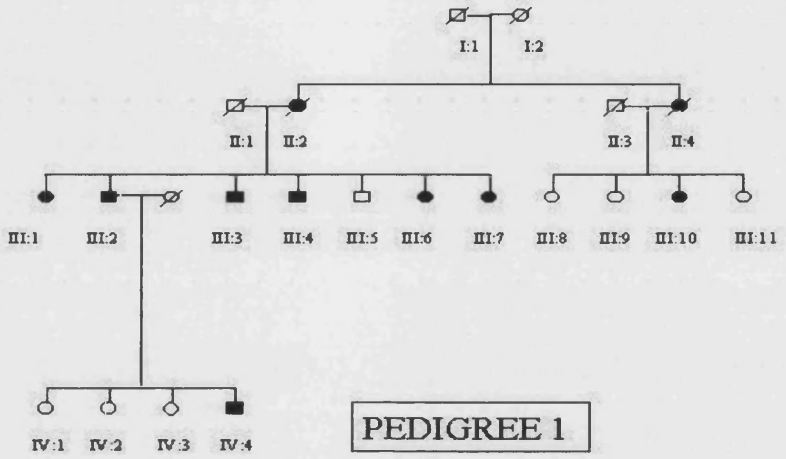

Figure 7.1. Pedigree 1. Phenotype information is included on the pedigrees: Narrow angle (filled symbol), normal individuals with open angles (unfilled symbol). Individuals' pedigree number is displayed.

Table 7.1 lists the following phenotypic data for members of Pedigree 1: gender, age, age at diagnosis, PACG classification (including history of previous acute episode), refraction, cup-disc ratio, gonioscopic findings (total gonioscopic angle width and presence of PAS), biometric measurements of axial length and anterior chamber depth, and glaucoma treatment if any.

Of the 8 affected subjects, there were 4 males and 4 females, with ages ranging from 48 to 88 years. Three subjects were diagnosed to have PACG, 4 with PAC and 1 with narrow angles only. Two of those with PAC and 1 with

PACG had a history of previous acute angle closure. Five of the subjects were diagnosed below the age of 60, the youngest at the age of 38 years only. All 3 subjects with previous acute angle closure were diagnosed before they were 60. The 3 subjects with PACG had advanced disease with CD ratio of 0.9, 0.7 and 0.9 respectively. Two of the PACG and one PAC subject had undergone trabeculectomy, and all but one of the other affected subjects had previous laser peripheral iridotomy.

All but one of the affected cases had PAS in the angles, and gonioscopy revealed extensive angle closure with total gonioscopic width score of 2.13 $\pm$ 1.4 (mean $\pm$ SD) in affected cases compared to 12.14 $\pm$ 2.0 in those unaffected ($p<0.001$). The mean anterior chamber depth in affected compared to unaffected cases was 2.56 $\pm$ 0.30 mm and 3.15 $\pm$ 0.31 mm respectively ($p<0.001$). The corresponding values for axial length were 22.8 $\pm$ 0.68 mm and 23.3 $\pm$ 0.36 mm ($p<0.001$)

Table 7.1. Clinical features of Pedigree 1. (Abbreviations used for Glaucoma Treatment: Trab= trabeculectomy; PI= peripheral iridotomy)

Patient Number	Sex	Age [years]	Age at diagnosis [years]	PACG classificat-ion	Previous acute episode	Refraction (spherical equivalent)	Cup-disc ratio at the time of examination	Total gonioscopic angle width	Presence of PAS	Anterior chamber depth (ACD) [mm]	Axial length (AXL) [mm]	Glaucoma treatment
III:1	Female	88	49	PACG	Nil	+1.0	0.9	1	+	2.27	22.7	Trab
III:2	Male	76	75	PAC	Nil	+2.0	0.6	3	+	2.76	22.17	PI
III:3	Male	74	72	PACG	Nil	-1.0	0.7	3	+	2.35	23.5	PI
III:4	Male	71	46	PAC	+	Plano	0.6	1	+	2.35	22.79	PI, Trab
III:5	Male	69	NA	Normal	Nil	Plano	0.3	9	Nil	2.69	23.19	Nil
III:6	Female	66	38	PAC	+	+2.0	0.5	3	+	2.6	21.8	PI
III:7	Female	63	59	PACG	+	+1.5	0.9	0	+	2.43	22.48	PI, Meds
III:8	Female	73	NA	Normal	Nil	Plano	0.3	15	Nil	3.5	23.12	Nil
III:9	Female	71	NA	Normal	Nil	Plano	0.5	11	Nil	2.94	23.1	Nil
III:10	Female	68	68	PAC	Nil	-1.2	0.5	2	+	2.54	23.1	PI
III:11	Female	65	NA	Normal	Nil	+0.75	0.3	11	Nil	2.89	23.07	Nil
IV:1	Female	52	NA	Normal	Nil	Plano	0.5	14	Nil	3.2	24.1	Nil
IV:2	Female	51	NA	Normal	Nil	-3.5	0.5	12	Nil	3.5	23.4	Nil
IV:3	Female	50	NA	Normal	Nil	-2.0	0.6	13	Nil	3.3	23.46	Nil
IV:4	Male	48	47	Narrow	Nil	-1.25	0.6	4	Nil	3.2	23.9	Nil

7.3.3. Ocular features of Pedigree 2

In Pedigree 2, there were 12 living affected subjects and 5 unaffected subjects (Figure 7.2). However, one of the affected individuals (IV:10) refused to be examined, leaving 16 subjects with phenotype data. Table 7.2 lists the phenotypic data for members of Pedigree 2.

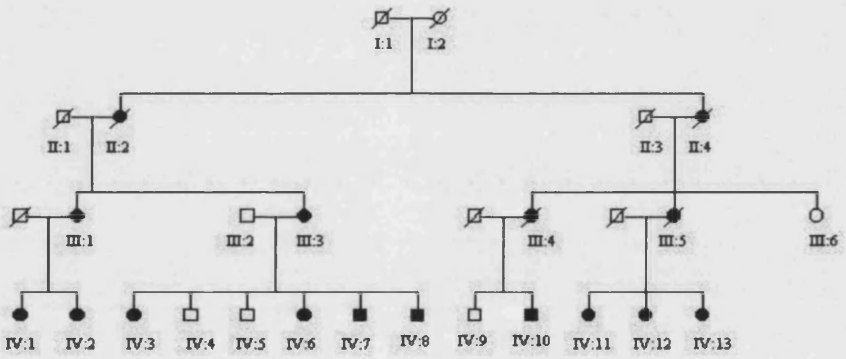

PEDIGREE 2

Figure 7.2. Pedigree 2. Phenotype information is included on the pedigrees: Narrow/occludable angle (filled symbol), normal individuals with open angles (unfilled symbol). Individuals' pedigree number is displayed.

Table 7.2. Clinical features of Pedigree 2. (Abbreviations used for Glaucoma Treatment: Trab= trabeculectomy; PI= peripheral iridotomy)

Patient No.	Sex	Age [years]	Age at diagnosis [years]	PACG classification	Previous acute episode	Refraction (spherical equiv)	Cup-disc ratio at the time of examination	Total gonioscopic angle width	Presence of PAS	Anterior chamber depth (ACD) [mm]	Axial length (AXL) [mm]	Glaucoma treatment
III:1	Female	84	60	PACG	Nil	+5.0	0.7	0	+	2.4	22.36	PI, Trab
III:2	Male	81	NA	Normal	Nil	Plano	0.6	10	Nil	3.9	22.4	Nil
III:3	Female	79	61	PACG	+	+2.0	0.95	1	+	2.8	19.97	Trab
III:6	Female	74	NA	Normal	Nil	Plano	0.6	16	Nil	3.6	22.6	Nil
IV:1	Female	53	53	PAC	Nil	-0.5	0.5	3	+	2.7	22.29	Nil
IV:2	Female	52	52	PAC	Nil	Plano	0.6	2	+	3.05	22.1	Nil
IV:3	Female	54	51	PAC	+	Plano	0.4	4	Nil	2.5	22.01	PI
IV:4	Male	52	NA	Normal	Nil	-6.0	0.3	9	Nil	2.8	25.2	Nil
IV:5	Male	51	NA	Normal	Nil	+1.0	0.3	10	Nil	3.2	23.5	Nil
IV:6	Female	50	49	Narrow	Nil	+1.0	0.4	2	Nil	2.57	22.14	Nil
IV:7	Male	40	49	PAC	+	+2.2	0.4	3	Nil	2.33	22.36	PI
IV:8	Male	47	40	PAC	+	-1.0	0.5	2	+	2.6	22.3	PI
IV:9	Male	47	NA	Normal	Nil	-1.75	0.4	8	Nil	3.17	23.5	Nil
IV:11	Female	66	58	PAC	+	-1.0	0.5	2	+	2.42	23.52	PI
IV:12	Female	55	55	Narrow	Nil	-0.5	0.4	3	Nil	2.31	22.84	PI
IV:13	Female	53	55	Narrow	Nil	-1.5	0.4	1	Nil	2.8	23.46	PI

Of the 12 affected subjects, there were 2 males and 10 females, with ages ranging from 40 to 84 years. Two subjects were diagnosed to have PACG, 6 with PAC and 3 with narrow angles only. One of those with PACG and 4 with PAC had a history of previous acute angle closure. All but 2 of the affected subjects were diagnosed below the age of 60, the youngest at the age of 40 years. Four out of the 5 subjects with previous acute angle closure were diagnosed before they were 60. The 2 subjects with PACG had CD ratio of 0.7 and 0.95 respectively. The visual field of subject III:3 (with CD ratio of 0.95) is shown in Figure 7.3. Both of the PACG subjects had undergone trabeculectomy, and 6 of the other 9 affected subjects had previous laser peripheral iridotomy. Two subjects were diagnosed to have PAC only in the course of this study, and had thus not received any prior treatment.

All but one of the PACG/PAC cases had PAS in the angles. The total gonioscpic width was 2.09 $\pm$ 1.1 (mean $\pm$ SD) in affected cases compared to 10.6 $\pm$ 3.1 in those unaffected ($p<0.001$). Figure 7.4 depicts the view of a closed angle on gonioscopy, of one of the affected subjects. The mean anterior chamber depth in affected compared to unaffected cases was 2.59 $\pm$ 0.23 mm and 3.33 $\pm$ 0.42 mm respectively ($p<0.001$). The corresponding values for axial length were 22.3 $\pm$ 0.93 mm and 23.24 $\pm$ 1.4 mm ($p<0.001$).

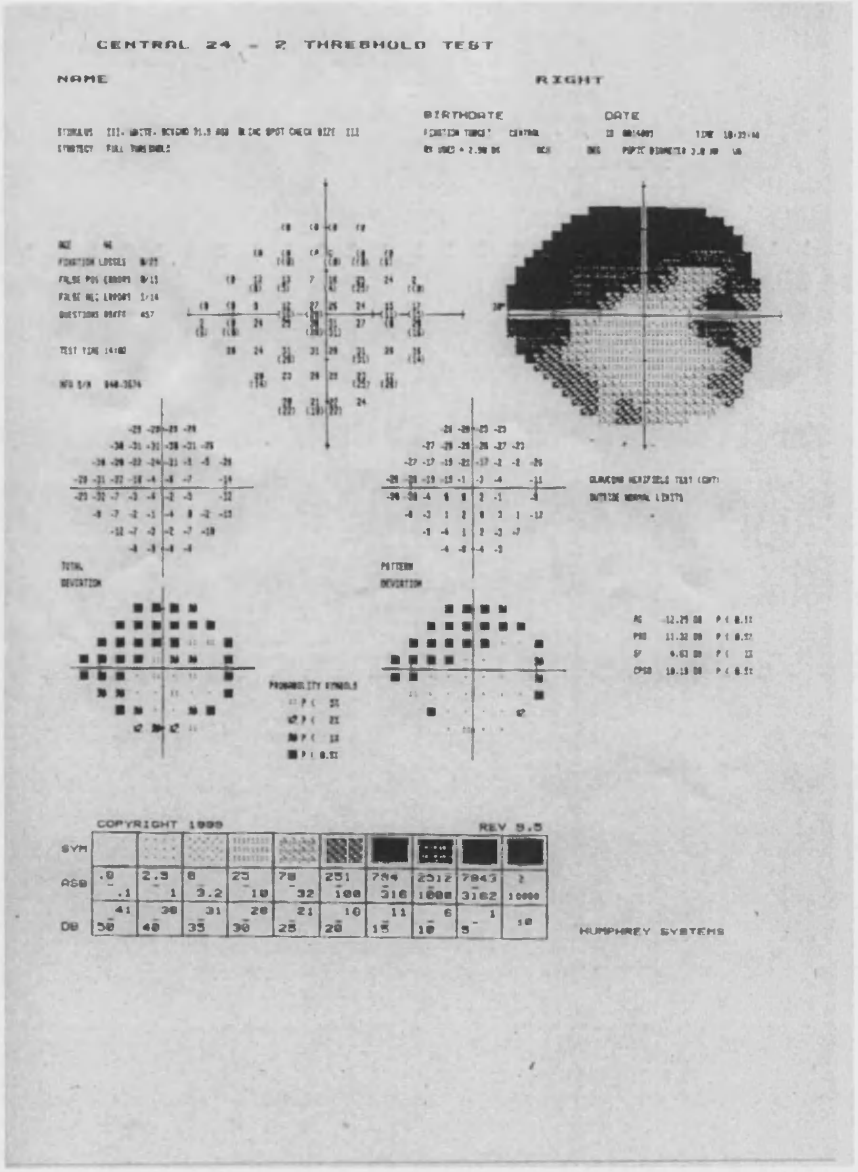

Figure 7.3. The visual field of subject III:3 (with CD ratio of 0.95) showing superior hemifield loss.

7.4. Discussion

Although an autosomal dominant mode of inheritance for primary angle closure glaucoma has been previously suggested (Tornquist, 1953), this study provides the first supporting evidence for this concept to date. Two large pedigrees with PACG have been characterised, and the disease was found to segregate in an autosomal dominant manner. Several reasons may account for the lack of previous literature on PACG heredity. There is firstly a paucity of research into PACG, which is probably related to the high prevalence of the condition in populations where glaucoma research has not been a major focus. The inheritance of PACG is difficult to determine due to the late onset of the disease and the lack of accurate clinical information on previous generations. There may also be under-reporting of a family history, as in POAG (McNaught *et al.*, 2000), leading to the impression that most affected patients are isolated cases.

Affected subjects from the 2 pedigrees appear to have quite a young age of diagnosis of the disease, with most being diagnosed before the age of 60 years, although there is likely to be some bias towards earlier diagnosis due to a positive family history. An early to mid adulthood age of diagnosis has also been noted in POAG families (Sheffield *et al.*, 1993; Stoilova *et al.*, 1996; Trifan *et al.*, 1998; Sarfarazi *et al.*, 1998), and suggests that the disease process manifests earlier in those with a genetic predisposition. Those with a history of acute symptomatic angle closure (Figure 7.5) in particular appeared to be diagnosed earlier (most in their 40s and 50s), compared to those with asymptomatic disease. It is likely that the acute symptoms made the patients seek medical help, while the absence of symptoms in chronic cases results in them being undiagnosed and untreated until later in life. It is interesting that some subjects developed acute PAC, while other subjects of the same pedigree had chronic disease. The reasons why some individuals develop an episode of

acute PAC while others develop asymptomatic disease still remain obscure.

Linkage studies to determine the genetics of POAG have concentrated on the presence of glaucomatous optic neuropathy (GON) and/or ocular hypertension as the basis of classifying the affection status of patients (Sheffield *et al.*, 1993; Stoilova *et al.*, 1996; Wirtz *et al.*, 1997; Trifan *et al.*, 1998; Sarfarazi *et al.*, 1998; Wirtz *et al.*, 1999). In contrast, the diagnostic criteria that was central to the phenotypic classification used in this study was the existence of a narrow angle, defined as the presence of at least 180 degrees of angle in which the trabecular meshwork was not visible on indentation gonioscopy. Thus, the affection status was established not by the presence of glaucomatous optic neuropathy, but by the angle configuration. This concept is critical, as it is likely that cases will be misclassified if based on the glaucoma status alone. For example, eyes with narrow angles (but without raised IOP, PAS or GON) would be classified as unaffected under the 'GON' classification but such eyes may actually have a significant degree of angle closure and with time, may develop GON and hence PACG.

A new diagnostic classification of PACG (Foster and Johnson, 2000; Foster *et al.*, 2002) was also used in this study, which provides a more uniform definition of the disease, and is in line with the classification used in POAG (as detailed in Section 1.3.4.2). The focus of the classification is the presence of end organ damage, namely glaucomatous damage to the optic nerve, and differentiates those with true disease as opposed to suspects who are at increased risk of disease. The term 'glaucoma' is thus reserved for people who have suffered injury to the optic nerve as judged by visual field abnormality, combined with enlargement of the cup/disc ratio. Thus, persons suffering an acute, symptomatic rise in intraocular pressure would not be considered to have glaucoma, unless they showed evidence of optic nerve damage. This is counter-intuitive for many Western ophthalmologists, who commonly associate PACG with the acute symptomatic angle closure episode, and

continue to label the presentation as acute angle closure 'glaucoma,' despite evidence that many episodes of symptomatic angle closure recover without visual loss developing as a sequel of the acute attack (Douglas *et al.*, 1975; Aung *et al.*, 2001). This was further illustrated in this study by the finding that several individuals with a history of acute symptomatic angle closure were classified as having PAC and not PACG, i.e. they had no evidence of glaucoma damage after the acute episode. Using this classification, it is interesting to note that different members of the same pedigree had varying degrees of angle closure, from narrow angles alone, to PAC and PACG. This is likely to reflect varying levels of damage secondary to the primary angle closure process. Thus, eyes in the earliest stage have just narrow angles, PAC cases develop PAS and/or raised IOP, while those in the advanced stage develop glaucomatous damage and hence PACG.

The association between a small eye and PACG has been recognized for some time (Lowe, 1974), and several studies have found that a small eye with a shallow anterior chamber is significantly associated with PACG (Tornquist, 1956; Lowe, 1969; Alsbirk, 1974a; Alsbirk, 1974b; Arkell *et al.*, 1987). Interestingly, affected subjects in the 2 pedigrees were also found to have significantly shorter axial lengths and shallower anterior chambers compared to unaffected cases. This finding makes one speculate that the gene responsible for PACG is a growth factor, probably related to eyeball or orbit growth. Having such small eyes may not result in disease at a young age, but with ageing, the lens becomes increasingly thicker and cataractous. It is plausible that this changing configuration of the lens will narrow the angle and lead to progressive angle closure and the eyes overtime will develop PAC and eventually PACG.

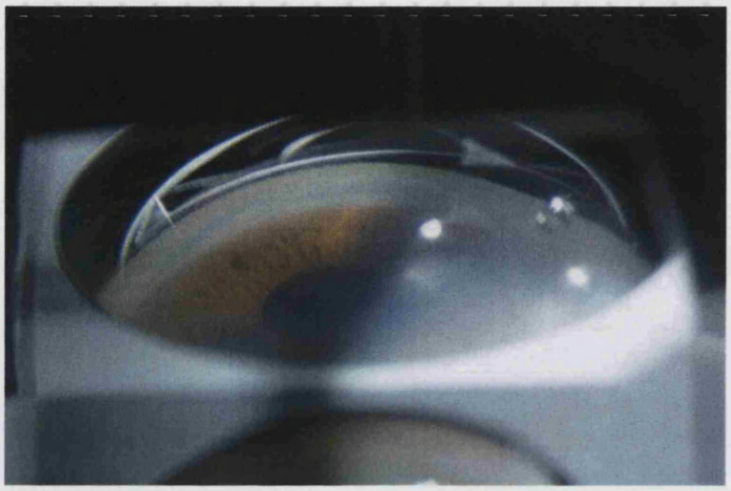

Figure 7.4. Gonioscopic view of the closed angle of an affected subject from Pedigree 2.

Figure 7.5. Clinical slide of a patient with acute angle closure, showing a hazy cornea, injected conjunctiva and a mid-dilated pupil.

CHAPTER 8

LINKAGE ANALYSIS OF PRIMARY ANGLE CLOSURE GLAUCOMA PEDIGREES

8.1. Introduction

Although primary angle closure glaucoma (PACG) is a major cause of blindness worldwide, no molecular genetic studies related to the condition have been performed to date. Two large Singaporean pedigrees with PACG were identified and the clinical phenotype described previously in Chapter 7. The families showed an autosomal dominant mode of inheritance.

Linkage analysis was used to assess if the disorder mapped to loci encompassing possible candidate genes. Loci associated with eyes having short axial lengths were first excluded, as were known primary open angle glaucoma loci. In order to identify a novel genetic locus, a genome-wide linkage scan was performed using fluorescent-labeled dinucleotide microsatellite markers. Subsequent genotyping confirmed linkage on chromosome 10q11 and refined the linked genetic interval. The genetic map of the linked interval was constructed from data derived from the Human Genome Project, which is available on web-based databases; the main one used being Ensembl (www.ensembl.org). Four candidate genes located in the linked interval were selected based on their expression pattern and function, and screened for mutations.

8.2. Methods

8.2.1. Linkage analysis

Linkage analysis was the method used to assess if the disorder mapped to a particular locus (described in Section 2.10). PCR-based microsatellite marker genotyping was performed on DNA samples extracted from venous blood provided by each subject. The methods used in genotyping have been described in Section 2.10.2.

8.2.2. Calculation of LOD scores for microsatellite markers

Two-point LOD scores for each marker analysed were calculated using the program MLINK of the LINKAGE package (version 5.1) via the HGMP Genetic Linkage User Environment (GLUE: www.hgmp.co.uk) (as detailed in section 2.10.3.). A fully penetrant dominant model with a disease frequency of 0.0001 (1 in 10,000) was assumed. Marker allele frequencies were assumed to occur at equal frequencies since population allele frequencies associated with Singaporean Chinese people were not available.

8.2.3. Direct sequencing

Coding regions of candidate genes were amplified by PCR and then directly sequenced using the ABI 3100 DNA sequencer (as detailed in Section 2.9.4.).

8.3. Results

8.3.1. Exclusion of loci for genes associated with nanophthalmos and microphthalmia

To determine the locus for PACG, the initial strategy of this study was to use linkage analysis across a number of candidate loci. These candidate loci were chosen as a result of similarities in the phenotype. As PACG is strongly associated with short axial length, the 2 large Singaporean families with PACG were studied with linkage analysis for evidence of linkage to loci for genes associated with eyes having a short axial length (microphthalmia). These loci and the markers studied are summarised in Table 8.1.

Table 8.1. Loci for genes associated with nanophthalmos and microphthalmia, chromosomal location and the microsatellite markers genotyped.

Candidate Disease	Symbol	Chromosomal localization	Markers
Autosomal dominant nanophthalmos	NNO1	11p13	D11S903 D11S1313
Autosomal dominant microphthalmia/ Nanophthalmos	NNO2	15q12	D15S1007 D15S1031
Autosomal recessive microphthalmia	MCOP	14q32	D14S65 D14S267
Syndromic microphthalmia with cataracts and iris abnormalities	CHX10	14q24.3	D14S77 D14S1025

Table 8.2 and 8.3 below lists the LOD scores obtained for these markers. LOD scores less then –2.0 were obtained for all loci. This is evidence that PACG in these 2 pedigrees is not linked to loci for nanophthalmos and microphthalmia.

Table 8.2. Two-point LOD scores obtained for Pedigree 1 for loci associated with nanophthalmos and microphthalmia (θ is the recombination fraction).

Markers \ θ	0.0	0.05	0.1	0.2	0.3	0.4
D11S903	-∞	-2.3	-1.26	-0.41	-0.21	-0.01
D11S1313	-∞	-1.85	-1.05	-0.39	-0.14	-0.05
D15S1007	-∞	-3.71	-2.15	-0.83	-0.5	-0.06
D14S65	-∞	-2.62	-1.52	-0.56	-0.17	-0.01
D14S267	-∞	-1.96	-1.25	-0.84	-0.23	-0.05
D14S77	-∞	-1.68	-0.96	-0.58	-0.11	-0.02
D14S1025	-∞	-3.45	-2.16	-0.95	-0.37	-0.05

Table 8.3. Two-point LOD scores obtained for Pedigree 2 for loci associated with nanophthalmos and microphthalmia.

Markers \ θ	0.0	0.05	0.1	0.2	0.3	0.4
D11S903	-∞	-2.7	-1.6	-0.68	-0.25	-0.06
D15S1007	-∞	-2.22	-1.29	-0.50	-0.18	-0.04
D15S1031	-∞	-3.54	-2.17	-0.94	-0.37	-0.09
D14S65	-∞	-2.26	-1.36	-0.56	-0.21	-0.05
D14S267	-∞	-1.83	-0.92	-0.21	0.05	0.02
D14S77	-∞	-3.01	-1.80	-0.74	-0.27	-0.06
D14S1025	-∞	-2.42	-1.40	-0.49	-0.13	-0.01

8.3.2. Exclusion of known loci for primary open angle glaucoma

After the exclusion of linkage to loci for genes associated with eyes having a short axial length, linkage analysis was performed for markers associated with a number of known POAG loci. This was to exclude the possibility that PACG and POAG shared similar genetic loci. The table 8.4 below lists the 6 known POAG loci and the microsatellite markers used in the linkage analysis.

Table 8.4. Known loci for POAG, chromosomal location and the microsatellite markers genotyped.

Locus symbol	**Gene symbol**	**Chromosomal localisation**	**Markers**
GLC1A	*MYOC*	1q23-q24	D1S196 D1S218
GLC1B		2cen-q13	D2S347
GLC1C		3q21-q24	D3S1569 D3S1279
GLC1D		8q23	D8S284 D8S272
GLC1E	*OPTN*	10p14	D10S1653
GLC1F		7q35	D7S661

Table 8.5 and 8.6 below lists the LOD scores obtained for these markers. From the data, linkage to known loci for POAG was excluded in these 2 pedigrees. Thus it is likely that there is a novel genetic locus associated with PACG.

Table 8.5. Two-point LOD scores obtained for Pedigree 1 for known POAG loci.

Markers \ θ	0.0	0.05	0.1	0.2	0.3	0.4
D1S196	-∞	-1.73	-1.11	-0.51	-0.2	-0.05
D2S347	-∞	-2.19	-1.33	-0.56	-0.21	-0.05
D3S1569	-3.5	-1.57	-0.82	-0.24	-0.04	0
D8S284	-∞	-2.23	-1.38	-0.60	-0.23	-0.05
D10S1653	-∞	-2.54	-1.48	-0.61	-0.26	-0.1
D7S661	-∞	-2.86	-1.61	-0.59	-0.2	-0.04

Table 8.6. Two-point LOD scores obtained for Pedigree 2 for known POAG loci.

Markers \ θ	0.0	0.05	0.1	0.2	0.3	0.4
D1S218	-∞	-2.19	-1.36	-0.63	-0.27	-0.08
D2S347	-∞	-1.90	-1.09	-0.42	-0.14	-0.03
D3S1279	-∞	-3.46	-2.14	-0.92	-0.34	-0.06
D8S272	-∞	-2.19	-1.52	-0.81	-0.42	-0.17
D10S548	-∞	-2.17	-1.37	-0.67	-0.33	-0.12
D7S661	-∞	-3.5	-2.0	-0.8	-0.27	-0.04

8.3.3. Genome wide linkage-scan

A total genome scan was undertaken utilizing markers from version 2.0 of the ABI MD-10 (Applied Biosystems). These allow approximately 10 cM resolution of the human genome.

The results of the genome scan are listed in the Appendix (Tables 1 to 22 for Pedigree 1 and in Tables 23 to 44 for Pedigree 2).

The markers showing LOD scores of >1.0 for pedigree 1 and 2 are summarized below in Tables 8.7 and 8.8 respectively.

Table 8.7. Genome wide scan: Markers with LOD score >1.0 for Pedigree 1. (θ is the recombination fraction and Z_{max} is the maximum lod score for each microsatellite marker).

Marker	**Theta=0**	**0.05**	**0.1**	**0.2**	**0.300**	**0.4**	**Z_{MAX}**
D1S2836	1.35	1.20	1.05	0.74	0.42	0.13	1.35
D3S1297	1.06	0.93	0.80	0.53	0.27	0.08	1.06
D3S1304	1.03	0.87	0.61	0.42	0.20	0.05	1.03
D7S507	1.13	1.12	1.04	0.81	0.50	0.18	1.13
D10S1780	1.24	1.13	1.01	0.75	0.43	0.18	1.24
D10S196	2.34	2.09	1.84	1.29	0.72	0.21	2.34
D10S210	-∞	1.57	1.56	1.20	0.70	0.20	1.57
D10S185	1.40	1.39	1.30	1.01	0.66	0.32	1.40
D10S192	1.06	0.98	0.90	0.71	0.48	0.23	1.06
D11S4175	1.22	1.05	0.91	0.66	0.42	0.19	1.22
D13S265	1.22	1.14	1.02	0.76	0.48	0.21	1.22
D18S452	1.34	1.28	1.19	0.94	0.61	0.23	1.34

Table 8.8. Genome wide scan: Markers with LOD score >1.0 for Pedigree 2.

Marker	**Theta=0**	**0.05**	**0.1**	**0.2**	**0.300**	**0.4**	**Z_{MAX}**
D2S162	1.15	1.11	1.03	0.78	0.44	0.08	1.15
D10S591	1.51	1.30	1.08	0.66	0.29	0.04	1.51
D12S345	-∞	1.36	1.36	1.05	0.63	0.21	1.36
D17S921	1.36	1.26	1.14	0.82	0.48	0.18	1.36
D19S418	1.43	1.40	1.32	1.08	0.76	0.38	1.43

There were no common markers with LOD score>1.0 in both pedigrees.

The highest LOD score was obtained in Pedigree 1 for the marker D10S196 (LOD=2.34 at θ=0) on chromosome 10q11 (Figure 8.1). However, for this marker, the LOD score for pedigree 2 was –2.23 at θ=0, which shows that the disease did not link to this locus for Pedigree 2, indicating genetic heterogeneity between the 2 pedigrees.

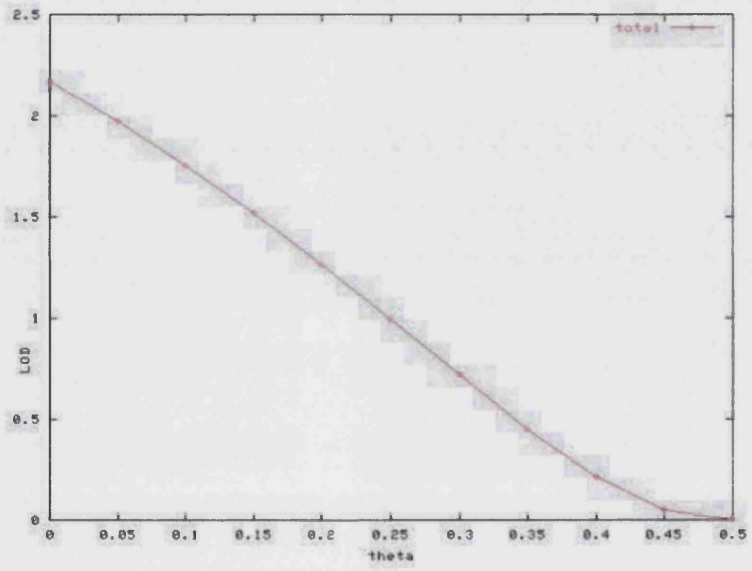

Figure 8.1. LOD score obtained for D10S196.

A targeted approach was taken to refine the linkage found for Pedigree 1, and stop further linkage studies on Pedigree 2. The remainder of the chapter will summarize the work done confirming this locus in Pedigree 1, as well as sequencing of candidate genes in this interval.

8.3.4. Refinement of locus of Chromosome 10

In order to refine the disease interval, fine mapping around marker D10S196 was performed using 35 additional microsatellite markers for Pedigree 1.
The following markers were not informative: D10S1566, D10S538, D10S1790, D10S524, D10S1642, D10S1470, D10S1869, D10S2283, D10S1766, D10S1577, D10S1464, D10S1577, D10S1220, D10S2283 and D10S1458.

The linkage results of markers with positive LOD scores are summarised below in Table 8.9. The maximum LOD score was obtained for marker D10S220 (LOD=3.4 at θ=0)(see Figure 8.2).

Table 8.9. Further markers genotyped on Chromosome 10: Markers with positive LOD score for Pedigree 1.

Markers \ θ	0	0.05	0.1	0.2	0.3	0.4	Z_{MAX}
D10S1100	1.12	1.0	0.86	0.55	0.28	0.08	1.12
D10S141	2.29	2.03	1.76	1.19	0.59	0.11	2.29
D10S1793	-∞	0.90	1.08	0.98	0.62	0.20	1.08
D10S225	-∞	0.89	1.08	0.98	0.63	0.20	1.08
NM2	2.95	2.69	2.42	1.84	1.20	0.5	2.95
D10S196	2.3	1.97	1.75	1.26	0.72	0.21	2.3
D10S220	3.4	3.15	2.86	2.2	1.45	0.64	3.4
NM3	2.57	2.32	2.05	1.46	0.82	0.27	2.32
NM1	1.2	1.0	0.86	0.55	0.28	0.08	1.2
D10S568	-∞	0.58	0.91	0.93	0.66	0.29	0.93
D10S539	-∞	0.72	0.85	0.73	0.44	0.17	0.85
D10S546	1.33	1.22	1.08	0.76	0.44	0.17	1.33
D10S1584	0.57	0.73	0.75	0.61	0.36	0.12	0.75
D10S1124	2.11	1.96	1.76	1.28	0.70	0.14	2.11

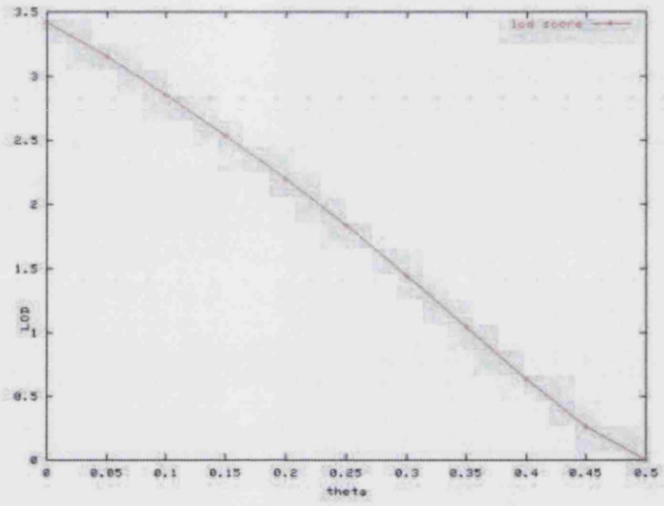

Figure 8.2. LOD score obtained for D10S220

8.3.5. Linkage of the PACG disease phenotype to chromosome 10: Haplotype analysis

Haplotype analysis (Figure 8.3) revealed a 5 cM genetic interval (Marshfield map distances) on chromosome 10q11 that linked to disease. The flanking markers for this region were D10S225 (centromeric end) and D10S568 (telomeric end).

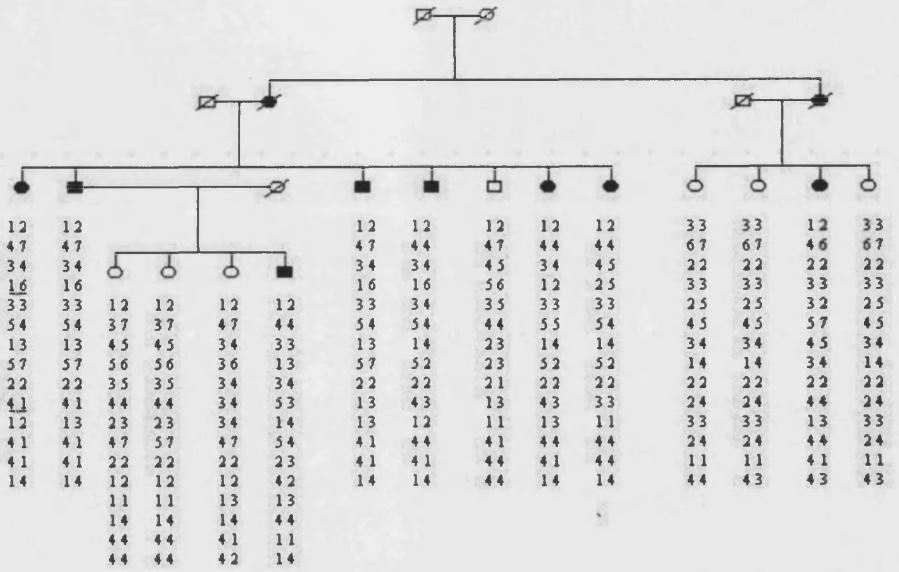

Figure 8.3. Haplotype analysis of microsatellite markers in the genetic interval.

The order of markers used to construct the haplotype (in Figure 8.1) are shown as follows in Table 8.10:

Markers	
D10S1100	
D10S141	
D10S1793	
D10S225	Flanking marker
NM2	
D10S196	
D10S220	Maximum LOD score
NM3	
NM1	
D10S568	Flanking marker
D10S539	
D10S546	
D10S1584	
D10S1124	

Table 8.10. Order of microsatellite markers used to construct the haplotype shown in Figure 8.1.

8.3.6. Genetic map for the PACG interval

The genetic map of the linked interval on chromosome 10 was constructed from data derived from the Human Genome Project, which is available on web-based databases. The main database used was Ensembl (www.ensembl.org), a joint project between the European Molecular Biology Laboratory-European Bioinformatics Institute (EMBL – EBI) and the Sanger Institute. All such databases present up-to-date sequence data and the best possible automatic annotation for the genome, and are updated regularly.

From the data available in July-August 2002 (Ensembl version 7.29), six known and several predicted genes were found to be present between the flanking markers, D10S225 and D10S568. The known genes and their position in relation to the microsatellite markers are shown in Figure 8.4.

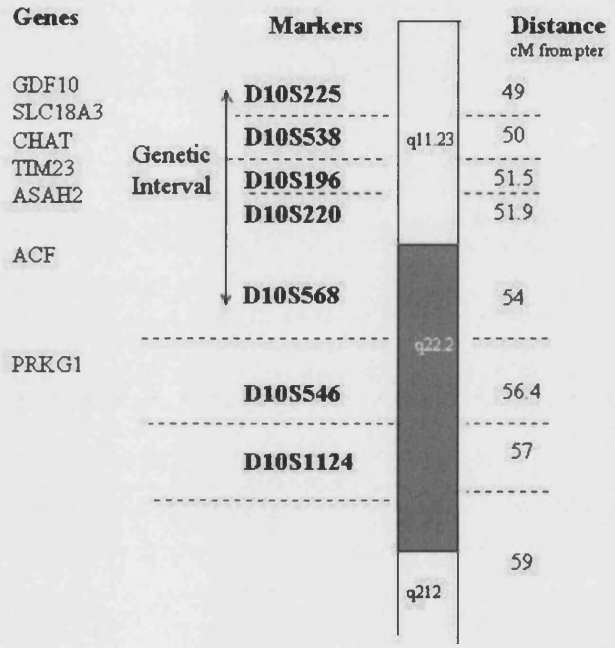

Figure 8.4. Genetic map for the linked PACG interval (August 2002). Known genes are in the left column, microsatellites are in bold, genetic distances in cM shown in the right column.

8.3.7. Candidate genes in the linked interval.

All the genes located in the linked genetic interval are possible candidates for PACG. Unfortunately, there is very little data available about the genes in the interval from the databases, and there was no obvious or good candidate gene

found in this interval. Information about the six known genes in the interval is summarized as follows:

8.3.7.1. GDF10: growth differentiation factor 10 gene.

The protein encoded by this gene is a member of the bone morphogenetic protein (BMP) family and the TGF-beta superfamily (Cunningham *et al.*, 1995). The members of this family are regulators of cell growth and differentiation in both embryonic and adult tissues. Studies in mice suggest that the protein encoded by this gene plays a role in skeletal morphogenesis (Wozney *et al.*, 1988).

8.3.7.2. SLC18A3: solute carrier family 18 (vesicular acetylcholine), member 3 gene.

The protein encoded by this gene is a vesicular proton-dependent acetylcholine transporter thought to be important for cholinergic neurotransmission (Erickson *et al.*, 1994).

8.3.7.3. CHAT: choline acetyltransferase gene.

The protein encoded by this gene synthesizes the neurotransmitter acetylcholine (Cohen-Haguenauer *et al.*, 1990). Cholinergic systems are implicated in numerous neurological functions, and alteration in some cholinergic neurons may account for diseases such as myasthenia gravis (Ohno *et al.*, 2001).

8.3.7.4. TIMM23: translocase of inner mitochondrial membrane 23 homolog gene

The gene is associated with the production of a mitochondrial inner membrane translocase subunit, which translocates nuclear-encoded proteins into the mitochondrion (Donzeau *et al.*, 2000).

8.3.7.5. ASAH2: N-acylsphingosine amidohydrolase 2 gene (non-lysosomal ceramidase).

The gene is related to mitochondrial ceramidase, which hydrolyzes ceramide and functions in sphingolipid metabolism.

8.3.7.6. ACF: apobec-1 complementation factor gene

The gene product belongs to the hnRNP R family of RNA-binding proteins. It has been proposed that this complementation factor functions as an RNA-binding subunit and may be involved in RNA editing or RNA processing events (Henderson *et al.*, 2001).

8.3.7.7. Selection of possible candidate genes

Three of the genes in the genetic interval, SLC18A3, TIMM23 and ASAH2, are known to be expressed in the eye and therefore represent good candidate

genes for PACG. A fourth gene, GDF10 was also considered to be a possible candidate gene, as it is a growth factor and it was thought that the gene responsible for PACG might affect eyeball growth. These 4 genes were thus selected for mutation screening.

8.3.8. Mutation screening of candidate genes by direct sequencing

All coding exons of GDF10, SLC18A3, TIMM23 and ASAH2 were amplified in two affected members and one unaffected member of Pedigree 1, using the primer pairs listed in Table 8.11. The PCR products were directly sequenced using the ABI 3100 DNA sequencer (as detailed in Section 2.9.4.) and compared to the known exon sequences. No changes were detected in the coding region of all 4 genes, ruling out the possibility that coding region mutations in these genes are responsible for the PACG seen in this family.

Gene	Exon	Forward primer	Reverse primer
TIMM23	1	GGAACCACTCGGTTTGCTG	CGCGCAACTTAGTGTAGACG
	2	CATGTAACAATCAGGAGCTGGA	AGCATAGCACTTGGCGTTTT
	3	GAGGGACACTCAGCTTGGTT	TTTGATTTTACGCACCCTCA
	4	GCTGTCTTTATCTGGGTGAATTG	TCAAGGTTGTACTCATCAAACCA
	5	TGGGTCTAGACATGTTAAATAGCC	TGTTCATGATATTTGTGCATTCTTT
	6	TTTTGTCACTGAGCACTTCCA	TGTAATTTCCTTGAAAACCATGAA
	7	CCCAGCCCATTTCACAGTA	GACTACTGAAGTGTCCTCCATTCA
GDF10	1	CCTTCCTCCTCCTGGACTTC	AATGAGGAGAAGGGGTCCTG
	2a	CACGAGCGAGAACTTCACAG	GGTCCCTCTCCTCAGAATCC
	2b	CCCAGCTGGATTCTGAGGA	GGCTGAGGAACTTGACGGTA
	3	CGGAGCTGAGGTAACCCTAC	CACAAGTCCTGGTTGCAGAA
SLC18A3	1	CTGAGGCACAGGGGAGTCT	TCTTCGCTCTCCGTAGGGTA
	2	CCTACACGGCCAACACCT	GGCGAACTCATAGAGGATGC
	3	GCCATGATCGCCGATAAGTA	AGGTAGACGCCCAGCACAT
	4	CACGTGGATGAAGCATACGA	CATAGAGCAGGTTGGCCAGT
	5	CATCGCCGACATCTCCTATT	CAGAGCAGCCCCCTTGAC
ASAH2	1	CAGGTTCTTGAGCTGTTCCTG	GGAGCCCATTGTCTACTTGC
	2	TTTCTTTGTTTTTCTGCAGTCG	TCCTGTCACATTCACCCACT
	3	TCCTGGATCAGTGATTGAACTC	TAAAGAACAGCTGCCTCTGG
	4	TGTCCCCACCAGGATTTCTA	CCCTAAAGGGAATGAAACGA
	5	TGTGTCAGCTGCTACTGTTCA	AAGAAAAGCTACCCGACAGAA
	6	TCATAGTTCTTGGCCCCAGT	TGCAGCATGAATGATGACAC
	7	TGCCTGCAAATGATTTTGAAT	GGCCAGTGTATACTAGAAGACAAGG
	8	CCTGAAAAGAAATGCAAGAATG	ACCTCCCAAGCTGACCTCTT
	9/ 10	CACTTTAGCCTTTTTGCTTGG	CAGAGAACAGAACCCAGAAGC
	11	TTGAGAGGGTTGGTTCAAGG	CCATTCATTACCTGACAGTTACAC
	12	AGAGGAAATTCTGGGACCACT	ACCAAGGGGTCAACACAGAA
	13	GCCAGTGTTTCTGTGTACTCTGC	CCTCTTCACCAAACATGAACA
	14	TCCATTGACTTGTCCAACTGT	AGCAAGTCCTGCATTTGACACA

Table 8.11. Candidate genes sequenced with the primer pairs shown.

8.4. Discussion

This study identified the first locus for primary angle closure glaucoma on chromosome 10q11. The locus, spanning a region of 5 cM, was flanked by the markers D10S225 and D10S568, with the maximum LOD score of 3.4 at $\theta=0$ obtained for the marker D10S220. Under the nomenclature and classification system for glaucoma genetics devised by the Human Genome Organisation (HUGO) Genome Database Nomenclature Committee, this locus would thus be termed GLC2A.

The finding that Pedigree 2 did not link to this locus implicates the existence of another genetic locus for PACG, and hence genetic heterogeneity for PACG. This is not surprising as there is likely to be more than one genetic locus for the condition, as illustrated in POAG by the identification of 6 different loci and 2 genes so far (Craig and Mackey, 1999). Further linkage analysis is ongoing for Pedigree 2 in order to identify the locus in this family.

The initial strategy of searching for linkage to potential candidate genes and known glaucoma loci was not successful. Genes associated with small eyeball dimensions such as microphthalmia and nanophthalmos are obvious candidates for PACG. This is because eyes with PACG have smaller dimensions including anterior chamber depth and axial length. It is speculated that the gene responsible for PACG is a growth factor, probably related to eyeball or orbit growth. Such small eyes may not result in disease at a young age, but with ageing, the lens becomes increasingly thicker and cataractous. It is likely that this new configuration of the lens will narrow the angle and lead to progressive angle closure. Identification of the causative gene for PACG may even improve the understanding of the mechanisms underlying human eye morphogenesis, including the development of myopia. However, the 2 pedigrees did not link to the four known loci for nanophthalmos and microphthalmia.

The six known POAG loci were also excluded in these 2 pedigrees. The exclusion of these POAG loci however, is perhaps not surprising. This is because POAG and PACG, though both leading to glaucoma, have different mechanisms. In PACG, the main pathology is the angle configuration, and glaucoma is thought to be secondary to the high IOP induced by angle closure. On the other hand, the angle configuration is normal in POAG, but there are other factors likely to be involved in the pathophysiology of the glaucomatous process such as increased outflow resistance at the angle, and optic nerve susceptibility to damage by increased IOP.

Apart from growth factors and other POAG loci and genes, it would be useful to propose other possible candidate genes or classes of genes for PACG. For example, there is some evidence that autonomic dysfunction may be a contributory factor in the development of pupil-block, and hence primary angle closure, as individuals with PACG have been found to have both ocular as well as systemic autonomic dysfunction (Clark, 1989; Clark, 1990). Thus it is speculated that a possible role for a PACG gene is in autonomic function. A gene related to intraocular inflammation may also be plausible. This is because eyes with angle closure get peripheral anterior synechiae (PAS) in the angles, which also occurs in inflammatory conditions of the eye such as uveitis, and one can hypothesize that eyes predisposed to PAS may develop angle closure.

The human genome project has made significant contributions to the mapping and characterisation of genes implicated in human disease. Once a disease locus has been genetically refined to a region, the identification of genes within this interval has been facilitated by positional candidate gene strategies utilising data of the sequence of the human genome that is continually updated on websites such as Ensembl (http://www.ensembl.org) and NCBI (http://www.ncbi.nlm.nih.gov). Using this approach, four genes, GDF10, SLC18A3, TIMM23 and ASAH2 were localised to be in the linked genetic interval. The genes were chosen based on their expression in the eye (for

SLC18A3, TIMM23 and ASAH2) and for function (GDF10). These genes were then analyzed and excluded as being responsible for PACG. The information about the position and annotation of these genes was obtained in July-August 2002 from Ensembl version 7.29 (Hubbard *et al.*, 2002). However, recent data from the latest sequence (Ensembl version 11 in February 2003) have since emerged that these 4 genes actually lie just **outside** the genetic interval. This new location of these genes outside the linked interval thus explains the exclusion of coding regions of these genes for the disease. The latest genetic map of the linked interval on chromosome 10 (constructed from Ensembl version 11) is shown below in Figure 8.5.

Three known genes, ACF, PRKG1 and DKK1, as well as 4 predicted genes, Q9P136, NM_018505, NM_014114 and Q96MTO, are now localized to be in this linked interval. The ACF (apobec-1 complementation factor) gene product functions as an RNA-binding subunit and the protein may be involved in RNA editing or RNA processing events. PRKG1 (protein kinase, cGMP-dependent, type I gene) is a type I cGMP-dependent protein kinase that is involved in vascular smooth muscle tone and inhibition of platelet aggregation. The DKK1 (dickkopf homolog 1) gene is involved in Wnt signalling and may influence DNA alkylation damage. None of these genes are obvious candidates for PACG. However, due to the localisation of these genes in the linked interval, they will be screened for mutations.

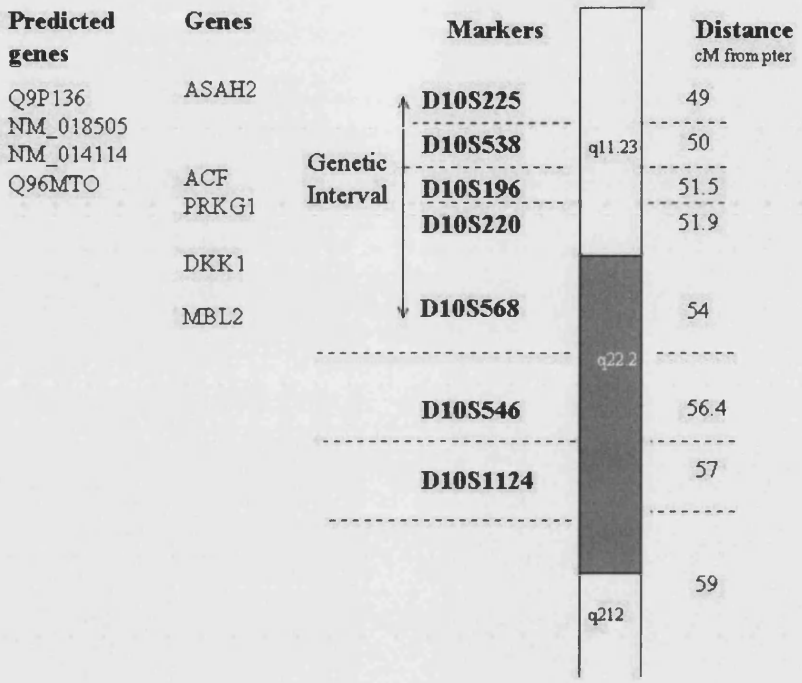

Figure 8.5. Latest genetic map for the linked PACG interval (constructed in February 2003). Predicted genes are in the extreme left column, known genes are in the next column, microsatellites are in bold, genetic distances in cM shown in the right column.

Chapter 9

GENERAL DISCUSSION

9.1. Overview of the research

Molecular genetics involves the identification of disease-causing genes, and the application of this information to unravel the pathophysiology of diseases. While the traditional approach to understanding disease has been 'outside in' i.e. a clinical observation spurs the formation of a hypothesis which is then tested, it is now possible to dissect a disease from the 'inside out' i.e. identify the molecular basis first, and then understand the disease pathophysiology and clinical implications. This approach has been a recurring feature of the research presented in this thesis, a summary of which is detailed below.

Single nucleotide polymorphisms on intervening sequence (IVS) 8 of the *OPA1* gene (genotype IVS 8 +4 C/T; +32 T/C) were found to be strongly associated with a fifth of normal tension glaucoma (NTG) cases and may be a marker for disease association, providing the first evidence of an association between *OPA1* and NTG. However this *OPA1* genotype was not found to be significantly associated with high tension glaucoma (HTG). Further work did not detect a significant difference in a range of phenotypic features in NTG patients with and without these *OPA1* polymorphisms, suggesting that these specific genetic variations do not underlie any major phenotypic diversity in NTG.

Although *Optineurin* (*OPTN*) gene variants were recently found in almost 15% of families with POAG (predominantly NTG), this prevalence was not replicated when a large panel of 315 adult POAG subjects were examined for the 2 most common *OPTN* sequence variants, E50K and M98K. The E50K

mutation was identified in only 1.5% of NTG subjects, making it an infrequent cause of sporadic NTG. The M98K variant was found to be associated specifically with NTG but not HTG, suggesting genetic heterogeneity between these 2 phenotypes. A characteristic NTG phenotype comprising a young-adult age of onset, advanced visual loss and progressive disease, was found in individuals carrying the E50K *OPTN* mutation.

Finally, two large Singaporean families with primary angle closure glaucoma (PACG) were examined by linkage analysis. The first locus for the disease was identified on chromosome 10, and the disease interval was refined to 5.0 cM on chromosome 10q11 flanked by the markers D10S225 and D10S568, with the maximum LOD score of 3.4 at θ=0 for D10S220. Several genes, *GDF10, TIM23, SLC18A3* and *ASAH2* were excluded as candidates for this condition.

9.2. Molecular genetic approaches towards identifying disease-causing genes

Identifying a disease-causing gene is a formidable task, given the complexity of the human genome. The route chosen for the identification of the disease gene rests on the type of information known about the disease. Two different approaches were employed in this research. The first method was the "candidate gene" approach, in which a biologically plausible candidate gene, *OPA1,* was tested directly for mutations in NTG subjects, on the basis that dominant optic atrophy and NTG share similarities in the phenotype. This approach led to the identification of an association between NTG and *OPA1* intronic polymorphisms. These polymorphisms are not likely to be directly causative of disease but may be may be a marker for disease association. It is thought that indirect mechanisms may be present, possibly by conferring

susceptibility in patients to other factor(s) that mediate the disease. In general, the candidate gene approach is limited by the fact that the number of identified genes with a known function represents only a small fraction of the estimated total number of genes in the human genome. In addition, there are a large number of disorders where the underlying cause and mechanism is not well understood. This approach may also be complicated by genetic heterogeneity and if a particular disease results from a combination of mutations in more than one gene.

The second approach used in this research was the "positional cloning" approach that compares within a family, the inheritance of a disease gene with the inheritance of specific DNA markers, and relies solely upon identifying the disease gene by its location in the genome rather than by its functional properties. What are required are precise diagnostic criteria and large families with affected individuals. Clear diagnostic criteria are critical to separate affected, suspect and unaffected individuals because misclassification can seriously undermine genetic linkage efforts. This method is laborious and time consuming, but has recently been increasingly successful due to the efforts from the Human Genome Project initiative, namely the production of high resolution genetic and physical maps which aid localisation of disease genes. Using this approach, a first locus for PACG was identified on chromosome 10. Potential genes have been investigated in the genetic interval and the disease gene may be identified with further work in the future.

9.3. Advances in the human genome project

The human genome project has made a significant contribution to the mapping and characterization of genes implicated in human disease through microsatellite analysis, physical mapping and ultimately genome sequencing. Novel microsatellite markers are now easier to identify with the new

information available. In addition, these markers are now supplemented by high-density single nucleotide polymorphism (SNP) maps enabling the fine mapping of disease loci, which has greatly enhanced the prospects of studying multifactorial or complex traits (Chanock, 2001). Once a disease locus has been genetically refined to the smallest region possible, the identification of genes within this interval has been facilitated by knowledge of the sequence of the human genome. Using this data, positional candidate gene strategies can be employed to identify and prioritize possible disease genes that map to the critical disease interval.

The human genome was estimated to be comprised of 60-80 000 genes (Fields *et al.,* 1994). However, the publication of the first draft sequence of the human genome (Lander *et al.,* 2001; Venter *et al.,* 2001) led to the revised estimate of 30-40 000 genes. Recently, Wiemann and colleagues (2001) sequenced 500 novel cDNAs and when these sequences were aligned to the sequences of finished chromosomes 21 and 22 a large proportion of the novel cDNAs had either been completely missed by the bioinformatic analysis of the genomic sequencing or had been incorrectly predicted. If this finding is extrapolated to the remaining chromosomes in the genome, then perhaps the estimate of 30-40 000 genes was too conservative. In addition, the complexity of the human genome, with many alternatively spliced products, translates to a greater number of proteins with modified locations and/or functions than first thought.

The frequent revisions, adjustments and evolution of the data derived from the Human Genome Project were well illustrated in the research presented. For example, sequence data derived from the Human Genome Project and pertaining to the linked genetic interval on chromosome 10, was not at the completed stage at the time of positional candidate gene identification. New data was regularly added and modified during the period of the research according to the progress of the Human Genome sequencing. The genetic map

of the linked interval constructed in 2002 thus differed from that in 2003. This led to genes thought to be in the linked interval to be erroneously sequenced. It is likely that the completion of the Human Genome Project in the coming year or two will greatly improve the chances of identifying the gene responsible for PACG.

As individual research groups take on the challenge of in depth functional analysis of gene and protein families ('post genomics'), bioinformatic tools are likely to become more accurate but will also evolve with the research. This in turn will aid annotation of cDNA and protein, as well as genomic sequence. In the post genomic era, the techniques collectively known as proteomics are useful for characterizing the protein phenotype of a particular tissue or cell, as well as quantitatively identifying differences in the levels of individual proteins following modulation of a tissue or cell. These tools will enable us to monitor changes in the expression of a given protein(s) and its post-translational modification, identify novel therapeutic targets and evaluate pharmacological effects on a given metabolic pathway. These technologies are now set to provide us with an immense amount of data for future analysis, which will hopefully pave the way to further understanding disease pathogenesis and therapies.

9.4. Heterogeneity of glaucoma

The molecular genetic studies described in this thesis encompassed the two main forms of glaucoma worldwide, POAG and PACG, and the findings highlight the genetic and phenotypic heterogeneity of glaucoma.

In POAG, there is controversy as to whether NTG and HTG are separate disease entities, or if they represent different ends of the phenotypic spectrum of POAG. While some studies have found that the conditions

cannot be distinguished in terms of clinical behaviour or pathophysiology (Motolko *et al.*, 1982; Lewis *et al.*, 1983; Miller and Quigley, 1987; Fazio *et al.*, 1990), other reports have noted optic disc and visual field differences between patients with HTG and NTG (Caprioli and Spaeth, 1984, Caprioli and Spaeth, 1985; Chauhan *et al.*, 1989; Tuulonen and Airaksinen, 1992; Edi *et al.*, 1997). The association of *OPA1* polymorphisms, IVS 8 +4 C/T; +32 T/C, and the M98K *OPTN* variant specifically with NTG but not HTG suggests genetic and/or allelic heterogeneity between these 2 phenotypes, and may be evidence that the diseases are distinct entities. Such genetic differences may imply different mechanisms of optic nerve damage, possibly by affecting susceptibility to factor(s) that mediate glaucoma.

For PACG, the first locus for this condition was found on chromosome 10 (Chapter 8). The finding that the second pedigree (Pedigree 2) did not link to this same locus suggests the existence of another genetic locus for this family, and is also evidence of genetic heterogeneity for PACG.

9.5. Genotype / Phenotype correlation

Research in molecular genetics unlocks the underlying mechanisms and inter-relationships of disease phenotypes at a molecular level. The knowledge of the clinical behavior of specific mutations is particularly helpful in disease management by providing patients and clinicians with useful information regarding the course and prognosis of their disease. A correlation between specific mutations in *MYOC* and the clinical course of glaucoma has been previously described (Alward *et al.*, 1998; Allingham *et al.*, 1998; Angius *et al.*, 2000; Craig *et al.*, 2001). In this research, a correlation between genotype and phenotype has been identified that is likely to be useful in predicting the course and prognosis of disease caused by the *OPTN* E50K mutation. The characteristic NTG phenotype produced

by this mutation comprises a young-adult age of onset, advanced visual loss and progressive disease, and it remains to be seen if other specific features distinguishing those with and without the mutation will become apparent in the future. With more detailed phenotyping and longer follow-up, it may even be possible to provide information on the rate of disease progression and the likely response of a given individual to specific or pharmacological agents (conventional and novel) or the need for early surgery.

9.6. The role of the clinician in the age of molecular genetics

The clinician plays a pivotal role alongside scientists in the process of gene discovery. Accurate phenotyping and establishment of precise diagnostic criteria by clinicians are essential first steps in genetic studies. The clinician can identify suitable pedigrees, sib-pairs and individual subjects for such studies, as well as enquire about family history in all patients to find disorders with a familial aggregation. Based on the knowledge obtained regarding the genetic mutation and relevant genetic epidemiological information, clinicians can identify genotype-phenotype correlations, which will be useful in counseling patients regarding the natural history of the disease and the identification of at risk individuals in the family. More detailed counseling may be given to patients regarding the risk of having children who will manifest the same disorder. Other vital roles for clinicians will be to develop and evaluate diagnostic tests, to help elucidate disease pathophysiology, and to develop novel pharmacological therapies based on molecular genetic findings.

9.7. Future perspectives for glaucoma genetics

Much progress has been achieved over the past few years on understanding the genetic basis of glaucoma and glaucoma-related disorders. Undoubtedly the answers will be far more complex than can be imagined at our current state of knowledge. Multiple putative genes on chromosomal loci linked to glaucoma have yet to be identified. As more pedigrees are studied and candidate genes analysed, new glaucoma-causing genes will be identified. As we continue to understand more about the known genes, we undoubtedly will learn more about the mechanisms of different types of glaucoma and their interactions. It is likely that isolation of the genes and characterization of the gene products concerned with glaucoma will offer considerable insight into retinal and optic nerve susceptibility factors in the disease process.

Recent developments in microarray technology, sequencing of the human genome, and bioinformatics may enhance our investigations into the genetic basis of glaucoma. The advent of more cost- and time-efficient mutation screening strategies may enable a more generalized population-based screening to be developed to identify at-risk individuals. The emerging field of pharmacogenetics holds promise to determine which therapeutic interventions are most likely to be effective in a given patient. Therapeutic application of this work (gene therapy) is not on the immediate horizon for glaucoma and is likely to require long-term expression capabilities. Nonetheless, the prospect of being able to correct or compensate for an underlying molecular defect in certain situations, thereby preventing the onset of disease or reversing early changes, is indeed exciting, and will find its niche among the methods to treat and possibly cure glaucoma. Finally genetic approaches to slow or prevent neuronal damage in glaucoma may provide another front for research. It is hoped that all these advances derived from molecular genetics will lead to improved understanding of the molecular basis of the disease, better treatments and even cures to conquer this major cause of world blindness.

References

Akarsu AN, Turacli ME, Aktan SG, Barsoum-Homsy M, Chevrette L, Sayli BS, Sarfarazi M. A second locus (GLC3B) for primary congenital glaucoma maps to the 1p36 region. Hum Mol Genet 1996; 5: 1199-1203

Alexander C, Votruba M, Pesch UE, Thiselton DL, Mayer S, Moore A, Rodriguez M, Rodriguez M, Kellner U, Leo-Kottler B, Auburger G, Bhattacharya SS, Wissinger B. OPA1, encoding a dynamin-related GTPase is mutated in autosomal dominant optic atrophy (OPA1) linked to chromosome 3q28. Nat Genet 2000; 26: 211-215

Allikmets R. Further evidence for an association of ABCR alleles with age-related macular degeneration. The International ABCR Screening Consortium. Am J Hum Genet 2000; 67: 487-91

Allingham RR, Wiggs JL, De La Paz MA, Vollrath D, Tallett DA, Broomer B, Jones KH, Del Bono EA, Kern J, Patterson K, Haines JL, Pericak-Vance MA. Gln368STOP myocilin mutation in families with late-onset primary open-angle glaucoma. Invest Ophthalmol Vis Sci 1998; 39: 2288-95

Alsbirk PH. Anterior chamber depth in Greenland Eskimos. I. A population study of variation with age and sex. Acta Ophthalmol 1974; 52: 551-564

Alsbirk PH. Anterior chamber depth in Greenland Eskimos. II. Geographical and ethnic variations. Acta Ophthalmol 1974; 52: 565-580

Alsbirk PH. Anterior chamber depth, genes and environment: a population study among long-term Greenland Eskimo immigrants in Copenhagen. Acta Ophthalmol (Copenh) 1975; 53: 223-234

Alsbirk PH. Anterior chamber depth and primary angle closure glaucoma: A genetic study. Acta Ophthalmol (Copenh) 1975; 53: 436-449

Alsbirk PH. Primary angle closure glaucoma: oculometry, epidemiology and genetics in a high-risk population. Acta Ophthalmol (Copenh) 1976; suppl 127: 5-31

Alward WLM, Fingert JH, Coote MA, et al. Clinical features associated with mutations in the chromosome 1 open angle glaucoma gene (GLC1A). N Engl J Med 1998; 338: 1022-7

Alward WL, Kwon YH, Khanna CL, Johnson AT, Hayreh SS, Zimmerman MB, Narkiewicz J, Andorf JL, Moore PA, Fingert JH, Sheffield VC, Stone

EM. Variations in the myocilin gene in patients with open-angle glaucoma. Arch Ophthalmol 2002; 120: 1189-97

Anderson DR. Glaucoma: the damage caused by pressure. XLVI Edward Jackson Memorial Lecture. Am J Ophthalmol 1989; 108: 485-95

Angius A, Spinelli P, Ghilotti G, Casu G, Sole G, Loi A, Totaro A, Zelante L, Gasparini P, Orzalesi N, Pirastu M, Bonomi L. Myocilin Gln368stop mutation and advanced age as risk factors for late-onset primary open-angle glaucoma. Arch Ophthalmol 2000; 118: 674-9

Arkell SM, Lightman DA, Sommer A, Taylor HR, Korshin OM, Tielsch JM. The prevalence of glaucoma among eskimos of Northwest Alaska. Arch Ophthalmol 1987; 105: 482-485

Aung T, Looi AL, Chew PT. The visual field following acute primary angle closure. Acta Ophthalmol Scand 2001; 79: 298-300

Bailly S, Israel N, Fay M, Gougerot-Pocidalo MA, Duff GW. An intronic polymorphic repeat sequence modulates interleukin-1 alpha gene regulation. Mol Immunol 1996; 33: 999-1006

Becker B, Shaffer RN. Diagnosis and therapy of the glaucomas. St Louis: CV Mosby; 1965.

Bejjani BA, Lewis RA, Tomey KF, Anderson KL, Dueker DK, Jabak M, Astle WF, Otterud B, Leppert M, Lupski JR. Mutations in CYP1B1, the gene for cytochrome P4501B1, are the predominant cause of primary congenital glaucoma in Saudi Arabia. Am J Hum Genet. 1998; 62: 325-333

Bejjani BA, Stockton DW, Lewis RA, Tomey KF, Dueker DK, Jabak M, Astle WF, Lupski JR. Multiple CYP1B1 mutations and incomplete penetrance in an inbred population segregating primary congenital glaucoma suggest frequent de novo events and a dominant modifier locus. Hum Mol Genet. 2000; 9: 367-74

Bennett SR, Alward WL, Folberg R. An autosomal dominant form of low tension glaucoma. Am J Ophthalmol 1989; 108: 238-44

Bessant DA, Khaliq S, Hameed A, Anwar K, Mehdi SQ, Payne AM, Bhattacharya SS. A locus for autosomal recessive congenital microphthalmia maps to chromosome 14q32. Am J Hum Genet.1998; 62: 1113-1116

Bhandari A, Crabb DP, Poinoosawmy D, Fitzke FW, Hitchings RA, Noureddin BN. Effect of surgery on visual field progression in normal-tension glaucoma. Ophthalmology 1997; 104: 1131-1137

Bonomi L, Marchini G, Marraffa M, Bernardi P, De Franco I, Perfetti S, Varotto A, Tenna V. Prevalence of glaucoma and intraocular pressure distribution in a defined population. The Egna-Neumarkt Study. Ophthalmology 1998; 105: 209-15

Botstein D, White RL, Skolnick M, Davis RW. Construction of a genetic linkage map in man using restriction fragment length polymorphisms. Am J Hum Genet 1980; 32: 314-31

Bullido MJ, Artiga MJ, Recuero M, Sastre I, Garcia MA, Aldudo J, Lendon C, Han SW, Morris JC, Frank A, Vazquez J, Goate A, Valdivieso F. A polymorphism in the regulatory region of APOE associated with risk for Alzheimer's dementia. Nat Genet 1998; 18: 69-71

Caprioli J, Spaeth GL. Comparison of visual fields defects in low-tension glaucoma with those in high tension glaucomas. *Am J Ophthalmol* 1984; 97: 730-737

Caprioli J, Spaeth GL. Comparison of the optic nerve head in high- and low-tension glaucoma. Arch Ophthalmol 1985; 103: 1145-1149

Carter CJ, Brooks DE, Doyle DL, Drance SM. Investigations into a vascular etiology for low-tension glaucoma. Ophthalmology. 1990; 97: 49-55

Cartwright MJ, Anderson DR. Correlation of asymmetric damage with asymmetric intraocular pressure in normal-tension glaucoma (low-tension glaucoma). Arch Ophthalmol 1988; 106: 898-900

Chanock S. Candidate genes and single nucleotide polymorphisms (SNPs) in the study of human disease. Dis Markers 2001; 17: 89-98

Chauhan BC, Drance SM, Douglas GR, Johnson CA. Visual field damage in normal tension and high tension glaucoma. Am J Ophthalmol 1989; 108: 636-642

Clamp M, Andrews D, Barker D, Bevan P, Cameron G, Chen Y, Clark L, Cox T, Cuff J, Curwen V, Down T, Durbin R, Eyras E, Gilbert J, Hammond M, Hubbard T, Kasprzyk A, Keefe D, Lehvaslaiho H, Iyer V, Melsopp C, Mongin E, Pettett R, Potter S, Rust A, Schmidt E, Searle S, Slater G, Smith J, Spooner W, Stabenau A, Stalker J, Stupka E, Ureta-Vidal A, Vastrik I, Birney E.Ensembl 2002: accommodating comparative genomics. Nucleic Acids Res 2003; 31: 38-42

Clark CV. Autonomic denervation hypersensitivity in the primary glaucomas. Eye 1989; 3: 349-354

Clark CV. The prevalence of autonomic neuropathy in the primary glaucomas.

[Review]. Doc Ophthalmol 1990; 74: 277-285

Cohen-Haguenauer O, Brice A, Berrard S, Van Cong N, Mallet J, Frezal J. Localization of the choline acetyltransferase (CHAT) gene to human chromosome 10. Genomics 1990; 6: 374-378.

Collaborative Normal-Tension Glaucoma Study Group. Comparison of glaucomatous progression between untreated patients with normal-tension glaucoma and patients with therapeutically reduced intraocular pressures [see comments]. Am J Ophthalmol 1998; 126: 487-97

Collaborative NTG Study Group, The effectiveness of IOP reduction in the treatment of NTG. Am J Ophthalmol 1998; 126: 498–505.

Congdon N, Wang F, Tielsch JM: Issues in the epidemiology and population based screening of primary angle-closure glaucoma. Surv Ophthalmol 1992; 36: 411-423

Copt RP, Thomas R, Mermoud A. Corneal thickness in ocular hypertension, primary open-angle glaucoma, and normal tension glaucoma. Arch Ophthalmol 1999; 117: 14-16

Craig JE, Mackey DA. Glaucoma genetics: where are we? Where will we go? Curr Opin Ophthalmol 1999; 10: 126-34

Craig JE, Baird PN, Healey DL, McNaught AI, McCartney PJ, Rait JL, Dickinson JL, Roe L, Fingert JH, Stone EM, Mackey DA. Evidence for genetic heterogeneity within eight glaucoma families, with the GLC1A Gln368STOP mutation being an important phenotypic modifier. Ophthalmology 2001; 108: 1607-20

Cruts M, Backhovens H, Martin JJ, van Broeckhoven C. Genetic analysis of the cellular oncogene fos in patients with chromosome 14 encoded Alzheimer's disease. Neurosci Lett 1994; 174: 97-100

Cunningham NS, Jenkins NA, Gilbert DJ, Copeland NG, Reddi AH, Lee SJ. Growth/differentiation factor-10: a new member of the transforming growth factor-beta superfamily related to bone morphogenetic protein-3. Growth Factors 1995; 12: 99-109

Dandona L, Dandona R, Mandal P, Srinivas M, John RK, McCarty CA, Rao GN. Angle closure glaucoma in an urban population in Southern India. The Andhra Pradesh Eye Disease Study. Ophthalmology 2000; 107: 1710-6

Delettre C, Lenaers G, Griffoin JM, Gigarel N, Lorenzo C, Belenguer P, Pelloquin L, Grosgeorge J, Turc-Carel C, Perret E, Astarie-Dequeker C, Lasquellec L, Arnaud B, Ducommun B, Kaplan J, Hamel CP. Nuclear gene

OPA1, encoding a mitochondrial dynamin-related protein, is mutated in dominant optic atrophy. Nat Genet 2000; 26: 207-210

Dib C, Faure S, Fizames C, Samson D, Drouot N, Vignal A, Millasseau P, Marc S, Hazan J, Seboun E, Lathrop M, Gyapay G, Morissette J,nWeissenbach J. A comprehensive genetic map of the human genome based on 5,264 microsatellites. Nature 1996; 380: 152-4

Donzeau M, Kaldi K, Adam A, Paschen S, Wanner G, Guiard B, Bauer MF, Neupert W, Brunner M. Tim23 links the inner and outer mitochondrial membranes. Cell 2000; 101: 401-412

Douglas GR, Drance SM, Schulzer M. The visual field and nerve head in angle-closure glaucoma. A comparison of the effects of acute and chronic angle closure. Arch Ophthalmol 1975; 93: 409-411

Drance SM. some factors in the production of low tension glaucoma. Br J Ophthalmol 1972; 56: 229-42

Drance SM, Sweeney VP, Morgan RW, Feldman F. Studies of factors involved in the production of low tension glaucoma. Arch Ophthalmol 1973; 89:457-65

Drance SM, Douglas GR, Wijsman K, Schulzer M, Britton RJ. Response of blood flow to warm and cold in normal and low-tension glaucoma patients. Am J Ophthalmol 1988; 105: 35-9

Edi TE, Spaeth GL, Moster MR, Augsburger JJ. Quantitative differences between the optic nerve head and peripapillary retina in low-tension and high-tension primary open angle glaucoma. Am J Ophthalmol 1997; 124: 805-813

Eiberg H, Kjer B, Kjer P, Rosenberg T. Dominant optic atrophy (OPA1) mapped to chromosome 3q region. I. Linkage analysis. Hum Mol Genetics 1994; 3: 977-980

Erickson JD, Varoqui H, Schafer MKH, Modi W, Diebler MF, Weihe E, Rand J, Eiden LE, Bonner TI, Usdin TB. Functional identification of a vesicular acetylcholine transporter and its expression from a 'cholinergic' gene locus. J Biol Chem 1994; 269: 21929-21932

Fazio P, Krupin T, Feitl ME, Werner EB, Carre DA. Optic disc topography in patients with low-tension and primary open angle glaucoma. Arch Ophthalmol 1990; 108: 705-708

Fields C, Adams MD, White O, Venter JC. How many genes in the human genome? Nat Genet 1994; 7: 345-6.

Fingert JH, Heon E, Liebmann JM, Yamamoto T, Craig JE, Rait J, Kawase K, Hoh ST, Buys YM, Dickinson J, Hockey RR, Williams-Lyn D, Trope G, Kitazawa Y, Ritch R, Mackey DA, Alward WL, Sheffield VC, Stone EM. Analysis of myocilin mutations in 1703 glaucoma patients from five different populations. Hum Mol Genet 1999; 8: 899-905

Fitzke FW, Hitchings RA, Poinoosawmy D, McNaught AI, Crabb DP. Analysis of visual-field progression in glaucoma. Br J Ophthalmol 1996; 80: 40-8

Foster PJ, Baasanhu J, Alsbirk PH, Munkhbayar D, Uranchimeg D, Johnson GJ. Glaucoma in Mongolia-a population-based survey in Hovsgol Province, Northern Mongolia. Arch Ophthalmol 1996; 114: 1235-41

Foster PJ, Oen FT, Machin D, Ng TP, Devereux JG, Johnson GJ, Khaw PT, Seah SK. The prevalence of glaucoma in Chinese residents of Singapore: a cross-sectional population survey of the Tanjong Pagar district. Arch Ophthalmol 2000; 118:1105-11

Foster PJ, Johnson GJ. Primary angle-closure-classification and clinical features. In: Hitchings RA, ed. Glaucoma. London: BMJ Publishing Group, 2000.

Foster PJ, Buhrmann RR, Quigley HA, Johnson GJ. The definition of glaucoma in prevalence surveys. Br J Ophthalmol 2002; 86: 238-42

Foster PJ, Johnson GJ. Glaucoma in China: how big is the problem? Br J Ophthalmol 2001; 85: 1277-82

Francois J. Multifactorial or polygenic inheritance in ophthalmology. In: Henkind P, ed. Acta: 24th International Congress of Ophthalmology, 1982, vol. 1 Philadelphia: Lippincott, 1983: 1-24.

Gottfredsdottir MS, Sverrisson T, Musch DC, Steffansson E. Chronic open angle glaucoma and associated ophthalmic findings in monozygotic twins and their spouses in Iceland. J Glaucoma 1999; 8:134-9.

Graham SL, Drance SM, Wijsman K, Douglas GR, Mikelberg FS. Ambulatory blood pressure monitoring in glaucoma: the nocturnal dip. Ophthalmology 1995; 102: 61-9

Haldi ML, Strickland C, Lim P, VanBerkel V, Chen X, Noya D, Korenberg JR, Husain Z, Miller J, Lander ES. A comprehensive large-insert yeast artificial chromosome library for physical mapping of the mouse genome. Mamm Genome 1996; 7: 767-9

Hamard P, Hamard H, Dufaux J, Quesnot S. Optic nerve head blood flow using a laser Doppler velocimeter and haemorheology in primary open angle glaucoma and normal pressure glaucoma. Br J Ophthalmol 1994; 78: 449-53

Hayreh SS, Zimmerman MB, Podhajsky P, Alward WL. Nocturnal arterial hypotension and its role in optic nerve head and ocular ischaemic disorders. Am J Ophthalmol 1994; 117: 603-24

Henderson JO, Blanc V, Davidson NO. Isolation, characterization and developmental regulation of the human apobec-1 complementation factor (ACF) gene. Biochim Biophys Acta 2001; 1522: 22-30

Heon E, Sheth BP, Kalenak JW, Sunden SL, Streb LM, Taylor CM, Alward WL, Sheffield VC, Stone EM.Linkage of autosomal dominant iris hypoplasia to the region of the Rieger syndrome locus (4q25). Hum Molec Genet 1995; 4: 1435-1439

Hernandez MR, Pena JD. The optic nerve head in glaucomatous optic neuropathy. Arch Ophthalmol 1997;115:389–95.

Hitchings RA, Wu J, Poinoosawmy D, McNaught A. Surgery for normal tension glaucoma. Br J Ophthalmol 1995; 79: 402-406

Horikawa Y, Oda N, Cox NJ, Li X, Orho-Melander M, Hara M, Hinokio Y, Lindner TH, Mashima H, Schwarz PE, del Bosque-Plata L, Horikawa Y, Oda Y, Yoshiuchi I, Colilla S, Polonsky KS, Wei S, Concannon P, Iwasaki N, Schulze J, Baier LJ, Bogardus C, Groop L, Boerwinkle E, Hanis CL, Bell GI. Genetic variation in the gene encoding calpain-10 is associated with type 2 diabetes mellitus. Nat Genet 2000; 26: 163-75

Hu Z, Zhao ZL, Dong FT. An epidemiological investigation of glaucoma in Beijing and Shun-Yi county. Chin J Ophthalmol 1989; 25: 115-8

Hubbard T, Barker D, Birney E, Cameron G, Chen Y, Clark L, Cox T, Cuff J, Curwen V, Down T, Durbin R, Eyras E, Gilbert J, Hammond M, Huminiecki L, Kasprzyk A, Lehvaslaiho H, Lijnzaad P, Melsopp C, Mongin E, Pettett R, Pocock M, Potter S, Rust A, Schmidt E, Searle S, Slater G, Smith J, Spooner W, Stabenau A, Stalker J, Stupka E, Ureta-Vidal A, Vastrik I, Clamp M. The Ensembl genome database project. Nucleic Acids Res 2002; 30: 38-41.

Jacob A, Thomas R, Koshi SP, Braganza A, Muliyil J. Prevalence of primary glaucoma in an urban south Indian population. Indian J Ophthalmol 1998; 46: 81-6

Jay JL, Murdoch JR. The rate of visual field loss in untreated primary open angle glaucoma. Br J Ophthalmol 1993; 77: 176-8

Jeffreys AJ, Wilson V, Thein SL. Hypervariable 'minisatellite' regions in human DNA. Nature 1985; 314: 67-73

Johnston PB, Gaster RN, Smith VC, Tripathi RC. A clinicopathologic study of autosomal dominant optic atrophy. Am J Ophthalmol 1979; 88: 868-75

Jonasdottir A, Eiberg H, Kjer B, Kjer P, Rosenberg T. Refinement of the dominant optic atrophy locus (OPA1) to a 1.4-cM interval on chromosome 3q28-3q29, within a 3-Mb YAC contig. Hum Genet 1997; 99: 115-120

Jordan BR. Genome programmes: an opportunity for biology. Biomed Pharmacother 1994; 48: 183-90

Kamal D, Hitchings R. Normal tension glaucoma- a practical approach. Br J Ophthalmol 1998; 82: 835-840

Keen J, Lester D, Inglehearn C, Curtis A, Bhattacharya SS. Rapid detection of single base mismatches as heteroduplexes on Hydrolink gels. Trends Genet 1991; 7: 5

Kerrison JB, Arnould VJ, Ferraz Sallum JM, Vagefi MR, Barmada MM, Li Y, Zhu D, Maumenee IH. Genetic heterogeneity of dominant optic atrophy, Kjer type: Identification of a second locus on chromosome 18q12.2-12.3. Arch Ophthalmol 1999; 117: 805-810

Kim BS, Savinova OV, Reedy MV, Martin J, Lun Y, Gan L, Smith RS, Tomarev SI, John SW, Johnson RL. Targeted Disruption of the Myocilin Gene (Myoc) Suggests that Human Glaucoma-Causing Mutations Are Gain of Function. Mol Cell Biol. 2001;21:7707-13.

Kjer P, Jensen OA, Klinken L. Histopathology of eye, optic nerve and brain in a case of dominant optic atrophy. Acta Ophthalmol (Copenh) 1983; 61: 300-312

Klein BE, Klein R, Sponsel WE, Franke T, Cantor LB, Martone J, Menage MJ.Prevalence of glaucoma. The Beaver Dam Eye Study. Ophthalmology 1992; 99: 1499-1504

Koseki N, Araie M, Shirato S, Yamamoto S. Effect of trabeculectomy on visual field performance in central 30 degrees field in progressive normal-tension glaucoma. Ophthalmology 1997; 104: 197-201

Kozlowski K, Walter MA. Variation in residual PITX2 activity underlies the phenotypic spectrum of anterior segment developmental disorders. Hum Mol Genet 2000; 9: 2131-9

Kubota R, Noda S, Wang Y, Minoshima S, Asakawa S, Kudoh J, Mashima Y, Oguchi Y, Shimizu N. A novel myosin-like protein (myocilin) expressed in the connecting cilium of the photocreceptor: molecular cloning, tissue expression and chromosomal mapping. Genomics 1997; 41: 360-9

Kulak SC, Kozlowski K, Semina EV, Pearce WG, Walter MA. Mutation in the RIEG1 gene in patients with iridogoniodysgenesis syndrome. Hum Molec Genet 1998; 7: 1113-1117

Lander ES. The new genomics: global views of biology. Science 1996; 274: 536-9

Lander ES, Linton LM, Birren B, Nusbaum C, Zody MC, Baldwin J, Devon K, Dewar K, Doyle M, FitzHugh W, Funke R, Gage D, Harris K, Heaford A, Howland J, Kann L, Lehoczky J, LeVine R, McEwan P, McKernan K, Meldrim J, Mesirov JP, Miranda C, Morris W, Naylor J, Raymond C, Rosetti M, Santos R, Sheridan A, Sougnez C, Stange-Thomann N, Stojanovic N, Subramanian A, Wyman D, Rogers J, Sulston J, Ainscough R, Beck S, Bentley D, Burton J, Clee C, Carter N, Coulson A, Deadman R, Deloukas P, Dunham A, Dunham I, Durbin R, French L, Grafham D, Gregory S, Hubbard T, Humphray S, Hunt A, Jones M, Lloyd C, McMurray A, Matthews L, Mercer S, Milne S, Mullikin JC, Mungall A, Plumb R, Ross M, Shownkeen R, Sims S, Waterston RH, Wilson RK, Hillier LW, McPherson JD, Marra MA, Mardis ER, Fulton LA, Chinwalla AT, Pepin KH, Gish WR, Chissoe SL, Wendl MC, Delehaunty KD, Miner TL, Delehaunty A, Kramer JB, Cook LL, Fulton RS, Johnson DL, Minx PJ, Clifton SW, Hawkins T, Branscomb E, Predki P, Richardson P, Wenning S, Slezak T, Doggett N, Cheng JF, Olsen A, Lucas S, Elkin C, Uberbacher E, Frazier M, Gibbs RA, Muzny DM, Scherer SE, Bouck JB, Sodergren EJ, Worley KC, Rives CM, Gorrell JH, Metzker ML, Naylor SL, Kucherlapati RS, Nelson DL, Weinstock GM, Sakaki Y, Fujiyama A, Hattori M, Yada T, Toyoda A, Itoh T, Kawagoe C, Watanabe H, Totoki Y, Taylor T, Weissenbach J, Heilig R, Saurin W, Artiguenave F, Brottier P, Bruls T, Pelletier E, Robert C, Wincker P, Smith DR, Doucette-Stamm L, Rubenfield M, Weinstock K, Lee HM, Dubois J, Rosenthal A, Platzer M, Nyakatura G, Taudien S, Rump A, Yang H, Yu J, Wang J, Huang G, Gu J, Hood L, Rowen L, Madan A, Qin S, Davis RW, Federspiel NA, Abola AP, Proctor MJ, Myers RM, Schmutz J, Dickson M, Grimwood J, Cox DR, Olson MV, Kaul R, Raymond C, Shimizu N, Kawasaki K, Minoshima S, Evans GA, Athanasiou M, Schultz R, Roe BA, Chen F, Pan H, Ramser J, Lehrach H, Reinhardt R, McCombie WR, de la Bastide M, Dedhia N, Blocker H, Hornischer K, Nordsiek G, Agarwala R, Aravind L, Bailey JA, Bateman A, Batzoglou S, Birney E, Bork P, Brown DG, Burge CB, Cerutti L, Chen HC, Church D, Clamp M, Copley RR, Doerks T, Eddy SR, Eichler EE, Furey TS, Galagan J, Gilbert JG, Harmon C, Hayashizaki Y, Haussler D, Hermjakob H, Hokamp K, Jang W, Johnson LS, Jones TA, Kasif S, Kaspryzk A, Kennedy S, Kent WJ, Kitts P, Koonin EV, Korf I, Kulp D, Lancet D, Lowe TM, McLysaght A, Mikkelsen T, Moran JV, Mulder N, Pollara VJ, Ponting CP,

Schuler G, Schultz J, Slater G, Smit AF, Stupka E, Szustakowski J, Thierry-Mieg D, Thierry-Mieg J, Wagner L, Wallis J, Wheeler R, Williams A, Wolf YI, Wolfe KH, Yang SP, Yeh RF, Collins F, Guyer MS, Peterson J, Felsenfeld A, Wetterstrand KA, Patrinos A, Morgan MJ, Szustakowki J, de Jong P, Catanese JJ, Osoegawa K, Shizuya H, Choi S, Chen YJ; International Human Genome Sequencing Consortium.. Initial sequencing and analysis of the human genome. Nature 2001; 409: 860-921

Lathrop GM, Lalouel JM. Easy calculations of lod scores and genetic risks on small computers. Am J Hum Genet 1984; 36: 460-465

Lee BL, Zangwill L, Weinreb RN. Change in optic disc topography associated with diurnal variation in intraocular pressure. J Glaucoma 1999;8:221-3.

Lee GA, Khaw PT, Ficker LA, Shah P. The corneal thickness and intraocular pressure story: where are we now? Clin Experiment Ophthalmol 2002; 30: 334-7

Lehmann OJ, Ebenezer ND, Jordan T, Fox M, Ocaka L, Payne A, Leroy BP, Clark BJ, Hitchings RA, Povey S, Khaw PT, Bhattacharya SS. Chromosomal duplication involving the forkhead transcription factor gene FOXC1 causes iris hypoplasia and glaucoma. Am J Hum Genet 2000; 67: 1129-35

Leighton DA. Survey of the first-degree relatives glaucoma patients. Trans Ophthalmol Soc UK 1976; 96: 28-32

Leske MC, Connell AM, Wu SY, Hyman LG, Schachat AP. Risk factors for open-angle glaucoma. The Barbados Eye Study. Arch Ophthalmol 1995; 113: 918-24

Levin LA. Retinal ganglion cells and neuroprotection for glaucoma. Surv Ophthalmol 2003;48: S21-24.

Lewis RA, Hayreh SS, Phelps CD. Optic disk and visual field correlations in primary open-angle and low-tension glaucoma. Am J Ophthalmol 1983; 96: 148-52.

Litt M, Luty JA. A hypervariable microsatellite revealed by in vitro amplification of a dinucleotide repeat within the cardiac muscle actin gene. Am J Hum Genet 1989; 44: 397-401

Liu JH, Kripke DF, Twa MD, Hoffman RE, Mansberger SL, Rex KM, Girkin CA, Weinreb RN. Twenty-four-hour pattern of intraocular pressure in the aging population. Invest Ophthalmol Vis Sci. 1999;40:2912-7.

Lowe RF. Primary angle-closure glaucoma: family histories and anterior chamber depths. Br J Ophthalmol 1964; 48: 191-5

Lowe RF. Causes of shallow anterior chamber in primary angle closure glaucoma. Ultrasonic biometry of normal and angle-closure eyes. Am J Ophthalmol 1969; 67: 87-93

Lowe RF. Primary angle-closure glaucoma: inheritance and environment. Br J Ophthalmol 1972; 56: 13-20

Lowe RF. Primary angle-closure glaucoma: A review of ocular biometry. Aust J Ophthalmol 1977; 5: 9-17

Lowe RF. Clinical types of primary angle-closure glaucoma. Aust NZ J Ophthalmol 1988; 16: 245-50

Mason RP, Kosoko O, Wilson MR, Martone JF, Cowan CL Jr, Gear JC, Ross-Degnan D. National survey of the prevalence and risk factors of glaucoma in St Lucia, West Indies. I. Prevalence findings. Ophthalmology 1989; 96: 1363-8

McNaught AI, Allen JG, Healey DL, McCartney PJ, Coote MA, Wong TL, Craig JE, Green CM, Rait JL, Mackey DA. Accuracy and implications of a reported family history of glaucoma: experience from the Glaucoma Inheritance Study in Tasmania. Arch Ophthalmol 2000; 118: 900-4

Membrey WL, Poinoosawmy DP, Bunce C, Fitzke FW, Hitchings RA. Comparison of visual field progression in patients with normal pressure glaucoma between eyes with and without visual field loss that threatens fixation. Br J Ophthalmol 2000; 84: 1154-8.

Membrey WL, Bunce C, Poinoosawmy DP, Fitzke FW, Hitchings RA. Glaucoma surgery with or without adjunctive antiproliferatives in normal tension glaucoma: 2. Visual field progression. Br J Ophthalmol 2001; 85: 696-701

Meyer JH, Brandi-Dohrn J, Funk J. Twenty four hour blood pressure monitoring in normal tension glaucoma. Br J Ophthalmol 1996; 80: 864-7

Miller KM, Quigley HA. Comparison of optic disc features in low-tension and typical open-angle glaucoma. Ophthalmic Surg 1987; 18: 882-9

Morad Y, Sharon E, Hefetz L, Nmemt P. Corneal thickness and curvature in normal-tension glaucoma. Am J Ophthalmol 1998; 125: 164–8

Morissette J, Clepet C, Moisan S, Dubois S, Winstall E, Vermeeren D, Nguyen TD, Polansky JR, Cote G, Anctil JL, Amyot M, Plante M, Falardeau P, Raymond V. Homozygotes carrying an autosomal dominant TIGR mutation do not manifest glaucoma. Nat Genet 1998; 19: 319-21

Morle L, Bozon M, Zech JC, Alloisio N, Raas-Rothschild A, Philippe C, Lambert JC, Godet J, Plauchu H, Edery P. A locus for autosomal dominant colobomatous microphthalmia maps to chromosome 15q12-q15. Am J Hum Genet 2000; 67: 1592-1597

Motolko M, Drance SM, Douglas GR. Visual field defects in low-tension glaucoma. Comparison of defects in low-tension glaucoma and chronic open angle glaucoma. Arch Ophthalmol 1982; 100: 1074-7

Nemesure B, Leske MC, He Q, Mendell N. Analyses of reported family history of glaucoma: a preliminary investigation. The Barbados Eye Study Group. Ophthalmic Epidemiol 1996; 3: 135-41

Nemesure B, He Q, Mendell N, Wu SY, Hejtmancik JF, Hennis A, Leske MC. Barbados Family Study Group. Inheritance of open-angle glaucoma in the Barbados family study. Am J Med Genet 2001; 103: 36-43

Neufeld AH, Hernandez MR, Gonzalez M. Nitric oxide synthase in the human glaucomatous optic nerve head. Arch Ophthalmol 1997;115: 497–503

Nishimura DY, Searby CC, Alward WL, Walton D, Craig JE, Mackey DA, Kawase K, Kanis AB, Patil SR, Stone EM, Sheffield VC. A spectrum of FOXC1 mutations suggests gene dosage as a mechanism for developmental defects of the anterior chamber of the eye. Am J Hum Genet 2001; 68: 364-72

O'Brien C, Butt Z, Ludlam C, Zetkova P. Activation of the coagulation cascade in untreated primary open-angle glaucoma. Ophthalmology 1997; 104: 725-30

Oh YG, Minelli S, Spaeth GL, Steinman WC. The anterior chamber angle is different in different racial groups, a gonioscopic study. Eye 1994; 8: 104-8

Ohno K, Tsujino A, Brengman JM, Harper CM, Bajzer Z, Udd B, Beyring R, Robb S, Kirkham FJ, Engel AG. Choline acetyltransferase mutations cause myasthenic syndrome associated with episodic apnea in humans. Proc Nat Acad Sci 2001; 8: 2017-2022.

Orban TI, Csokay B, Olah E. Sequence alterations can mask each other's presence during screening with SSCP or heteroduplex analysis: BRCA genes as examples. Biotechniques 2000; 29: 94-8

Orita M, Iwahana H, Kanazawa H, Hayashi K, Sekiya T. Detection of polymorphisms of human DNA by gel electrophoresis as single-strand conformation polymorphisms. Proc Nat Acad Sci 1989; 86: 2766-70

Othman MI, Sullivan SA, Skuta GL, Cockrell DA, Stringham HM, Downs CA, Fornes A, Mick A, Boehnke M, Vollrath D, Richards JE. Autosomal dominant nanophthalmos (NNO1) with high hyperopia and angle-closure glaucoma maps to chromosome 11. Am J Hum Genet 1998; 63: 1411-1418

Ott J. Analysis of human genetic linkage. 3rd ed. Johns Hopkins University Press, 1997.

Paterson G. Studies on siblings of patients with both angle closure and chronic simple glaucoma. Trans Ophthalmol Soc UK 1961; 81: 561-76

Percin EF, Ploder LA, Yu JJ, Arici K, Horsford DJ, Rutherford A, Bapat B, Cox DW, Duncan AMV, Kalnins VI, Kocak-Altintas A, Sowden JC, Traboulsi E, Sarfarazi M, McInnes RR. Human microphthalmia associated with mutations in the retinal homeobox gene CHX10. Nature Genet 2000; 25: 397-401

Pesch UE, Leo-Kottler B, Mayer S, Jurklies B, Kellner U, Apfelstedt-Sylla E, Zrenner E, Alexander C, Wissinger B. OPA1 Mutations in patients with autosomal dominant optic atrophy and evidence for semi-dominant inheritance. Hum Mol Genet 2001; 10: 1359-1368

Phelps CD, Corbett JJ. Migraine and low-tension glaucoma. A case-control study. Invest Ophthalmol Vis Sci 1985; 26: 1105-8

Phillips JC, Del Bono EA, Haines JL, Pralea AM, Cohen JS, Greff LJ, Wiggs JL. A second locus for Rieger syndrome maps to chromosome 13q14. Am J Hum Genet 1996; 59: 613-9

Polansky JR, Fauss DJ, Chen P, Chen H, Lutjen-Drecoll E, Johnson D, Kurtz RM, Ma ZD, Bloom E, Nguyen TD. Cellular pharmacology and molecular biology of the trabecular meshwork inducible glucocorticoid response gene product. Ophthalmologica 1997; 211: 126-39

Quigley HA. Number of people with glaucoma worldwide. Br J Ophthalmol 1996; 80: 389-93

Rezaie T, Child A, Hitchings R, Brice G, Miller L, Coca-Prados M, Heon E, Krupin T, Ritch R, Kreutzer D, Crick RP, Sarfarazi M.Adult-onset primary open-angle glaucoma caused by mutations in optineurin. Science 2002; 295: 1077-9

Richards JE, Ritch R, Lichter PR, Rozsa FW, Stringham HM, Caronia RM, Johnson D, Abundo GP, Willcockson J, Downs CA, Thompson DA, Musarella MA, Gupta N, Othman MI, Torrez DM, Herman SB, Wong DJ, Higashi M, Boehnke M. Novel trabecular meshwork inducible glucocorticoid response mutation in an eight-generation juvenile-onset primary open-angle glaucoma pedigree. Ophthalmology 1998; 105: 1698-707

Ritch R, Lowe RF: Angle closure glaucoma, in Ritch R, Shields MB, Krupin T: The Glaucomas. St Louis,CV Mosby, 1996 ed 2.

Salmon JF, Swanevelder SA, Donald MA. The dimensions of eyes with chronic angle closure glaucomas. J Glaucoma 1994; 3: 237-43

Sachidanandam R, Weissman D, Schmidt SC, Kakol JM, Stein LD, Marth G, Sherry S, Mullikin JC, Mortimore BJ, Willey DL, Hunt SE, Cole CG, Coggill PC, Rice CM, Ning Z, Rogers J, Bentley DR, Kwok PY, Mardis ER, Yeh RT, Schultz B, Cook L, Davenport R, Dante M, Fulton L, Hillier L, Waterston RH, McPherson JD, Gilman B, Schaffner S, Van Etten WJ, Reich D, Higgins J, Daly MJ, Blumenstiel B, Baldwin J, Stange-Thomann N, Zody MC, Linton L, Lander ES, Altshuler D; The International SNP Map Working Group. A map of human genome sequence variation containing 1.42 million single nucleotide polymorphisms. Nature 2001; 409: 928-33

Salmon JF, Mermoud A, Ivey A, Swanevelder SA, Hoffman M. The prevalence of primary angle -closure glaucoma and open angle glaucoma in Mamre, Western Cape, South Africa. Arch Ophthalmol 1993; 111: 1263-1269

Salmon JF, Swanevelder SA, Donald MA. The dimensions of eyes with chronic angle closure glaucomas. J Glaucoma 1994; 3: 237-43

Sarfarazi M, Child A, Stoilova D, Brice G, Desai T, Trifan OC, Poinoosawmy D, Crick RP. Localization of the fourth locus (GLC1E) for adult onset primary open angle glaucoma to the 10p15-p14 region. Am J Hum Genet 1998; 62: 641-52

Scheie HG. Width and pigmentation of the angle of the anterior chamber. A system of grading by gonioscopy. Arch Ophthalmol 1957; 58: 510-2

Schuler GD, Boguski MS, Stewart EA, Stein LD, Gyapay G, Rice K, White RE, Rodriguez-Tome P, Aggarwal A, Bajorek E, Bentolila S, Birren BB, Butler A, Castle AB, Chiannilkulchai N, Chu A, Clee C, Cowles S, Day PJ, Dibling T, Drouot N, Dunham I, Duprat S, East C, Hudson TJ, et al. A gene map of the human genome. Science 1996; 274: 540-6

Semina EV, Reiter R, Leysens NJ, Alward WL, Small KW, Datson NA, Siegel-Bartelt J, Bierke-Nelson D, Bitoun P, Zabel BU, Carey JC, Murray JC. Cloning and characterization of a novel bicoid-related homeobox transcription

factor gene, RIEG, involved in Rieger syndrome. Nature Genet 1996; 14: 392-399

Sheffield VC, Stone EM, Alward WL, Drack AV, Johnson AT, Streb LM, Nichols BE. Genetic linkage of open angle familial glaucoma to chromosome 1q21-q31. Nat Genetics 1993; 4: 47-50

Shepard A, Jacobson N, Fingert JH, Stone EM. Sheffield VC, Clark AF. Delayed secondary glucocorticoid responsiveness of MYOC in human trabecular meshwork cells. Invest Ophthal Vis Sci 2001;42:3173-81

Shiose Y, Kitazawa Y, Tsukahara S, Akamatsu T, Mizokami K, Futa R, Katsushima H, Kosaki H. Epidemiology of glaucoma in Japan- a nationwide glaucoma survey. Jpn J Ophthalmol 1991; 35: 133-5

Sivagnanasundaram S, Morris AG, Gaitonde EJ, McKenna PJ, Mollon JD, Hunt DM. A cluster of single nucleotide polymorphisms in the 5'-leader of the human dopamine D3 receptor gene (DRD3) and its relationship to schizophrenia. Neurosci Lett 2000; 279: 13-6

Sommer A, Tielsch JM, Katz J, Quigley HA, Gottsch JD, Javitt J, Singh K. Relationship between intraocular pressure and primary open angle glaucoma among white and black Americans: the Baltimore Eye Survey. Arch Ophthalmol 1991; 109: 1090-5

Spaeth GL. The normal development of the human anterior chamber angle: a new system of descriptive grading. Trans Ophthalmol Soc UK 1971; 91: 709-739

Spaeth GL. Gonioscopy: uses old and new- the inheritance of occludable angles. Ophthalmology 1978; 85: 222-32

Stam LF, Laurie CC. Molecular dissection of a major gene effect on a quantitative trait: the level of alcohol dehydrogenase expression in Drosophila melanogaster. Genetics 1996; 144: 1559-64

Stoilova D, Child A, Trifan O. C, Crick R. P, Coakes RL, Sarfarazi M. Localization of a locus (GLC1B) for adult-onset primary open angle glaucoma to the 2cen-q13 region Genomics 1996; 36: 142-150

Stoilov I, Akarsu AN, Sarfarazi M. Identification of three different truncating mutations in cytochrome P4501B1 (CYP1B1) as the principal cause of primary congenital glaucoma (buphthalmos) in families linked to the GLC3A locus on chromosome 2p21. Hum Molec Genet 1997; 6: 641-647

Stone EM, Fingert JH, Alward WLM, Nguyen TD, Polansky JR, Sunden SL, Nishimura D, Clark AF, Nystuen A, Nichols BE, Mackey DA, Ritch R, Kalenak JW, Craven ER, Sheffield VC. Identification of a gene that causes primary open angle glaucoma. Science 1997; 275: 668-70

Suzuki Y, Shirato S, Taniguchi F, Ohara K, Nishimaki K, Ohta S.Mutations in the TIGR gene in familial primary open-angle glaucoma in Japan. Am J Hum Genet 1997; 61: 1202-4

Tang YM, Wo YY, Stewart J, Hawkins AL, Griffin CA, Sutter TR, Greenlee WF.Isolation and characterization of the human cytochrome P450 CYP1B1 gene. J Biol Chem 1996; 271: 28324-28330

Takenaka K, Sakai H, Yamakawa H, Yoshimura S, Kumagai M, Yamakawa H, Nakashima S, Nozawa Y, Sakai N. Polymorphism of the endoglin gene in patients with intracranial saccular aneurysms. J Neurosurg 1999; 90: 935-8

Teikari JM. Genetic factors in open-angle (simple and capsular) glaucoma. A population based twin study. Acta Ophthalmologica 1987;65:715-20

Thylefors B, Negrel AD, Pararajasegaram R, Dadzie KY. Global data on blindness. Bull WHO 1995; 73(1): 115-21

Tielsch JM, Sommer A, Katz J, Royall RM, Quigley HA, Javitt J. Racial variations in prevalence of primary open angle glaucoma. JAMA 1991; 266: 369-74

Tielsch JM, Katz J, Sommer A, Quigley HA, Javitt JC. Family history and risk of primary open angle glaucoma. The Baltimore Eye Survey. Arch Ophthalmol 1994; 112: 69-73

Tomlinson A, Leighton DA. Ocular dimensions in the heredity of angle-closure glaucoma. Br J Ophthalmol 1973; 57: 475-485

Ton CC, Hirvonen H, Miwa H, Weil MM, Monaghan P, Jordan T, van Heyningen V, Hastie ND, Meijers-Heijboer H, Drechsler M, et al. Positional cloning and characterization of a paired box- and homeobox-containing gene from the aniridia region. Cell 1991; 67: 1059-74

Toomes C, Marchbank NJ, Mackey DA, Craig JE, Newbury-Ecob RA, Bennett CP, Vize CJ, Desai SP, Black GC, Patel N, Teimory M, Markham AF, Inglehearn CF, Churchill AJ. Spectrum, frequency and penetrance of OPA1 mutations in dominant optic atrophy. Hum Mol Genet 2001; 10: 1369-78

Törnquist R. Shallow anterior chamber in acute angle-closure. A clinical and genetic study. Acta Ophthalmol 1953; 31(Suppl. 39): 1-74

Tornquist R. Chamber depth in primary acute glaucoma. Br J Ophthalmol 1956; 40: 421-9

Trifan OC, Traboulsi E, Stoilova D, Alozie I, Nguyen R, Raja S, Sarfarazi M. A third locus (GLC1D) for adult onset primary open angle glaucoma maps to the 8q23 region. Am J Ophthalmol 1998; 126: 17-28

Tuulonen A, Airaksinen PJ. Optic disc size in exfoliative, primary open angle, and low-tension glaucoma. Arch Ophthalmol 1992; 110: 211-213

Venter JC, Adams MD, Myers EW, Li PW, Mural RJ, Sutton GG, Smith HO, Yandell M, Evans CA, Holt RA, Gocayne JD, Amanatides P, Ballew RM, Huson DH, Wortman JR, Zhang Q Kodira CD, Zheng XH, Chen L, Skupski M, Subramanian G, Thomas PD, Zhang J, Gabor Miklos GL, Nelson C, Broder S, Clark AG, Nadeau J, McKusick VA, Zinder N, Levine AJ, Roberts RJ, Simon M, Slayman C, Hunkapiller M, Bolanos R, Delcher A, Dew I, Fasulo D, Flanigan M, Florea L, Halpern A, Hannenhalli S, Kravitz S, Levy S, Mobarry C, Reinert K, Remington K, Abu-Threideh J, Beasley E, Biddick K, Bonazzi V, Brandon R, Cargill M, Chandramouliswaran I, Charlab R, Chaturvedi K, Deng Z, Di Francesco V, Dunn P, Eilbeck K, Evangelista C, Gabrielian AE, Gan W, Ge W, Gong F, Gu Z, Guan P, Heiman TJ, Higgins ME, Ji RR, Ke Z, Ketchum KA, Lai Z, Lei Y, Li Z, Li J, Liang Y, Lin X, Lu F, Merkulov GV, Milshina N, Moore HM, Naik AK, Narayan VA, Neelam B, Nusskern D, Rusch DB, Salzberg S, Shao W, Shue B, Sun J, Wang Z, Wang A, Wang X, Wang J, Wei M, Wides R, Xiao C, Yan C, Yao A, Ye J, Zhan M, Zhang W, Zhang H, Zhao Q, Zheng L, Zhong F, Zhong W, Zhu S, Zhao S, Gilbert D, Baumhueter S, Spier G, Carter C, Cravchik A, Woodage T, Ali F, An H, Awe A, Baldwin D, Baden H, Barnstead M, Barrow I, Beeson K, Busam D, Carver A, Center A, Cheng ML, Curry L, Danaher S, Davenport L, Desilets R, Dietz S, Dodson K, Doup L, Ferriera S, Garg N, Gluecksmann A, Hart B, Haynes J, Haynes C, Heiner C, Hladun S, Hostin D, Houck J, Howland T, Ibegwam C, Johnson J, Kalush F, Kline L, Koduru S, Love A, Mann F, May D, McCawley S, McIntosh T, McMullen I, Moy M, Moy L, Murphy B, Nelson K, Pfannkoch C, Pratts E, Puri V, Qureshi H, Reardon M, Rodriguez R, Rogers YH, Romblad D, Ruhfel B, Scott R, Sitter C, Smallwood M, Stewart E, Strong R, Suh E, Thomas R, Tint NN, Tse S, Vech C, Wang G, Wetter J, Williams S, Williams M, Windsor S, Winn-Deen E, Wolfe K, Zaveri J, Zaveri K, Abril JF, Guigo R, Campbell MJ, Sjolander KV, Karlak B, Kejariwal A, Mi H, Lazareva B, Hatton T, Narechania A, Diemer K, Muruganujan A, Guo N, Sato S, Bafna V, Istrail S, Lippert R, Schwartz R, Walenz B, Yooseph S, Allen D, Basu A, Baxendale J, Blick L, Caminha M, Carnes-Stine J, Caulk P, Chiang YH, Coyne M, Dahlke C, Mays A, Dombroski M, Donnelly M, Ely D, Esparham S, Fosler C, Gire H, Glanowski S, Glasser K, Glodek A, Gorokhov M, Graham K, Gropman B, Harris M, Heil J, Henderson S, Hoover J, Jennings D, Jordan C, Jordan J, Kasha J, Kagan L, Kraft C, Levitsky A, Lewis M, Liu X, Lopez J, Ma D, Majoros W, McDaniel

J, Murphy S, Newman M, Nguyen T, Nguyen N, Nodell M, Pan S, Peck J, Peterson M, Rowe W, Sanders R, Scott J, Simpson M, Smith T, Sprague A, Stockwell T, Turner R, Venter E, Wang M, Wen M, Wu D, Wu M, Xia A, Zandieh A, Zhu X. The sequence of the human genome. Science 2001; 291: 1304-51

Vincent AL, Billingsley G, Buys Y, Levin AV, Priston M, Trope G, Williams-Lyn D, Heon E. Digenic inheritance of early-onset glaucoma: CYP1B1, a potential modifier gene. Am J Hum Genet 2002; 70: 448-60

Vittitow JL, Borras T. Expression of optineurin, a glaucoma-linked gene, is influenced by elevated intraocular pressure. Biochem Biophys Res Commun 2002; 298: 67-74

Wang DG, Fan JB, Siao CJ, Berno A, Young P, Sapolsky R, Ghandour G, Perkins N, Winchester E, Spencer J, Kruglyak L, Stein L, Hsie L, Topaloglou T, Hubbell E, Robinson E, Mittmann M, Morris MS, Shen N, Kilburn D, Rioux J, Nusbaum C, Rozen S, Hudson TJ, Lander ES, et al. Large-scale identification, mapping, and genotyping of single-nucleotide polymorphisms in the human genome. Science 1998; 280: 1077-82

Wax MB. Is there a role for the immune system in glaucomatous optic neuropathy? Curr Opin Ophthalmol 2000;11:145–50.

Weber JL, May PE. Abundant class of human DNA polymorphisms which can be typed using the polymerase chain reaction. Am J Hum Genet 1989; 44: 388-96.

Wei J, Hemmings GP. The NOTCH4 locus is associated with susceptibility to schizophrenia. Nat Genet 2000; 25: 376-7

Wiemann S, Weil B, Wellenreuther R, Gassenhuber J, Glassl S, Ansorge W, Bocher M, Blocker H, Bauersachs S, Blum H, Lauber J, Dusterhoft A, Beyer A, Kohrer K, Strack N, Mewes HW, Ottenwalder B, Obermaier B, Tampe J, Heubner D, Wambutt R, Korn B, Klein M, Poustka A. Toward a catalog of human genes and proteins: sequencing and analysis of 500 novel complete protein coding human cDNAs. Genome Res 2001; 11: 422-35

Wiggs JL, Allingham RR, Vollrath D, Jones KH, De La Paz M, Kern J, Patterson K, Babb VL, Del Bono EA, Broomer BW, Pericak-Vance MA, Haines JL. Prevalence of mutations in TIGR/myocilin in patients with adult and juvenile primary open angle glaucoma. Am J Hum Genet 1998; 63: 1549-52

Wilson RP, Steinmann WC. Use of trabeculectomy with postoperative 5-fluorouracil in patients requiring extremely low intraocular pressure levels to limit further glaucoma progression. Ophthalmology 1991; 98: 1047-1052

Wirtz MK, Samples JR, Kramer PL, Rust K, Topinka JR, Yount J, Koler RD, Acott TS. Mapping of a gene for adult-onset primary open angle glaucoma to chromosome 3q. Am J Hum Genet 1997; 60: 296-304.

Wirtz MK, Samples JR, Rust K, Lie J, Nordling L, Schilling K, Acott TS, Kramer PL. GLC1F, a new primary open-angle glaucoma locus, maps to 7q35-q36. Arch Ophthalmol. 1999; 117: 237-41

Wolfs RC, Klaver CC, Vingerling JR, Grobbee DE, Hofman A, de Jong PT. Distribution of central corneal thickness and its association with intraocular pressure: the Rotterdam study. Am J Ophthalmol 1997; 123: 767-72

Wolfs RC, Klaver CC, Ramrattan RS, van Duijn CM, Hofman A, de Jong PT. Genetic risk of primary open-angle glaucoma. Arch Ophthalmol 1998; 116: 1640-5

Wozney JM, Rosen V, Celeste AJ, Mitsock LM, Whitters MJ, Kriz RW, Hewick RM, Wang EA. Novel regulators of bone formation: molecular clones and activities. Science 1988; 242: 1528-1534

Appendix: Genome Scan Data

Table 1. Pedigree 1: Chromosome 1 markers

Marker	Theta=0	0.05	0.1	0.15	0.2	0.25	0.300	0.35	0.	0.45
D1S468	-∞	-1.42	-0.66	-0.29	-0.08	0.03	0.07	0.07	0.05	0.02
D1S214	-∞	-0.31	-0.04	-0.06	-0.08	-0.07	-0.05	-0.03	-0.01	0.00
D1S450	-∞	-2.26	-1.27	-0.74	-0.42	-0.21	-0.08	0	0.03	0
D1S2667	-∞	-2.21	-1.19	-0.66	-0.35	-0.15	-0.03	-0.04	-0.06	0
D1S2697	-0.10	-0.05	-0.02	0	0	-0.01	-0.01	-0.01	0	0
D1S199	-∞	-2.86	-1.84	-1.28	-0.89	-0.60	-0.38	-0.21	-0.09	-0.02
D1S234	-∞	-2.00	-1.20	-0.75	-0.47	-0.28	-0.16	-0.08	-0.03	-0.01
D1S255	-0.31	-0.31	-0.29	-0.25	-0.21	-0.16	-0.11	-0.07	-0.03	-0.01
D1S2797	-∞	-0.26	-0.04	0.05	0.09	0.09	0.08	0.05	0.03	0.01
D1S2890	-0.04	-0.05	-0.05	-0.03	-0.02	-0.01	0	0	0	0
D1S230	-∞	-1.53	-1.00	-0.70	-0.5	-0.36	-0.25	-0.16	-0.09	-0.04
D1S2841	-∞	-1.19	-0.55	-0.24	-0.07	0.01	0.05	0.05	0.03	0.01
D1S207	0.17	0.18	0.17	0.14	0.11	0.08	0.05	0.03	0.01	0.00
D1S2868	-∞	-2.12	-1.25	-0.79	-0.50	-0.31	-0.18	-0.10	-0.04	-0.01

D1S206	-∞	-0.59	-0.32	-0.18	-0.10	-0.05	-0.02	-0.00	-0.01	-0.01
D1S2726	-∞	-1.76	-1.03	-0.63	-0.37	-0.20	-0.10	-0.03	-0.01	-0.01
D1S252	-∞	-2.96	-1.80	-1.15	-0.72	-0.43	-0.23	-0.09	-0.02	0.01
D1S498	-0.09	-0.08	-0.07	-0.06	-0.04	-0.03	-0.02	-0.01	-0.01	0
D1S484	-∞	-2.07	-1.27	-0.81	-0.5	-0.3	-0.16	-0.07	-0.02	0
D1S2878	-∞	-1.13	-0.61	-0.29	-0.09	0.03	0.08	0.10	0.08	0.05
D1S196	-∞	-1.73	-1.11	-0.76	-0.51	-0.33	-0.20	-0.11	-0.05	-0.01
D1S218	-∞	0.54	0.66	0.63	0.54	0.42	0.28	0.14	0.04	0.00
D1S238	-∞	-1.32	-0.76	-0.48	-0.33	-0.23	-0.17	-0.12	-0.08	-0.04
D1S413	-∞	-2.45	-1.57	-1.10	-0.79	-0.57	-0.40	-0.26	-0.15	-0.06
D1S249	-∞	-3.74	-2.37	-1.58	-1.06	-0.68	-0.42	-0.22	-0.01	-0.02
D1S425	-∞	-1.44	-0.86	-0.54	-0.34	-0.21	-0.12	-0.06	-0.03	-0.01
D1S213	-∞	-2.22	-1.19	-0.67	-0.37	-0.20	-0.09	-0.04	-0.01	0.0
D1S2800	-0.01	-0.02	-0.03	-0.03	-0.03	-0.02	-0.01	-0.01	-0.01	0
D1S2785	-∞	-1.43	-0.63	-0.26	-0.07	0.017	0.04	0.03	0.013	0.002
D1S2842	-0.32	-0.27	-0.21	-0.16	-0.11	-0.07	-0.04	-0.02	-0.01	0.0
D1S2836	1.35	1.20	1.05	0.90	0.74	0.58	0.42	0.27	0.13	0.04

Table 2. Pedigree 1: Chromosome 2 markers

Marker	**Theta=0**	**0.05**	**0.1**	**0.15**	**0.2**	**0.25**	**0.300**	**0.35**	**0.4**	**0.45**
D2S319	-∞	-1.69	-0.84	-0.4	-0.13	0.02	0.1	0.12	0.1	0.05
D2S2211	-0.4	-0.38	-0.33	-0.26	-0.19	-0.14	-0.09	-0.05	-0.02	-0.01
D2S162	-∞	-1.92	-1.35	-1.07	-0.92	-0.80	-0.68	-0.53	-0.35	-0.17
D2S168	-∞	-2.3	-1.26	-0.73	-0.41	-0.22	-0.10	-0.04	-0.02	0
D2S305	-0.18	-0.15	-0.13	-0.09	-0.06	-0.03	-0.01	-0.01	-0.0	-0.0
D2S165	-0.18	-0.15	-0.13	-0.10	-0.07	-0.05	-0.03	-0.02	-0.01	0
D2S367	-∞	-1.85	-1.05	-0.64	-0.39	-0.24	-0.14	-0.08	-0.05	-0.02
D2S2259	-∞	-1.43	-0.83	-0.53	-0.35	-0.24	-0.16	-0.1	-0.06	-0.03
D2S391	-∞	-1.47	-0.84	-0.49	-0.26	-0.12	-0.04	0	0	-0.02
D2S337	-∞	-1.48	-0.77	-0.41	-0.21	-0.1	-0.04	-0.01	0	0
D2S2368	-∞	-2.16	-1.33	-0.88	-0.58	-0.38	-0.23	-0.12	-0.05	-0.01
D2S286	-∞	-2.69	-1.63	-1.07	-0.71	-0.46	-0.28	-0.15	-0.06	-0.02
D2S2333	-∞	-3.71	-2.15	-1.33	-0.83	-0.5	-0.28	-0.14	-0.06	-0.01
D2S2216	-1.82	-0.28	-0.05	0.06	0.11	0.13	0.11	0.08	0.04	0.01
D2S160	-∞	-1.03	-0.54	-0.30	-0.16	-0.08	-0.04	-0.01	-0.01	0

D2S347	-∞	-2.19	-1.33	-0.86	-0.56	-0.36	-0.21	-0.11	-0.05	-0.01
D2S112	-∞	-1.49	-0.93	-0.62	-0.41	-0.27	-0.16	-0.09	-0.04	-0.01
D2S151	-∞	-0.96	-0.49	-0.26	-0.14	-0.07	-0.03	-0.01	-0.01	0
D2S142	-∞	-1.26	-0.7	-0.41	-0.25	-0.14	-0.08	-0.04	-0.02	0
D2S2330	-∞	-1.15	-0.66	-0.39	-0.23	-0.13	-0.06	-0.03	-0.01	0
D2S335	-∞	-1.74	-1.08	-0.67	-0.4	-0.21	-0.09	-0.02	0.02	0.03
D2S364	-∞	-2.62	-1.52	-0.93	-0.56	-0.32	-0.17	-0.07	-0.01	0.01
D2S117		-1.15	-0.66	-0.42	-0.28	-0.18	-0.11	-0.07	-0.03	-0.01
D2S325	0.47	0.42	0.38	0.33	0.28	0.23	0.18	0.13	0.08	0.04
D2S2382	-∞	-1.2	-0.66	-0.35	-0.16	-0.03	0.05	0.08	0.09	0.06
D2S126	-0.13	-0.04	0	0.02	0.03	0.03	0.02	0.02	0.01	0
D2S396	-∞	-1.82	-1.03	-0.63	-0.38	-0.23	-0.13	-0.06	-0.03	
D2S206	-∞	-2.56	-1.47	-0.89	-0.53	-0.29	-0.14	-0.04	0.01	0.02
D2S338	-∞	-0.62	-0.36	-0.23	-0.15	-0.09	-0.06	-0.03	-0.01	0
D2S125	-∞	-0.48	0.15	0.41	0.50	0.49	0.43	0.32	0.20	0.09

Table 3. Pedigree 1: Chromosome 3 markers

Marker	**Theta=0**	**0.05**	**0.1**	**0.15**	**0.2**	**0.25**	**0.300**	**0.35**	**0.4**	**0.45**
D3S1297	1.06	0.93	0.80	0.66	0.53	0.40	0.27	0.16	0.08	0.02
D3S1304	1.03	0.87	0.61	0.56	0.42	0.30	0.20	0.11	0.05	0.01
D3S1263	0.33	0.45	0.43	0.35	0.25	0.13	0.01	-0.08	-0.12	-0.09
D3S2338	-∞	-1.96	-1.25	-0.84	-0.57	-0.37	-0.23	-0.12	-0.05	-0.01
D3S1266	-∞	-1.37	-0.96	-0.68	-0.47	-0.31	-0.19	-0.10	-0.04	-0.01
D3S1277	-0.54	-0.41	-0.31	-0.23	-0.17	-0.12	-0.07	-0.04	-0.02	-0.01
D3S1289	-∞	-3.35	-2.14	-1.44	-0.97	-0.63	-0.38	-0.21	-0.09	-0.02
D3S1300	-∞	-1.9	-1.18	-0.77	-0.49	-0.30	-0.18	-0.09	-0.04	-0.01
D3S1285	0.38	0.42	0.41	0.38	0.33	0.28	0.22	0.15	0.09	0.03
D3S1566	-∞	0.33	0.55	0.60	0.57	0.49	0.39	0.28	0.17	0.07
D3S3681	-∞	-1.68	-0.96	-0.58	-0.34	-0.20	-0.11	-0.05	-0.02	-0.01
D3S1271	-0.05	-0.06	-0.05	-0.03	-0.01	0	0	0	0	0
D3S1278	-0.04	-0.04	-0.03	-0.03	-0.02	-0.02	-0.01	-0.01	0	
D3S1267	-∞	-3.43	-2.09	-1.36	-0.89	-0.57	-0.34	-0.19	-0.08	-0.02
D3S1292	-∞	-1.42	-0.45	-0.01	0.22	0.32	0.32	0.27	0.17	0.06

D3S1569	-3.5	-1.57	-0.82	-0.45	-0.24	-0.12	-0.04	-0.01	0	0
D3S1279	-0.12	-0.12	-0.11	-0.09	-0.07	-0.05	-0.03	-0.02	-0.01	0
D3S1565	-0.24	-0.06	0.02	0.05	0.06	0.06	0.04	0.03	0.01	0
D3S1262	0.98	0.89	0.79	0.68	0.57	0.45	0.32	0.20	0.10	0.03
D3S1580	-∞	-1.02	-0.64	-0.52	-0.50	-0.51	-0.49	-0.42	-0.30	-0.16
D3S1601	0.03	0.04	0.04	0.03	0.03	0.02	0.01	0.01	0.00	0.00
D3S1311	-0.01	-0.02	-0.03	-0.03	-0.04	-0.03	-0.02	-0.02	-0.01	0

Table 4. Pedigree 1: Chromosome 4 markers

Marker	**Theta=0**	**0.05**	**0.1**	**0.15**	**0.2**	**0.25**	**0.300**	**0.35**	**0.4**	**0.45**
D4S412	-∞	-0.63	-0.37	-0.24	-0.15	-0.09	-0.05	-0.02	0.01	0.01
D4S2935	-0.03	-0.01	-0.02	-0.03	-0.04	-0.03	-0.03	-0.02	-0.01	0
D4S403	-∞	-0.42	-0.04	0.10	0.14	0.13	0.10	0.07	0.03	0.01
D4S419	-∞	-3.45	-2.16	-1.43	-0.95	-0.61	-0.37	-0.20	-0.09	-0.02
D4S391	-∞	-0.63	-0.21	-0.02	0.06	0.09	0.08	0.06	0.03	0.01
D4S405	-∞	-1.3	-0.65	-0.33	-0.14	-0.03	0.02	0.05	0.05	0.03
D4S1592	-∞	-0.58	0.06	0.31	0.41	0.41	0.35	0.26	0.15	0.05
D4S392	-∞	-0.36	0.24	0.46	0.52	0.49	0.41	0.29	0.17	0.07

D4S2964	-∞	-0.05	0.32	0.43	0.43	0.36	0.26	0.16	0.07	0.02
D4S1534	-0.82	-0.45	-0.25	-0.12	-0.05	-0.01	0.01	0.01	0.01	0.0
D4S414	-∞	-0.24	0.01	0.13	0.19	0.21	0.20	0.17	0.12	0.07
D4S1572	-∞	-2.44	-1.45	-0.97	-0.70	-0.54	-0.42	-0.31	-0.19	-0.08
D4S406	-∞	-0.87	-0.60	-0.44	-0.32	-0.23	-0.15	-0.09	-0.04	-0.01
D4S402	-∞	-1.92	-1.04	-0.60	-0.35	-0.20	-0.11	-0.06	-0.03	-0.01
D4S1575	-∞	-1.50	-0.97	-0.64	-0.41	-0.25	-0.14	-0.07	-0.03	-0.01
D4S424	-∞	-3.86	-2.29	-1.45	-0.93	-0.58	-0.34	-0.18	-0.08	-0.02
D4S413	-0.77	-0.52	-0.36	-0.25	-0.17	-0.12	-0.08	-0.05	-0.03	-0.01
D4S1597	-∞	-1.51	-0.93	-0.61	-0.40	-0.25	-0.15	-0.08	-0.03	-0.01
D4S1539	-∞	-0.28	-0.05	0.06	0.11	0.13	0.12	0.11	0.08	0.04
D4S415	0.042	0.02	0.001	-0.01	-0.02	-0.02	-0.01	-0.001	-0.004	-0.001
D4S1535	0.13	0.10	0.07	0.05	0.04	0.03	0.02	0.01	0	0
D4S426	-∞	-1.07	-0.51	-0.24	-0.10	-0.02	0.02	0.03	0.03	0.02

Table 5. Pedigree 1: Chromosome 5 markers

Marker	Theta=0	0.05	0.1	0.15	0.2	0.25	0.300	0.35	0.4	0.45
D5S1981	0.16	0.19	0.19	0.17	0.14	0.11	0.07	0.04	0.02	0.01
D5S406	0.63	0.51	0.41	0.33	0.26	0.19	0.13	0.08	0.04	0.01
D5S630	-∞	-0.45	-0.25	-0.17	-0.12	-0.10	-0.08	-0.06	-0.04	-0.02
D5S416	-∞	-2.58	-1.60	-1.05	-0.70	-0.45	-0.28	-0.16	-0.07	-0.02
D5S419	-∞	-3.02	-1.84	-1.21	-0.81	-0.53	-0.33	-0.18	-0.08	-0.02
D5S426	0.34	0.30	0.26	0.21	0.17	0.12	0.08	0.05	0.03	0.01
D5S418	-∞	-1.33	-0.61	-0.28	-0.10	-0.02	0.02	0.02	0.01	0
D5S407	0.15	0.18	0.17	0.15	0.13	0.10	0.07	0.04	0.02	0.00
D5S647	-∞	-1.02	-0.55	-0.33	-0.20	-0.13	-0.08	-0.04	-0.02	0
D5S424	-∞	-1.20	-0.77	-0.52	-0.35	-0.23	-0.14	-0.08	-0.03	-0.01
D5S641	-0.72	-0.45	-0.30	-0.20	-0.13	-0.08	-0.05	-0.03	-0.01	0
D5S428	-∞	-0.3	-0.09	0	0.03	0.04	0.04	0.03	0.01	0
D5S644	-∞	-2.04	-1.55	-0.69	-0.42	-0.24	-0.14	-0.07	-0.03	-0.007
D5S433	-∞	-0.24	-0.05	0.03	0.06	0.06	0.05	0.03	0.02	0.00
D5S2027	0.93	0.84	0.75	0.66	0.56	0.45	0.35	0.25	0.16	0.07

D5S471	-∞	-2.54	-1.49	-0.94	-0.60	-0.37	-0.21	-0.11	-0.05	-0.01
D5S2115	-∞	-1.37	-0.67	-0.34	-0.17	-0.07	-0.02	-0.002	0.003	0.001
D5S436	-0.05	0.24	0.32	0.33	0.31	0.26	0.19	0.13	0.06	0.02
D5S410	-∞	-0.77	-0.27	-0.02	0.11	0.17	0.19	0.18	0.13	0.07
D5S422	0.11	0.15	0.16	0.15	0.12	0.09	0.06	0.04	0.02	0.00
D5S400	-∞	-3.03	-1.71	-1.02	-0.60	-0.32	-0.14	-0.04	0.01	0.02
D5S408	-∞	-0.15	0.04	0.10	0.12	0.11	0.09	0.06	0.03	0.01

Table 6. Pedigree 1: Chromosome 6 markers

Marker	**Theta=0**	**0.05**	**0.1**	**0.15**	**0.2**	**0.25**	**0.300**	**0.35**	**0.4**	**0.45**
D6S1574	-∞	0.06	0.21	0.23	0.21	0.16	0.11	0.06	0.02	0.01
D6S309	-0.69	-0.46	-0.31	-0.21	-0.14	-0.09	-0.05	-0.03	-0.01	-0.0
D6S470	0.07	0.07	0.06	0.05	0.04	0.03	0.02	0.01	0.01	-0.0
D6S289	-∞	-0.59	-0.27	-0.12	-0.05	-0.02	-0.01	-0.01	-0.01	-.0.01
D6S276	-0.53	-0.27	-0.13	-0.05	0	0.02	0.02	0.01	-0.01	0
D6S1610	-∞	-1.41	-0.93	-0.62	-0.41	-0.26	-0.15	-0.08	-0.03	-0.01
D6S257	0.39	0.29	0.21	0.15	0.10	0.06	0.04	0.02	0.01	0.0

D6S460	-∞	-0.49	-0.23	-0.11	-0.05	-0.02	-0.01	-0.01	0	0
D6S462	0.19	0.19	0.17	0.15	0.12	0.09	0.06	0.03	0.02	0
D6S434	-∞	-0.68	-0.43	-0.29	-0.20	-0.13	-0.08	-0.04	-0.02	-0.01
D6S287	0.16	0.17	0.15	0.13	0.11	0.08	0.05	0.03	0.02	0.0
D6S262	-∞	-0.9	-0.44	-0.22	-0.09	-0.02	0.02	0.04	0.038	0.02
D6S292	-∞	-1.56	-0.79	-0.39	-0.13	0.02	0.11	0.15	0.13	0.08
D6S308	-0.08	-0.04	-0.02	-0.01	0	0	0	0	0	0
D6S441	0.21	0.20	0.19	0.16	0.13	0.09	0.06	0.04	0.02	0
D6S1581	-∞	0.02	0.18	0.22	0.20	0.16	0.11	0.06	0.03	0
D6S264	0.38	0.34	0.29	0.24	0.18	0.14	0.09	0.05	0.02	0.01
D6S446	-0.45	-0.31	-0.20	-0.10	-0.01	0.02	0.02	0.01	0.01	0
D6S281	0.10	0.10	0.10	0.08	0.07	0.05	0.03	0.02	0.01	0

Table 7. Pedigree 1: Chromosome 7 markers

Marker	**Theta=0**	**0.05**	**0.1**	**0.15**	**0.2**	**0.25**	**0.300**	**0.35**	**0.4**	**0.45**
D7S531	-0.23	-0.204	-0.17	-0.14	-0.1	-0.07	-0.04	-0.02	-0.01	-0.002
D7S517	-0.12	-0.03	0.02	0.04	0.05	0.05	0.04	0.02	0.01	0
D7S513	-∞	-2.18	-1.38	-0.94	-0.65	-0.44	-0.29	-0.18	-0.10	-0.04
D7S507	1.13	1.12	1.04	0.94	0.81	0.66	0.50	0.34	0.18	0.05
D7S493	-∞	-6.5	-3.19	-1.19	-0.75	-0.46	-0.25	-0.12	-0.04	0.002
D7S516	-∞	-2.7	-1.6	-1.04	-0.67	-0.42	-0.25	-0.13	-0.06	-0.01
D7S484	-∞	-2.08	-1.23	-0.77	-0.48	-0.28	-0.14	-0.05	-0.01	-0.01
D7S510	-∞	-1.03	-0.69	-0.49	-0.34	-0.23	-0.14	-0.08	-0.04	-0.01
D7S519	-∞	-2.46	-1.41	-0.87	-0.54	-0.32	-0.18	-0.09	-0.04	-0.01
D7S502	-∞	-4.141	-2.55	-1.7	-1.1	-0.7	-0.4	-0.23	-0.1	-0.26
D7S669	-∞	-0.77	-0.43	-0.25	-0.14	-0.08	-0.04	-0.02	-0.01	0
D7S630	-∞	-0.28	-0.07	0.01	0.04	0.05	0.04	0.03	0.01	0
D7S657	0.48	0.62	0.62	0.57	0.49	0.40	0.3	0.2	0.11	0.04
D7S515	-∞	-2.22	-1.29	-0.80	-0.50	-0.31	-0.18	-0.09	-0.04	-0.01
D7S486	-∞	-2.23	-1.38	-0.91	-0.60	-0.39	-0.23	-0.13	-0.05	-0.01

D7S530	0.03	0.05	0.06	0.06	0.06	0.05	0.04	0.04	0.03	0.02
D7S640	-∞	-3.04	-1.78	-1.11	-0.68	-0.4	-0.2	-0.08	-0.01	0.02
D7S684	-∞	-0.78	-0.12	0.160	0.28	0.31	0.28	0.21	0.122	0.045
D7S661	-∞	-2.86	-1.61	-0.97	-0.59	-0.35	-0.20	-0.10	-0.04	-0.01
D7S798	0.26	0.43	0.44	0.39	0.32	0.24	0.16	0.09	0.04	0.01
D7S2465	-∞	-2.96	-1.87	-1.27	-0.86	-0.57	-0.35	-0.19	-0.08	-0.02

Table 8. Pedigree 1: Chromosome 8 markers

Marker	**Theta= 0**	**0.05**	**0.1**	**0.15**	**0.2**	**0.25**	**0.300**	**0.35**	**0.4**	**0.45**
D8S264	-∞	-2.63	-1.58	-1.02	-0.67	-0.43	-0.26	-0.14	-0.07	-0.02
D8S277	-∞	-2.33	-1.35	-0.85	-0.54	-0.35	-0.22	-0.13	-0.07	-0.03
D8S550	-∞	-0.75	-0.48	-0.34	-0.24	-0.16	-0.11	-0.06	-0.03	-0.01
D8S549	-0.39	-0.36	-0.29	-0.22	-0.16	-0.11	-0.07	-0.04	-0.02	0
D8S258	-∞	-0.68	-0.41	-0.27	-0.18	-0.11	-0.07	-0.03	-0.01	0
D8S1771	-0.79	-0.57	-0.43	-0.33	-0.24	-0.17	-0.11	-0.06	-0.03	-0.01
D8S505	-∞	-0.29	-0.06	0.04	0.08	0.09	0.09	0.08	0.06	0.03
D8S285	-0.81	-0.55	-0.37	-0.24	-0.16	-0.10	-0.06	-0.03	-0.01	0

D8S260	-∞	-2	-1.31	-0.9	-0.62	-0.4	-0.25	-0.13	-0.05	-0.01
D8S270	-∞	-1.65	-1.0	-0.65	-0.42	-0.27	-0.16	-0.09	-0.04	-0.01
D8S1784	-∞	-0.65	-0.40	-0.27	-0.19	-0.13	-0.09	-0.06	-0.04	-0.02
D8S514	-∞	-1.12	-0.62	-0.37	-0.23	-0.13	-0.08	-0.04	-0.02	-0.01
D8S284	-∞	-2.23	-1.38	-0.91	-0.60	-0.39	-0.23	-0.13	-0.05	-0.01
D8S272	-∞	-2.38	-1.46	-0.96	-0.63	-0.4	-0.24	-0.13	-0.05	-0.01

Table 9 Pedigree 1: Chromosome 9 markers

Marker	**Theta= 0**	**0.05**	**0.1**	**0.15**	**0.2**	**0.25**	**0.300**	**0.35**	**0.4**	**0.45**
D9S288	-∞	-1.95	-0.95	-0.46	-0.18	-0.03	0.05	0.06	0.05	0.02
D9S286	-∞	-0.75	-0.23	0.01	0.11	0.14	0.13	0.09	0.05	0.01
D9S285	-∞	-1.76	-0.92	-0.51	-0.27	-0.14	-0.07	-0.03	-0.01	-0.00
D9S157	-∞	-2.09	-1.21	-0.76	-0.48	-0.30	-0.18	-0.10	-0.04	-0.01
D9S171	-0.03	-0.04	-0.04	-0.03	-0.02	-0.02	-0.01	-0.00	-0.00	0.00
D9S161	-∞	-1.74	-0.93	-0.54	-0.33	-0.21	-0.14	-0.10	-0.06	-0.03
D9S1817	-∞	-0.53	-0.19	-0.06	-0.02	-0.03	-0.04	-0.06	-0.05	-0.03
D9S273	-∞	-0.41	-0.16	-0.05	-0.01	0.02	0.02	0.01	0.01	0.01
D9S175	-∞	-2.26	-1.36	-0.88	-0.58	-0.38	-0.24	-0.14	-0.08	-0.03

D9S167	-∞	-0.96	-0.57	-0.40	-0.33	-0.31	-0.30	0.28	-0.22	-0.12
D9S283	-0.70	-0.11	0.04	0.08	0.07	0.02	-0.03	-0.06	-0.07	-0.04
D9S287	-∞	-1.21	-0.71	-0.48	-0.35	-0.27	-0.21	-0.16	-0.10	-0.04
D9S1690	-∞	-0.99	-0.53	-0.30	-0.17	-0.09	-0.04	-0.02	-0.01	0
D9S1677	-∞	-2.10	-1.28	-0.84	-0.56	-0.37	-0.23	-0.14	-0.07	-0.03
D9S1776	-1.99	-1.40	-0.93	-0.61	-0.40	-0.25	-0.15	-0.08	-0.03	-0.01
D9S1682	-0.23	-0.09	0.02	0.10	0.13	0.14	0.12	0.09	0.05	0.01
D9S290		0.05	0.19	0.21	0.18	0.14	0.09	0.05	0.023	
D9S164	-∞	-3.54	-2.17	-1.42	-0.94	-0.61	-0.37	-0.20	-0.09	-0.02
D9S1826	-∞	-2.81	-1.79	-1.27	-0.94	0.72	-0.54	-0.38	-0.24	-0.11
D9S158	-0.13	-0.11	-0.09	-0.06	-0.04	-0.02	-0.01	0	0	0

Table 10 Pedigree 1: Chromosome 10 markers

Marker	**Theta=0**	**0.05**	**0.1**	**0.15**	**0.2**	**0.25**	**0.300**	**0.35**	**0.4**	**0.45**
D10S249	-∞	0.04	0.42	0.53	0.54	0.48	0.39	0.27	0.14	0.04
D10S591	-∞	-1.17	-0.67	-0.40	-0.24	-0.14	-0.07	-0.03	-0.01	0
D10S189	-∞	-1.78	-1.07	-0.67	-0.41	-0.24	-0.13	-0.06	-0.02	-0.01
D10S547	-∞	-1.40	-0.86	-0.57	-0.39	-0.26	-0.16	-0.09	-0.04	-0.01
D10S1653	-∞	-2.54	-1.48	-0.94	-0.61	-0.40	-0.26	-0.17	-0.10	-0.05
D10S548	-∞	-0.33	0.07	0.22	0.27	0.25	0.20	0.14	0.07	0.02
D10S197	-∞	-0.91	-0.57	-0.4	-0.3	-0.24	-0.19	-0.14	-0.09	-0.04
D10S213	-∞	-2.34	-1.41	-0.93	-0.63	-0.42	-0.26	-0.15	-0.08	-0.03
D10S208	0.6	0.74	0.74	0.68	0.59	0.48	0.35	0.23	0.11	0.03
D10S1780	1.24	1.13	1.01	0.89	0.75	0.61	0.43	0.32	0.18	0.07
D10S578	-∞	-1.26	-0.58	-0.28	-0.12	-0.05	-0.03	-0.03	-0.03	-0.02
D10S196	2.34	2.09	1.84	1.57	1.29	1.01	0.72	0.44	0.21	0.05
D10S1790	-0.32	0.5	0.6	0.58	0.5	0.38	0.26	0.14	0.05	0.00
D10S1652	-∞	0.58	0.69	0.67	0.6	0.5	0.37	0.25	0.13	0.04
D10S581	-∞	-2.26	-1.36	-0.88	-0.56	-0.35	-0.21	-0.11	-0.05	-0.01

D10S210	-∞	1.57	1.56	1.41	1.20	0.96	0.70	0.43	0.20	0.05
D10S537	-∞	-1.22	-0.72	-0.48	-0.36	-0.30	-0.26	-0.22	-0.16	-0.08
D10S580	-∞	-0.71	-0.09	0.14	0.21	0.18	0.11	0.02	-0.04	-0.05
D10S1730	-∞	0.57	0.65	0.61	0.51	0.39	0.26	0.15	0.06	0.01
D10S1686	-∞	-0.39	0.01	0.20	0.30	0.33	0.31	0.27	0.19	0.10
D10S185	1.40	1.39	1.30	1.16	1.01	0.84	0.66	0.49	0.32	0.15
D10S1709	-∞	-1.06	-0.4	-0.11	-0.04	0.12	0.14	0.13	0.10	0.06
D10S192	1.06	0.98	0.90	0.81	0.71	0.60	0.48	0.36	0.23	0.11
D10S597	-0.06	0	0.03	0.04	0.04	0.04	0.03	0.02	0.01	0
D10S1693	-0.59	-0.38	-0.26	-0.17	-0.12	-0.07	-0.05	-0.02	-0.01	0
D10S587	-∞	-0.87	-0.50	-0.28	-0.14	-0.07	-0.04	-0.03	-0.04	-0.04
D10S1656	-∞	-3.01	-1.86	-1.23	-0.81	-0.52	-0.32	-0.17	-0.07	-0.02
D10S217	-0.32	-0.32	-0.28	-0.22	-0.14	-0.08	-0.04	-0.02	-0.01	0
D10S1651	-∞	-0.83	-0.19	0.08	0.20	0.23	0.22	0.18	0.12	0.06
D10S212	-0.31	-0.32	-0.31	-0.28	-0.24	-0.18	-0.13	-0.08	-0.03	-0.01

Table 11 Pedigree 1: Chromosome 11 markers

Marker	**Theta=0**	**0.05**	**0.1**	**0.15**	**0.2**	**0.25**	**0.300**	**0.35**	**0.4**	**0.45**
D11S4046	-∞	-1.14	-0.55	-0.26	-0.11	-0.02	-0.01	0.02	0.01	0
D11S1338	-0.75	-0.51	-0.35	-0.24	-0.16	-0.10	-0.06	-0.03	-0.01	0
D11S902	-∞	-1.73	-0.74	-0.26	-0.01	0.12	0.16	0.15	0.09	0.03
D11S904	-∞	-0.27	-0.06	0.03	0.07	0.08	0.08	0.07	0.05	0.03
D11S935	-∞	-2.00	-1.07	-0.58	-0.29	-0.11	-0.01	0.05	0.06	0.04
D11S905	-∞	-0.29	0.02	0.14	0.19	0.20	0.18	0.14	0.10	0.05
D11S4191	-∞	-1.77	-0.81	-0.35	-0.10	0.04	0.10	0.09	0.05	0
D11S987	-∞	-0.99	-0.42	-0.16	-0.03	0.02	0.03	0.02	0.01	0.0
D11S1314	-0.13	-0.13	-0.10	-0.07	-0.04	-0.02	-0.00	0	0	0
D11S901	0.19	0.28	0.26	0.18	0.08	-0.03	-0.13	-0.19	-0.18	-0.11
D11S937	-0.35	-0.35	-0.33	-0.28	-0.21	-0.15	-0.09	-0.05	-0.02	-0.00
D11S4175	1.22	1.05	0.91	0.78	0.66	0.54	0.42	0.30	0.19	0.08
D11S898	0.007	0.04	0.06	0.06	0.055	0.043	0.03	0.017	0.008	0.002
D11S908	0.10	0.09	0.07	0.06	0.05	0.03	0.02	0.01	0.01	0.0
D11S925	-0.35	-0.15	-0.06	-0.02	0.01	0.01	0.01	0.01	0	0

D11S1320	-0.05	-0.06	-0.05	-0.05	-0.04	-0.02	-0.02	-0.01	0	0
D11S968	-∞	-1.45	-0.72	-0.36	-0.15	-0.03	0.04	0.07	0.07	0.04

Table 12. Pedigree 1: Chromosome 12 markers

Marker	**Theta=0**	**0.05**	**0.1**	**0.15**	**0.2**	**0.25**	**0.300**	**0.35**	**0.4**	**0.45**
D12S352	-∞	-0.1	0.1	0.19	0.22	0.22	0.2	0.17	0.12	0.06
D12S99	-∞	-0.78	-0.29	-0.09	-0.02	-0.01	-0.02	-0.03	-0.03	-0.2
D12S336	-∞	-0.47	-0.17	-0.04	0.02	0.04	0.04	0.03	0.02	0
D12S364	-∞	-0.77	-0.11	0.17	0.29	0.32	0.29	0.22	0.14	0.07
D12S310	-0.18	-0.01	0.08	0.12	0.14	0.14	0.12	0.10	0.07	0.03
D12S1617	-∞	-2.371	-1.51	-1.0	-0.7	-0.46	-0.28	-0.15	-0.07	-0.01
D12S345	-∞	-2.71	-1.57	-0.95	-0.55	-0.29	-0.12	-0.02	0.03	0.03
D12S85	-∞	-4.16	-2.53	-1.65	-1.08	-0.69	-0.42	-0.22	-0.10	-0.02
D12S368	-∞	-0.31	-0.04	0.06	0.08	0.07	0.05	0.03	0.01	0
D12S83	-∞	-3.02	-1.89	-1.29	-0.90	-0.63	-0.43	-0.28	-0.16	-0.07
D12S326	-∞	-1.59	-0.83	-0.46	-0.26	-0.14	-0.07	-0.04	-0.03	-0.02
D12S351	-∞	-1:3	-0.75	-0.46	-0.29	-0.18	-0.11	-0.06	-0.03	-0.01

D12S346	-∞	-1.07	-0.41	-0.14	-0.03	-0.01	-0.04	-0.07	-0.08	-0.05
D12S78	-∞	-1.05	-0.57	-0.34	-0.20	-0.12	-0.06	-0.03	-0.01	0
D12S79	-∞	-2.46	-1.21	-0.61	-0.27	-0.08	0.01	0.03	0	0
D12S86	-∞	-2.4	-1.15	-0.55	-0.22	-0.04	0.044	0.054	0.019	-0.02
D12S324	-∞	-0.81	-0.57	-0.43	-0.32	-0.23	-0.15	-0.09	-0.04	-0.01
D12S1659	-∞	-2.8	-1.7	-1.1	-0.75	-0.49	-0.3	-0.19	-0.1	-0.04
D12S1723	-0.21	-0.06	0.02	0.05	0.06	0.05	0.04	0.03	0.01	0.0

Table 13. Pedigree 1: Chromosome 13 markers

Marker	**Theta=0**	**0.05**	**0.1**	**0.15**	**0.2**	**0.25**	**0.300**	**0.35**	**0.4**	**0.45**
D13S175	-0.04	-0.03	-0.01	0.02	0.03	0.04	0.03	0.02	0.01	0
D13S217	-∞	-1.83	-0.92	-0.47	-0.21	-0.06	0.02	0.05	0.05	0.03
D13S171	-∞	-1.02	-0.55	-0.33	-0.21	-0.13	-0.09	-0.06	-0.04	-0.02
D13S218	-∞	-0.32	-0.08	0.03	0.08	0.10	0.09	0.07	0.05	0.02
D13S263	-∞	-1.19	-0.82	-0.62	-0.47	-0.33	-0.22	-0.13	-0.06	-0.01
D13S153	-∞	-3.93	-2.29	-1.41	-0.85	-0.48	-0.24	-0.08	0.01	0.03
D13S156	-∞	-1.5	-0.8	-0.5	-0.3	-0.16	-0.08	-0.03	-0.01	-0.01

D13S170	-∞	-0.64	-0.09	0.17	0.30	0.34	0.33	0.28	0.20	0.10
D13S265	1.22	1.14	1.02	0.90	0.76	0.62	0.48	0.35	0.21	0.09
D13S159	-∞	-1.67	-0.87	-0.45	-0.19	-0.04	0.05	0.08	0.08	0.05
D13S158	-∞	-1.47	-0.72	-0.34	-0.12	0	0.06	0.08	0.06	0.03
D13S173	-∞	-2.4	-1.41	-0.85	-0.5	-0.28	-0.15	-0.07	-0.02	-0.01
D13S1265	-0.13	-0.13	-0.12	-0.09	-0.06	-0.04	-0.02	-0.01	0	0
D13S285	-∞	-4.26	-2.73	-1.89	-1.33	-0.92	-0.61	-0.38	-0.20	-0.08

Table 14. Pedigree 1: Chromosome 14 markers

Marker	**Theta=0**	**0.05**	**0.1**	**0.15**	**0.2**	**0.25**	**0.300**	**0.35**	**0.4**	**0.45**
D14S261	-2.04	-0.95	-0.60	-0.38	-0.23	-0.13	-0.07	-0.03	-0.01	0
D14S283	-∞	-1.3	-0.48	-0.09	0.11	0.2	0.22	0.19	0.13	0.06
D14S275	-∞	-1.75	-0.98	-0.59	-0.38	-0.26	-0.20	-0.16	-0.13	-0.08
D14S70	-∞	-0.90	-0.37	-0.11	0.03	0.10	0.11	0.09	0.05	0.02
D14S288	-∞	-3.10	-1.93	-1.26	-0.81	-0.51	-0.31	-0.17	-0.08	-0.03
D14S276	-∞	-3.15	-2.05	-1.44	-1.02	-0.72	-0.49	-0.31	-0.17	-0.07
D14S63	-∞	-0.63	-0.32	-0.18	-0.12	-0.09	-0.07	-0.06	-0.04	-0.02
D14S258	-∞	-2.11	-1.21	-0.74	-0.44	-0.25	-0.13	-0.05	-0.01	0

D14S74	-∞	-3.01	-1.80	-1.15	-0.74	-0.46	-0.27	-0.14	-0.06	-0.02
D14S68	-∞	-2.28	-1.47	-0.97	-0.64	-0.41	-0.24	-0.13	-0.05	-0.01
D14S280	-∞	-2.56	-1.44	-0.87	-0.52	-0.31	-0.17	-0.09	-0.04	-0.01
D14S65	-∞	-1.98	-1.15	-0.66	-0.36	-0.18	-0.07	-0.02	-0.01	0
D14S985	-∞	-2.09	-1.32	-0.90	-0.62	-0.43	-0.29	-0.19	-0.11	-0.05
D14S292	-∞	-3.41	-2.03	-1.27	-0.79	-0.46	-0.25	-0.10	-0.02	0.01

Table 15. Pedigree 1: Chromosome 15 markers

Marker	**Theta=0**	**0.05**	**0.1**	**0.15**	**0.2**	**0.25**	**0.300**	**0.35**	**0.4**	**0.45**
D15S128	-∞	-2.15	-1.14	-0.62	-0.31	-0.11	0	0.06	0.08	0.05
D15S1002	-∞	-1.74	-0.90	-0.47	-0.23	-0.08	0	0.05	0.06	0.04
D15S165	0.046	0.026	0.008	-0.01	-0.01	-0.01	-0.01	-0.01	-0.00	-0.001
D15S1007	-∞	-2.66	-1.42	-0.78	-0.40	-0.17	-0.03	0.04	0.06	0.05
D15S1012	0.24	0.21	0.18	0.14	0.11	0.08	0.05	0.03	0.01	0
D15S994	-1.652	-0.636	-0.28	-0.07	0.03	0.08	0.083	0.064	0.035	0.01
D15S978	-∞	-1.34	-0.55	-0.15	0.05	0.14	0.16	0.13	0.08	0.02
D15S117	-∞	-1.30	-0.71	-0.42	-0.24	-0.13	-0.07	-0.03	-0.01	0
D15S153	-∞	-1.49	-0.75	-0.39	-0.19	-0.08	-0.02	0	0.01	0

D15S131	-∞	0.35	0.46	0.45	0.38	0.30	0.21	0.13	0.06	0.02
D15S205	-∞	-0.23	-0.02	0.06	0.09	0.09	0.07	0.05	0.03	0.02
D15S127	-∞	-0.89	-0.37	-0.15	-0.05	-0.01	0.003	0.005	0.003	0.001
D15S130	-∞	-0.87	-0.4	-0.2	-0.12	-0.07	-0.04	-0.02	-0.01	-0.003
D15S120	-0.26	-0.26	-0.22	-0.17	-0.12	-0.07	-0.03	-0.01	-0.01	0

Table 16. Pedigree 1: Chromosome 16 markers

Marker	**Theta=0**	**0.05**	**0.1**	**0.15**	**0.2**	**0.25**	**0.300**	**0.35**	**0.4**	**0.45**
D16S423	-∞	-2.68	-1.42	-0.79	-0.41	-0.17	-0.03	0.05	0.07	0.05
D16S404	-0.23	-0.23	-0.23	-0.20	-0.17	-0.13	-0.09	-0.05	-0.03	-0.01
D16S3075	-∞	-2.64	-1.40	-0.77	-0.39	-0.16	-0.02	0.06	0.08	0.06
D16S3103	-∞	-1.99	-1.42	-1.04	-0.73	-0.49	-0.30	-0.17	-0.07	-0.02
D16S3046	-0.32	-0.18	-0.16	-0.17	-0.17	-0.15	-0.11	-0.07	-0.03	-0.01
D16S3068	-0.04	-0.04	-0.04	-0.03	-0.02	-0.02	-0.01	-0.01	0	0
D16S3136	0.41	0.48	0.49	0.47	0.43	0.37	0.31	0.24	0.16	0.08
D16S415	-∞	0.78	0.89	0.87	0.80	0.69	0.55	0.40	0.25	0.11
D16S503	-∞	-0.7	-0.25	-0.03	0.09	0.14	0.15	0.13	0.09	0.05
D16S515	-∞	-4.13	-2.51	-1.63	-1.07	-0.68	-0.41	-0.22	-0.10	-0.02

D16S516	0.163	0.14	0.12	0.1	0.07	0.05	0.03	0.02	0.01	0.003
D16S3091	-∞	-0.13	0.25	0.43	0.49	0.47	0.41	0.30	0.18	0.08
D16S520	-∞	1.008	1.09	1.019	0.09	0.75	0.58	0.39	0.2	0.06

Table 17. Pedigree 1: Chromosome 17 markers

Marker	**Theta=0**	**0.05**	**0.1**	**0.15**	**0.2**	**0.25**	**0.300**	**0.35**	**0.4**	**0.45**
D17S849	-∞	-2.10	-1.37	-0.93	-0.63	-0.41	-0.25	-0.14	-0.06	-0.02
D17S831	-∞	-2.42	-1.40	-0.84	-0.49	-0.27	-0.13	-0.05	-0.01	0.01
D17S938	-∞	-0.88	-0.41	-0.19	-0.07	-0.02	0	0	-0.01	-0.01
D17S1852	-∞	-0.86	-0.41	-0.20	-0.09	-0.03	-0.01	-0.01	-0.02	-0.02
D17S799	-∞	-0.84	-0.44	-0.29	-0.23	-0.22	-0.20	-0.18	-0.13	-0.06
D17S921	-∞	-2.05	-1.17	-0.7	-0.42	-0.23	-0.12	-0.05	-0.01	0
D17S1857	0.29	0.36	-0.34	-0.29	-0.23	0.17	0.11	0.06	0.03	-0.01
D17S798	-∞	-0.34	0.07	0.22	0.27	0.26	0.22	0.16	0.09	0.04
D17S1868	-∞	0.11	0.36	0.44	0.44	0.39	0.32	0.22	0.11	0.03
D17S787	-∞	-0.92	-0.53	-0.39	-0.34	-0.32	-0.30	-0.26	-0.19	-0.11
D17S944	-∞	-2.08	-1.25	-0.81	-0.52	-0.33	-0.20	-0.11	-0.06	-0.02

D17S949	-∞	-1.14	-0.57	-0.30	-0.16	-0.09	-0.05	-0.03	-0.03	-0.02
D17S785	-∞	-1.24	-0.58	-0.26	-0.09	-0.02	0.01	0	-0.01	-0.01
D17S784	-0.39	-0.23	-0.14	-0.08	-0.04	-0.02	-0.01	0	0	0
D17S928	-∞	-0.27	0.21	0.39	0.44	0.42	0.34	0.24	0.13	0.04

Table 18. Pedigree 1: Chromosome 18 markers

Marker	**Theta=0**	**0.05**	**0.1**	**0.15**	**0.2**	**0.25**	**0.300**	**0.35**	**0.4**	**0.45**
D18S59	-∞	-0.90	-0.34	-0.09	0.04	0.1	0.11	0.09	0.04	-0.01
D18S63	-∞	0.27	0.47	0.49	0.44	0.35	0.24	0.15	0.07	0.02
D18S452	1.34	1.28	1.19	1.07	0.94	0.78	0.61	0.42	0.23	0.07
D18S464	-∞	-2.63	-1.59	-1.05	-0.70	-0.46	-0.28	-0.15	-0.07	-0.02
D18S53	-0.17	-0.20	-0.21	-0.20	-0.15	-0.1	-0.06	-0.03	-0.01	0
D18S478	0.51	0.448	0.39	0.33	0.29	0.24	0.19	0.137	0.08	0.028
D18S1102	-∞	-3.57	-2.12	-1.34	-0.85	-0.51	-0.28	-0.13	-0.03	0.01
D18S474	-∞	0.54	0.87	0.95	0.92	0.82	0.67	0.50	0.32	0.14
D18S64	-∞	0.45	0.57	0.56	0.51	0.42	0.33	0.23	0.14	0.06
D18S68	-∞	-1.28	-0.75	-0.47	-0.30	-0.19	-0.11	-0.06	-0.02	-0.01
D18S61	-∞	-1.65	-0.69	-0.24	0.01	0.14	0.19	0.20	0.16	0.09

D18S1161	-∞	-1.74	-0.83	-0.37	-0.11	0.04	0.11	0.12	0.10	0.05
D18S462	0.56	0.58	0.52	0.42	0.29	0.17	0.05	-0.04	-0.07	-0.06
D18S70	-∞	-3.95	-2.31	-1.43	-0.87	-0.50	-0.25	-0.09	-0.01	0.02

Table 19. Pedigree 1: Chromosome 19 markers

Marker	**Theta=0**	**0.05**	**0.1**	**0.15**	**0.2**	**0.25**	**0.300**	**0.35**	**0.4**	**0.45**
D19S216	-∞	-1.95	-1.17	-0.76	-0.51	-0.35	-0.24	-0.17	-0.11	-0.06
D19S884	-∞	-1.92	-1.29	-0.93	-0.69	-0.51	-0.37	-0.25	-0.16	-0.08
D19S221	-∞	-1.46	-0.88	-0.57	-0.36	-0.23	-0.13	-0.07	-0.03	-0.01
D19S226	-∞	-0.90	-0.31	-0.04	0.09	0.14	0.15	0.12	0.08	0.04
D19S414	-∞	-0.81	-0.22	-0.01	0.068	0.077	0.058	0.028	-0.01	-0.023
D19S220	-∞	-3.55	-2.00	-1.2	-0.7	-0.4	-0.2	-0.1	-0.02	-0.005
D19S420	-∞	-3.25	-1.91	-1.20	-0.74	-0.44	-0.24	-0.10	-0.02	0.01
D19S902	-∞	-3.16	-1.84	-1.16	-0.74	-0.46	-0.28	-0.16	-0.07	-0.02
D19S571	-∞	-0.92	-0.59	-0.39	-0.26	-0.17	-0.10	-0.06	-0.03	-0.01
D19S418	-∞	-1.23	-0.31	0.10	0.29	0.35	0.34	0.27	0.17	0.07
D19S210	-∞	-2.79	-1.5	-0.8	-0.46	-0.2	-0.07	0.02	0.05	0.04

Table 20. Pedigree 1: Chromosome 20 markers

Marker	Theta=0	0.05	0.1	0.15	0.2	0.25	0.300	0.35	0.4	0.45
D20S117	-∞	-1.33	-0.75	-0.44	-0.25	-0.14	-0.07	-0.03	-0.01	-0.003
D20S889	-∞	-3.67	-2.19	-1.38	-0.87	-0.52	-0.28	-0.12	-0.03	0.01
D20S115	-∞	-0.63	-0.35	-0.21	-0.12	-0.06	-0.03	-0.01	0	0
D20S186	-0.18	-0.07	-0.01	0.02	0.03	0.03	0.02	0.01	0.01	0
D20S112	-∞	-1.62	-0.90	-0.54	-0.34	-0.21	-0.12	-0.07	-0.03	-0.01
D20S195	-∞	-1.80	-0.94	-0.50	-0.25	-0.11	-0.04	-0.01	-0.01	-0.01
D20S107	-∞	-3.30	-2.06	-1.38	-0.93	-0.61	-0.39	-0.23	-0.11	-0.04
D20S119	-∞	-3.58	-2.26	-1.50	-0.99	-0.63	-0.37	-0.19	-0.07	-0.01
D20S178	-∞	-3.79	-2.32	-1.52	-1.0	-0.64	-0.38	-0.21	-0.09	-0.02
D20S196	-∞	-0.76	-0.40	-0.22	-0.14	-0.11	-0.11	-0.11	-0.09	-0.06
D20S100	-0.05	-0.03	-0.02	-0.01	0	0	0	0	0	0
D20S173	-1.41	-0.95	-0.63	-0.41	-0.26	-0.16	-0.09	-0.05	-0.02	-0.01
D20S171	-∞	-1.94	-0.98	-0.52	-0.26	-0.12	-0.05	-0.02	-0.01	-0.01

Table 21. Pedigree 1: Chromosome 21 markers

Marker	Theta=0	0.05	0.1	0.15	0.2	0.25	0.300	0.35	0.4	0.45
D21S1256	-∞	-0.44	-0.16	-0.05	0.001	0.015	0.014	0.008	0.003	0.00
D21S1914	-∞	-0.70	-0.27	-0.05	0.06	0.12	0.13	0.12	0.08	0.04
D21S263	-∞	-0.32	-0.1	-0.01	0.03	0.04	0.03	0.02	0.01	0
D21S1252	-∞	-2.0	-0.98	-0.47	-0.18	0	0.09	0.13	0.12	0.07
D21S266	-∞	0.16	0.50	0.61	0.61	0.54	0.45	0.33	0.20	0.09

Table 22. Pedigree 1: Chromosome 22 markers

Marker	Theta=0	0.05	0.1	0.15	0.2	0.25	0.300	0.35	0.4	0.45
D22S420	-∞	-2.08	-1.05	-0.55	-0.26	-0.09	-0.01	0.02	0.02	0
D22S539	-∞	-2.18	-1.31	-0.85	-0.55	-0.36	-0.22	-0.13	-0.07	-0.03
D22S315	-∞	-2.25	-1.50	-1.10	-0.84	-0.64	-0.46	-0.31	-0.18	-0.08
D22S280	-∞	-2.78	-1.78	-1.20	-0.81	-0.53	-0.33	-0.18	-0.09	-0.03
D22S283	-∞	-3.51	-2.30	-1.63	-1.17	-0.84	-0.58	-0.37	-0.21	-0.08
D22S423	-∞	-1.58	-0.92	-0.57	-0.36	-0.22	-0.13	-0.07	-0.03	-0.01
D22S274	-∞	-1.8	-1.0	-0.67	-0.44	-0.28	-0.17	-0.09	-0.04	-0.01

Table 23. Pedigree 2: Chromosome 1 markers

Marker	Theta=0	0.05	0.1	0.15	0.2	0.25	0.300	0.35	0.4	0.45
D1S468	-∞	-1.88	-1.15	-0.78	-0.55	-0.39	-0.27	-0.17	-0.1	-0.04
D1S214	-∞	-2.54	-1.64	-1.15	-0.82	-0.59	-0.41	-0.27	-0.15	-0.07
D1S450	-0.13	-0.01	0.03	0.04	0.04	0.03	0.02	0.02	0.01	0.01
D1S2667	-1.9	-0.5	-0.22	-0.1	-0.04	-0.02	-0.01	-0.01	-0.01	-0.01
D1S2697	-∞	-0.73	-0.45	-0.29	-0.19	-0.12	-0.07	-0.04	-0.02	-0.01
D1S199	-∞	-2.20	-1.42	-0.99	-0.69	-0.46	-0.28	-0.15	-0.07	-0.02
D1S234	-∞	-2.11	-1.23	-0.75	-0.46	-0.27	-0.16	-0.08	-0.04	-0.01
D1S255	-0.18	-0.1	-0.05	-0.03	-0.01	0	0	0	0	0
D1S2797	-∞	-0.56	-0.16	0.05	0.17	0.22	0.23	0.21	0.15	0.08
D1S2890	-0.76	0.40	0.54	0.57	0.56	0.51	0.43	0.32	0.19	0.08
D1S230	-∞	-0.99	-0.45	-0.19	-0.05	0.02	0.05	0.05	0.04	0.02
D1S2841	-∞	-0.92	-0.51	-0.34	-0.24	-0.18	-0.12	-0.08	-0.04	-0.01
D1S207	-∞	-0.95	-0.56	-0.33	-0.19	-0.09	-0.03	0.01	0.02	0.02
D1S2868	-∞	-2.5	-1.57	-1.04	-0.69	-0.45	-0.27	-0.15	-0.06	-0.02
D1S206	-∞	-2.35	-1.47	-0.96	-0.62	-0.37	-0.21	-0.09	-0.03	0

D1S2726	-∞	-1.66	-0.99	-0.63	-0.4	-0.25	-0.15	-0.08	-0.04	-0.01
D1S252	-∞	-0.62	-0.31	-0.19	-0.16	-0.16	-0.19	-0.2	-0.17	-0.1
D1S498	-∞	-0.84	-0.28	0.03	0.20	0.27	0.28	0.24	0.16	0.08
D1S484	-∞	-0.7	-0.43	-0.29	-0.19	-0.12	-0.07	-0.04	-0.01	0
D1S2878	-∞	-1.07	-0.45	-0.21	-0.1	-0.06	-0.04	-0.03	-0.02	-0.01
D1S196	-∞	-0.93	-0.58	-0.37	-0.24	-0.15	-0.08	-0.04	-0.01	0
D1S218	-∞	-2.19	-1.36	-0.92	-0.63	-0.42	-0.27	-0.16	-0.08	-0.03
D1S238	-∞	-1.06	-0.59	-0.37	-0.23	-0.15	-0.09	-0.04	-0.02	0
D1S413	-∞	-3.83	-2.49	-1.7	-1.17	-0.79	-0.52	-0.31	-0.16	-0.06
D1S249	0.09	-0.01	-0.09	-0.15	-0.17	-0.17	-0.15	-0.11	-0.08	-0.04
D1S425	0.01	0.11	0.15	0.15	0.14	0.12	0.09	0.06	0.04	0.02
D1S213	-∞	-1.26	-0.8	-0.54	-0.36	-0.24	-0.16	-0.1	-0.06	-0.03
D1S2800	-∞	-1.74	-1.09	-0.71	-0.47	-0.31	-0.19	-0.11	-0.06	-0.02
D1S2785	-∞	-3.2	-1.9	-1.2	-0.77	-0.5	-0.3	-0.14	-0.06	-0.01
D1S2842	-∞	-0.78	-0.32	-0.13	-0.05	-0.02	-0.02	-0.02	-0.02	-0.01
D1S2836	-0.07	-0.04	-0.03	-0.01	0	0.01	0.01	0.01	0	0

Table 24. Pedigree 2: Chromosome 2 markers

Marker	Theta=0	0.05	0.1	0.15	0.2	0.25	0.300	0.35	0.4	0.45
D2S319	-∞	-1.41	-0.86	-0.58	-0.41	-0.30	-0.22	-0.16	-0.1	-0.05
D2S2211	-∞	-1.18	-0.77	-0.53	-0.36	-0.24	-0.15	-0.09	-0.04	-0.02
D2S162	1.15	1.11	1.03	0.92	0.78	0.61	0.44	0.25	0.08	-0.03
D2S168	-∞	-1.14	-0.69	-0.49	-0.37	-0.29	-0.23	-0.16	-0.10	-0.05
D2S305	-1.7	-0.28	-0.1	-0.03	0.004	0.016	0.017	0.014	0.009	0.004
D2S165	-0.54	-0.39	-0.29	-0.21	-0.14	-0.1	-0.06	-0.03	-0.01	0
D2S367	-∞	-0.55	-0.03	0.21	0.32	0.35	0.34	0.28	0.2	0.1
D2S2259	-∞	-1.37	-0.65	-0.29	-0.09	0.02	0.07	0.07	0.05	0.02
D2S391	-1.33	-0.94	-0.67	-0.47	-0.33	-0.21	-0.13	-0.07	-0.03	-0.01
D2S337	-∞	-0.01	0.2	0.25	0.23	0.19	0.14	0.09	0.05	0.02
D2S2368	-∞	-2.33	-1.22	-0.65	-0.31	-0.11	0.01	0.07	0.08	0.06
D2S286	-∞	-2.53	-1.63	-1.11	-0.76	-0.50	-0.31	-0.17	-0.07	-0.02
D2S2333	-∞	-0.9	-0.3	-0.02	0.1	0.16	0.15	0.12	0.07	0.03
D2S2216	-∞	-2.92	-1.82	-1.22	-0.83	-0.55	-0.35	-0.21	-0.10	-0.04
D2S160	-∞	-0.22	0.1	0.2	0.2	0.16	0.1	0.03	-0.01	-0.02

D2S347	-∞	-1.90	-1.09	-0.68	-0.42	-0.25	-0.14	-0.07	-0.03	0
D2S112	-∞	-3.05	-1.87	-1.22	-0.80	-0.51	-0.31	-0.17	-0.08	-0.03
D2S151	-∞	-0.68	-0.3	-0.13	-0.05	-0.01	0	0	0	0.01
D2S142	-∞	-1.51	-0.90	-0.57	-0.37	-0.23	-0.14	-0.08	-0.04	-0.02
D2S2330	-∞	-2.07	-1.27	-0.85	-0.6	-0.43	-0.31	-0.22	-0.14	-0.07
D2S335	-∞	-2.92	-1.71	-1.04	-0.61	-0.33	-0.14	-0.03	0.03	0.04
D2S364	0.24	0.2	0.17	0.14	0.11	0.08	0.06	0.03	0.02	0.01
D2S117	-∞	-2.63	-1.57	-1.0	-0.6	-0.4	-0.2	-0.15	-0.07	-0.02
D2S325	-∞	-0.88	-0.55	-0.4	-0.32	-0.28	-0.24	-0.2	-0.15	-0.08
D2S2382	-0.01	0.11	0.19	0.22	0.22	0.19	0.14	0.08	0.02	-0.01
D2S126	-∞	-0.41	-0.19	-0.09	-0.04	-0.01	0	0.01	0.01	0.01
D2S396	-∞	0.48	0.55	0.5	0.42	0.33	0.24	0.15	0.07	0.02
D2S206	-∞	-1.43	-0.84	-0.52	-0.32	-0.19	-0.1	-0.04	-0.01	0.01
D2S338	0.57	0.53	0.49	0.44	0.38	0.32	0.25	0.18	0.12	0.05
D2S125	-∞	-3.47	-2.23	-1.53	-1.05	-0.71	-0.45	-0.26	-0.13	-0.04

Table 25. Pedigree 2: Chromosome 3 markers

Marker	Theta=0	0.05	0.1	0.15	0.2	0.25	0.300	0.35	0.4	0.45
D3S1297	-∞	-1.9	-1.22	-0.82	-0.56	-0.37	-0.23	-0.13	-0.07	-0.02
D3S1304	-1.26	0.44	0.62	0.65	0.63	0.56	0.47	0.37	0.24	0.12
D3S1263	-∞	-1.78	-1.35	-0.99	-0.69	-0.46	-0.29	-0.16	-0.08	-0.02
D3S2338	-∞	-2.82	-1.72	-1.1	-0.7	-0.43	-0.24	-0.12	-0.04	-0.01
D3S1266	-0.06	-0.03	-0.01	0.01	0.01	0.01	0.01	0	0	-0.01
D3S1277	0.68	0.68	0.64	0.56	0.46	0.34	0.21	0.09	-0.01	-0.05
D3S1289	-∞	-0.91	-0.57	-0.37	-0.24	-0.15	-0.09	-0.04	-0.02	0
D3S1300	-∞	-2.31	-1.37	-0.87	-0.55	-0.33	-0.19	-0.1	-0.04	-0.01
D3S1285	0.15	0.27	0.32	0.33	0.31	0.27	0.21	0.14	0.07	0.02
D3S1566	-∞	-3.37	-2.19	-1.49	-1.01	-0.66	-0.41	-0.23	-0.1	-0.03
D3S3681	-∞	-2.54	-1.66	-1.13	-0.78	-0.52	-0.33	-0.20	-0.1	-0.04
D3S1271	-0.8	-0.52	-0.35	-0.24	-0.16	-0.1	-0.06	-0.03	-0.02	-0.01
D3S1278	-0.18	-0.13	-0.1	-0.07	-0.05	-0.03	-0.02	-0.01	-0.01	0
D3S1267	-∞	-3.11	-1.96	-1.33	-0.9	-0.6	-0.38	-0.21	-0.1	-0.03
D3S1292	-0.79	-0.38	-0.23	-0.14	-0.1	-0.06	-0.05	-0.03	-0.03	-0.01

D3S1569	-0.44	-0.26	-0.18	-0.16	-0.14	-0.14	-0.13	-0.11	-0.08	-0.05
D3S1279	-∞	-3.46	-2.14	-1.4	-0.92	-0.58	-0.34	-0.17	-0.06	-0.01
D3S1614	-∞	-0.52	-0.21	-0.06	0.03	0.07	0.09	0.09	0.07	0.04
D3S1565	-∞	-2.64	-1.63	-1.08	-0.71	-0.46	-0.28	-0.16	-0.08	-0.03
D3S1262	-0.16	0.08	0.16	0.18	0.18	0.16	0.13	0.10	0.07	0.03
D3S1580	-∞	-2.92	-1.88	-1.24	-0.8	-0.5	-0.28	-0.13	-0.04	0.01
D3S1601	-∞	-2.27	-1.45	-0.99	-0.69	-0.47	-0.3	-0.17	-0.08	-0.02
D3S1311	-∞	-1.37	-0.76	-0.46	-0.29	-0.19	-0.13	-0.09	-0.06	-0.03

Table 26. Pedigree 2: Chromosome 4 markers

Marker	**Theta=0**	**0.05**	**0.1**	**0.15**	**0.2**	**0.25**	**0.300**	**0.35**	**0.4**	**0.45**
D4S412	-∞	-0.52	-0.27	-0.14	-0.07	-0.02	0.01	0.02	0.02	0.02
D4S2935	-∞	-3.43	-2.06	-1.33	-0.87	-0.56	-0.34	-0.19	-0.09	-0.03
D4S403	-∞	-2.51	-1.58	-1.06	-0.72	-0.48	-0.31	-0.18	-0.09	-0.03
D4S419	0.36	0.46	0.47	0.44	0.38	0.31	0.23	0.15	0.08	0.02
D4S391	-∞	-0.74	-0.16	0.12	0.25	0.3	0.29	0.23	0.15	0.06
D4S405	-1.87	-1.04	-0.64	-0.39	-0.22	-0.11	-0.04	0.01	0.02	0.02
D4S1592	-∞	0.07	0.36	0.46	0.48	0.43	0.36	0.27	0.16	0.07

D4S392	-∞	-1.61	-0.85	-0.48	-0.28	-0.16	-0.08	-0.03	-0.01	0.01
D4S2964	-∞	-2.71	-1.63	-1.05	-0.69	-0.45	-0.28	-0.16	-0.08	-0.03
D4S1534	-∞	-2.07	-1.23	-0.78	-0.49	-0.3	-0.17	-0.09	-0.04	-0.01
D4S414	-∞	-0.09	0.24	0.36	0.38	0.35	0.27	0.18	0.09	0..03
D4S1572	-∞	-2.06	-1.24	-0.79	-0.51	-0.32	-0.19	-0.1	-0.04	-0.01
D4S406	0.46	0.39	0.34	0.28	0.23	0.18	0.13	0.09	0.05	0.02
D4S402	-∞	-1.45	-0.95	-0.63	-0.42	-0.26	-0.15	-0.07	-0.03	-0.01
D4S1575	-0.03	0.01	0.03	0.04	0.04	0.04	0.03	0.02	0.01	0.01
D4S424	-0.5	-0.4	-0.29	-0.19	-0.11	-0.04	0	0.02	0.03	0.02
D4S413	-∞	-2.37	-1.46	-0.98	-0.67	-0.46	-0.31	-0.2	-0.11	-0.04
D4S1597	-0.1	-0.06	-0.03	-0.01	0	0.01	0.01	0.01	0.01	0.01
D4S1539	-0.34	-0.29	-0.24	-0.19	-0.14	-0.1	-0.06	-0.03	-0.01	0
D4S1535	0.132	0.133	0.114	0.082	0.046	0.013	-0.01	-0.03	-0.03	-0.02
D4S426	0.08	0.13	0.13	0.11	0.07	0.04	0.01	-0.02	-0.03	-0.02

Table 27. Pedigree 2: Chromosome 5 markers

Marker	Theta=0	0.05	0.1	0.15	0.2	0.25	0.300	0.35	0.4	0.45
D5S1981	-∞	-0.71	-0.26	-0.06	0.03	0.07	0.07	0.06	0.04	0.01
D5S406	-∞	-2.59	-1.62	-1.08	-0.71	-0.46	-0.28	-0.15	-0.07	-0.02
D5S630	-1.31	-1.05	-0.7	-0.46	-0.29	-0.17	-0.09	-0.04	-0.01	0.01
D5S416	0.12	0.14	0.15	0.15	0.14	0.13	0.11	0.09	0.06	0.03
D5S419	-∞	-1.25	-0.52	-0.19	-0.01	0.07	0.1	0.09	0.06	2
D5S426	-∞	-0.23	-0.04	0.04	0.07	0.08	0.08	0.06	0.05	0.02
D5S418	-∞	-1.79	-.15	-0.77	-0.51	-0.31	-0.17	-0.08	-0.02	0.01
D5S407	-∞	-0.79	-0.48	-0.32	-0.22	-0.16	-0.12	-0.09	-0.07	-0.03
D5S647	-1.69	-1.08	-0.74	-0.51	-0.34	-0.22	-0.14	-0.08	-0.03	-0.01
D5S424	-0.06	-0.05	-0.04	-0.03	-0.02	-0.02	-0.01	-0.01	-0.01	0
D5S641	0.16	0.21	0.19	0.16	0.11	0.05	0	0	-0.05	-0.04
D5S428	-0.37	-0.3	-0.26	-0.23	-0.19	-0.16	-0.13	-0.09	-0.06	-0.03
D5S644	-∞	-1.1	-0.65	-0.4	-0.3	-0.2	-0.15	-0.09	-0.5	0.02
D5S433	-∞	-0.46	-0.22	-0.1	-0.04	0	0.01	0.02	0.02	0.01
D5S2027	-∞	-0.83	-0.44	-0.24	-0.12	-0.05	-0.01	0	0.01	0

D5S471	-∞	-1.5	-0.97	-0.62	-0.39	-0.22	-0.12	-0.05	-0.02	0
D5S2115	-∞	-4.0	-2.4	-1.5	-1.0	-0.67	-0.4	-0.23	-0.1	-0.03
D5S436	-0.3	-0.21	-0.15	-0.1	-0.07	-0.04	-0.03	-0.01	-0.01	0
D5S410	-0.45	-0.33	-0.24	-0.18	-0.12	-0.08	-0.05	-0.03	-0.01	0
D5S422	-∞	-0.46	-0.04	0.13	0.19	0.19	0.16	0.12	0.07	0.03
D5S400	-0.68	-0.53	-0.39	-0.28	-0.19	-0.12	-0.07	-0.04	-0.02	0
D5S408	-∞	-1.02	-0.66	-0.44	-0.29	-0.19	-0.11	-0.05	-0.02	-0.01

Table 28. Pedigree 2: Chromosome 6 markers

Marker	**Theta=0**	**0.05**	**0.1**	**0.15**	**0.2**	**0.25**	**0.300**	**0.35**	**0.4**	**0.45**
D6S1574	-0.25	0.04	0.12	0.14	0.13	0.11	0.09	0.06	0.04	0.02
D6S309	0.39	0.37	0.33	0.28	0.22	0.16	0.11	0.06	0.02	0
D6S470	-0.78	-0.38	-0.23	-0.14	-0.08	-0.04	-0.01	0	0.01	0.01
D6S289	-0.25	0.04	0.12	0.14	0.13	0.11	0.09	0.06	0.04	0.02
D6S422	-∞	-1.3	-0.9	-0.7	-0.6	-0.5	-0.3	-0.1	-0.01	-0.01
D6S276	-∞	-2.0	-1.3	-0.89	-0.61	-0.41	-0.26	-0.16	-0.08	-0.03
D6S1610	-∞	-1.93	-1.28	-0.91	-0.66	-0.48	-0.33	-0.22	-0.12	-0.05

D6S257	-∞	-2.82	-1.81	-1.22	-0.82	-0.54	-0.33	-0.18	-0.08	-0.02
D6S460	0.84	0.81	0.73	0.63	0.53	0.43	0.33	0.23	0.14	0.06
D6S462	0.42	0.32	0.22	0.12	0.03	-0.04	-0.08	-0.09	-0.08	-0.05
D6S434	-0.06	-0.05	-0.04	-0.03	-0.02	-0.02	-0.01	-0.01	-0.01	0
D6S287	-∞	-0.04	0.15	0.21	0.2	0.17	0.13	0.08	0.04	0.01
D6S262	-∞	0.3	0.5	0.5	0.4	0.35	0.24	0.14	0.05	0
D6S292	-∞	-1.28	-0.65	-0.36	-0.19	-0.09	-0.03	-0.01	0.01	0.01
D6S308	-∞	-0.54	-0.3	-0.19	-0.12	-0.08	-0.05	-0.02	-0.01	0
D6S441	-∞	-1.86	-1.01	-0.56	-0.29	-0.12	-0.02	0.04	0.06	0.04
D6S1581	-∞	-1.02	-0.66	-0.44	-0.29	-0.19	-0.11	-0.05	-0.02	0
D6S264	0.2	0.21	0.21	0.19	0.15	0.1	0.04	-0.01	-0.04	-0.04
D6S446	-0.82	-0.55	-0.37	-0.25	-0.16	-0.09	-0.05	-0.02	0	0.01
D6S281	-∞	0.23	0.39	0.41	0.38	0.32	0.24	0.15	0.08	0.02

Table 29. Pedigree 2: Chromosome 7 markers

Marker	Theta=0	0.05	0.1	0.15	0.2	0.25	0.300	0.35	0.4	0.45
D7S517	-∞	-1.24	-0.71	-0.44	-0.27	-0.17	-0.1	-0.06	-0.03	-0.01
D7S513	-∞	-0.27	0.05	0.12	0.1	0.05	-0.01	-0.05	-0.06	-0.04
D7S507	-∞	-1.05	-0.66	-0.42	-0.25	-0.14	-0.06	-0.01	0.01	0.02
D7S493	0.108	0.131	0.133	0.12	0.1	0.075	0.05	0.03	0.01	0.003
D7S516	0.369	0.368	0.363	0.317	0.260	0.198	0.140	0.088	0.048	0.019
D7S484	-∞	0.42	0.50	0.45	0.36	0.24	0.12	0	-0.08	-0.09
D7S510	-∞	-1.52	-0.94	-0.6	-0.39	-0.24	-0.14	-0.08	-0.04	-0.01
D7S519	-∞	0.24	0.48	0.57	0.57	0.53	0.44	0.34	0.22	0.11
D7S502	-∞	-1.8	-1.0	-0.7	-0.4	-0.3	-0.2	-0.1	-0.07	-0.03
D7S669	-∞	-1.4	-0.91	-0.62	-0.42	-0.28	-0.18	-0.11	-0.05	-0.02
D7S630	-∞	-2.27	-1.46	-0.97	-0.64	-0.4	-0.23	-0.12	-0.05	-0.01
D7S657	-∞	-1.97	-1.26	-0.85	-0.58	-0.39	-0.25	-0.14	-0.07	-0.02
D7S486	0.27	0.25	0.22	0.18	0.14	0.10	0.06	0.03	0.01	0
D7S530	-∞	-1.29	-0.76	-0.49	-0.31	-0.19	-0.11	-0.06	-0.03	-0.01
D7S640	-∞	-2.27	-1.48	-1.04	-0.75	-0.54	-0.38	-0.26	-0.15	-0.06

D7S684	-∞	-2.9	-1.6	-1.0	-0.6	-0.36	-0.19	-0.08	-0.03	0
D7S661	-∞	-3.5	-2.0	-1.3	-0.8	-0.5	-0.27	-0.12	-0.04	-0.002
D7S636	-∞	-1.14	-0.69	-0.49	-0.37	-0.29	-0.23	-0.16	-0.10	-0.05
D7S798	-∞	-3.01	-1.84	-1.20	-0.78	-0.5	-0.3	-0.16	-0.07	-0.02
D7S2465	-∞	-0.33	0.02	0.12	0.12	0.08	0.03	-0.02	-0.03	-0.02

Table 30. Pedigree 2: Chromosome 8 markers

Marker	**Theta= 0**	**0.05**	**0.1**	**0.15**	**0.2**	**0.25**	**0.300**	**0.35**	**0.4**	**0.45**
D8S264	-∞	-1.19	-0.54	-0.23	-0.07	0.01	0.04	0.03	0.02	0.01
D8S277	-∞	-3.51	-2.28	-1.54	-1.04	-0.69	-0.43	-0.24	-0.11	-0.03
D8S550	-∞	-1.09	-0.53	-0.24	-0.08	0	0.05	0.06	0.05	0.03
D8S549	-∞	-0.75	-0.46	-0.31	-0.20	-0.13	-0.08	-0.04	-0.02	-0.01
D8S258	-∞	-1.12	-0.73	-0.5	-0.34	-0.22	-0.14	-0.08	-0.04	-0.01
D8S1771	-2.0	-0.35	-0.14	-0.05	0.01	0.04	0.05	0.05	0.04	0.02
D8S505	-0.23	-0.15	-0.10	-0.06	-0.04	-0.02	-0.01	0	0	0
D8S285	-∞	-1.57	-0.98	-0.63	-0.41	-0.25	-0.15	-0.08	-0.03	-0.01
D8S260	-∞	-1.97	-1.28	-0.87	-0.59	-0.38	-0.24	-0.13	-0.06	-0.02

D8S270	-∞	-2.24	-1.25	-0.74	-0.42	-0.22	-0.10	-0.02	0.01	0.02
D8S1784	-0.68	-0.17	-0.02	0.03	0.04	0.04	0.03	0.02	0.01	0
D8S514	0.09	0.12	0.12	0.11	0.09	0.07	0.05	0.04	0.02	0.01
D8S284	-1.38	-1.19	-0.93	-0.73	-0.56	-0.42	-0.31	-0.21	-0.13	-0.06
D8S272	-∞	-2.19	-1.52	-1.10	-0.81	-0.59	-0.42	-0.28	-0.17	-0.07

Table 31. Pedigree 2: Chromosome 9 markers

Marker	**Theta =0**	**0.05**	**0.1**	**0.15**	**0.2**	**0.25**	**0.300**	**0.35**	**0.4**	**0.45**
D9S288	-∞	-2.31	-1.35	-0.82	-0.48	-0.25	-0.1	-0.02	0.03	0.03
D9S285	0.33	0.3	0.27	0.24	0.21	0.17	0.14	0.1	0.06	0.03
D9S157	-∞	-2.14	-1.21	-0.76	-0.50	-0.34	-0.24	-0.16	-0.1	-0.04
D9S171	-0.25	-0.17	-0.12	-0.08	-0.05	-0.04	-0.02	-0.01	-0.01	0
D9S161	-∞	-1.96	-1.11	-0.66	-0.37	-0.18	-0.06	0.01	0.04	0.04
D9S1817	-∞	-0.65	-0.27	-0.09	0	0.05	0.07	0.06	0.05	0.03
D9S273	0.06	0.07	0.07	0.06	0.05	0.04	0.02	0.01	0.01	0
D9S175	-∞	-1.26	-0.73	-0.45	-0.28	-0.16	-0.09	-0.04	-0.01	0
D9S167	-∞	-2.06	-1.29	-0.85	-0.57	-0.37	-0.23	-0.13	-0.06	-0.02
D9S283	-∞	-0.84	-0.47	-0.26	-0.14	-0.06	-0.01	0.01	0.02	0.02

D9S287	-∞	-2.08	-1.27	-0.82	-0.54	-0.34	-0.21	-0.11	-0.05	-0.02
D9S1690	-∞	-1.0	-0.48	-0.24	-0.12	-0.06	-0.05	-0.06	-0.07	-0.05
D9S1677	-∞	-0.73	-0.46	-0.31	-0.21	-0.14	-0.09	-0.06	-0.03	-0.01
D9S1776	-∞	0.38	0.5	0.51	0.46	0.39	0.29	0.18	0.07	0
D9S1682	-∞	-0.4	0.07	0.26	0.32	0.3	0.23	0.13	0.02	-0.04
D9S290	0.047	0.16	0.2	0.18	0.15	0.11	0.07	0.04	0.02	0
D9S164	-∞	-1.61	-0.85	-0.48	-0.26	-0.13	-0.06	-0.02	0	0.01
D9S1826	-∞	-2.02	-1.06	-0.55	-0.25	-0.06	0.04	0.08	0.08	0.05
D9S158	-∞	-2.08	-1.21	-0.76	-0.49	-0.32	-0.21	-0.13	-0.07	-0.03

Table 32. Pedigree 2: Chromosome 10 markers

Marker	**Theta=0**	**0.05**	**0.1**	**0.15**	**0.2**	**0.25**	**0.300**	**0.35**	**0.4**	**0.45**
D10S249	-∞	-1.13	-0.78	-0.6	-0.48	-0.38	-0.29	-0.21	-0.13	-0.06
D10S591	1.51	1.30	1.08	0.87	0.66	0.47	0.29	0.14	0.04	-0.01
D10S189	0.35	0.37	0.39	0.38	0.35	0.3	0.22	0.13	0.05	-0.01
D10S547	0.10	0.11	0.10	0.09	0.07	0.05	0.03	0.01	0.01	0
D10S1653	-∞	-0.1	0.3	0.45	0.48	0.44	0.37	0.28	0.19	0.09
D10S548	-∞	-2.17	-1.37	-0.94	-0.67	-0.48	-0.33	-0.21	-0.12	-0.05

D10S197	-∞	-0.45	-0.1	0.02	0.04	0.03	0	-0.02	-0.04	-0.03
D10S213	-∞	-1.2	-0.6	-0.34	-0.22	-0.16	-0.14	-0.11	-0.09	-0.05
D10S208	-∞	-1.06	-0.47	-0.18	-0.01	0.08	0.11	0.12	0.09	0.05
D10S1780	-∞	-1.22	-0.51	-0.17	-0.01	0.09	0.12	0.12	0.09	0.05
D10S578	-∞	-0.1	0.04	0.06	0.04	0.01	-0.02	-0.04	-0.04	-0.03
D10S196	-∞	-3.65	-2.23	-1.46	-0.96	-0.61	-0.36	-0.19	-0.08	-0.01
D10S1790	-∞	0.59	0.9	0.94	0.87	0.73	0.55	0.36	0.19	0.06
D10S1652	-1.56	-0.56	-0.3	-0.2	-0.13	-0.09	-0.06	-0.03	-0.02	-0.01
D10S581	-∞	-1.92	-0.95	-0.48	-0.22	-0.07	-0.01	0.01	0.01	-0.01
D10S537	-∞	-2.69	-1.63	-1.08	-0.72	-0.48	-0.31	-0.19	-0.11	-0.05
D10S580	-∞	-1.03	-0.56	-0.33	-0.19	-0.11	-0.06	-0.03	-0.01	0
D10S1686	-∞	-1.02	-0.58	-0.34	-0.19	-0.1	-0.05	-0.02	-0.01	0
D10S185	-∞	-2.17	-1.29	-0.82	-0.53	-0.33	-0.19	-0.1	-0.04	-0.01
D10S1709	-∞	-1.24	-0.54	-0.22	-0.05	0.04	0.07	0.08	0.07	0.04
D10S192	-∞	-0.79	-0.47	-0.31	-0.2	-0.13	-0.07	-0.03	0	0.01
D10S597	-∞	-1.26	-0.87	-0.61	-0.42	-0.28	-0.17	-0.10	-0.05	-0.01
D10S1693	-∞	-0.91	-0.58	-0.42	-0.32	-0.25	-0.20	-0.15	-0.1	-0.05

D10S587	-∞	-0.81	-0.47	-0.27	-0.14	-0.05	0	0.03	0.04	0.03
D10S1656	-∞	-1.64	-0.9	-0.54	-0.33	-0.21	-0.14	-0.09	-0.05	-0.03
D10S217	-∞	-2.78	-1.60	-0.97	-0.58	-0.32	-0.15	-0.04	0.02	0.03
D10S1651	-∞	-1.47	-0.81	-0.51	-0.35	-0.26	-0.19	-0.14	-0.09	-0.04
D10S212	-∞	-1.38	-0.87	-0.58	-0.4	-0.27	-0.18	-0.11	-0.06	-0.03

Table 33. Pedigree 2: Chromosome 11 markers

Marker	**Theta=0**	**0.05**	**0.1**	**0.15**	**0.2**	**0.25**	**0.300**	**0.35**	**0.4**	**0.45**
D11S4046	0.40	0.39	0.36	0.32	0.27	0.21	0.16	0.11	0.06	0.02
D11S1338	-∞	0.22	0.44	0.51	0.51	0.47	0.41	0.32	0.21	0.11
D11S902	-∞	-1.63	-0.78	-0.38	-0.16	-0.04	0.02	0.04	0.04	0.02
D11S904	-∞	-1.06	-0.67	-0.44	-0.29	-0.18	-0.1	-0.05	-0.02	0
D11S935	-∞	-2.28	-1.43	-0.94	-0.6	-0.37	-0.21	-0.1	-0.04	-0.01
D11S905	-∞	-1.95	-1.03	-0.54	-0.24	-0.06	0.04	0.08	0.08	0.05
D11S4191	-∞	-2.62	-1.75	-1.20	-0.82	-0.53	-0.32	-0.17	-0.07	-0.01
D11S987	-∞	-0.22	0.08	0.19	0.22	0.2	0.16	0.1	0.04	0.01
D11S1314	-0.2	-0.08	-0.01	0.04	0.07	0.09	0.09	0.08	0.06	0.03

D11S901	-∞	-2.70	-1.72	-1.16	-0.78	-0.51	-0.32	-0.18	-0.08	-0.02
D11S937	-∞	-2.09	-1.22	-0.76	-0.47	-0.28	-0.16	-0.07	-0.02	0
D11S898	0.5	0.5	0.4	0.35	0.3	0.22	0.16	0.1	0.06	0.02
D11S908	-∞	-0.15	0.31	0.49	0.54	0.53	0.46	0.36	0.23	0.1
D11S925	-∞	-1.53	-0.97	-0.67	-0.49	-0.37	-0.28	-0.2	-0.13	-0.07
D11S4151	-∞	-2.65	-1.59	-1.03	-0.68	-0.45	-0.29	-0.18	-0.10	-0.04
D11S1320	-∞	-2.29	-1.54	-1.07	-0.73	-0.48	-0.30	-0.16	-0.07	-0.02
D11S968	-∞	-0.74	-0.27	-0.05	0.07	0.13	0.14	0.13	0.09	0.05

Table 34. Pedigree 2: Chromosome 12 markers

Marker	**Theta=0**	**0.05**	**0.1**	**0.15**	**0.2**	**0.25**	**0.300**	**0.35**	**0.4**	**0.45**
D12S352	-∞	-2.74	-1.66	-1.0	-0.71	-0.45	-0.27	-0.15	-0.07	-0.02
D12S99	-∞	-2.2	-1.17	-0.6	-0.3	-0.12	-0.02	0.03	0.036	0.02
D12S336	-∞	-2.37	-1.38	-0.85	-0.52	-0.31	-0.17	-0.08	-0.03	0
D12S364	-∞	-1.67	-0.97	-0.63	-0.44	-0.33	-0.25	-0.18	-0.12	-0.06
D12S310	-0.32	-0.21	-0.14	-0.09	-0.06	-0.04	-0.02	-0.01	0	0.01
D12S1617	-∞	0.26	0.2	0.15	0.12	0.1	0.1	0.08	0.02	0.01

D12S345	-∞	1.36	1.36	1.23	1.05	0.85	0.63	0.41	0.21	0.05
D12S85	-∞	0.24	0.47	0.53	0.51	0.44	0.34	0.21	0.09	0
D12S368	-∞	-0.92	-0.56	-0.37	-0.26	-0.18	-0.13	-0.09	-0.05	-0.03
D12S83	-∞	-1.65	-1.04	-0.71	-0.50	-0.35	-0.24	-0.16	-0.09	-0.04
D12S326	-0.12	0.03	0.09	0.11	0.11	0.10	0.08	0.06	0.04	0.02
D12S351	-∞	-0.36	-0.15	-0.06	-0.03	-0.02	-0.02	-0.03	-0.03	-0.02
D12S346	-∞	-1.79	-0.93	-0.51	-0.26	-0.12	-0.05	-0.01	0	0
D12S78	-∞	-1.5	-0.84	-0.5	-0.29	-0.16	-0.08	-0.02	0	0.01
D12S79	-∞	-0.28	0.14	0.30	0.35	0.34	0.29	0.21	0.13	0.05
D12S86	-∞	-1.7	-1.0	-0.6	-0.4	-0.3	-0.2	-0.15	-0.1	-0.05
D12S324	0.51	0.39	0.28	0.18	0.10	0.04	-0.01	-0.03	-0.03	-0.02
D12S1659	0.446	0.4	0.35	0.28	0.022	0.165	0.112	0.07	0.03	0.01
D12S1723	0.14	0.25	0.28	0.27	0.24	0.19	0.14	0.08	0.04	0.01

Table 35. Pedigree 2: Chromosome 13 markers

Marker	Theta=0	0.05	0.1	0.15	0.2	0.25	0.300	0.35	0.4	0.45
D13S175	-0.19	-0.03	0.08	0.14	0.17	0.17	0.16	0.13	0.09	0.05
D13S217	-∞	-1.29	-0.71	-0.39	-0.18	-0.04	0.04	0.08	0.09	0.06
D13S171	-∞	-1.25	-0.75	-0.46	-0.28	-0.16	-0.08	-0.03	-0.01	0
D13S218	-∞	0.47	0.63	0.63	0.56	0.45	0.32	0.20	0.10	0.03
D13S263	-∞	-1.49	-0.8	-0.48	-0.3	-0.2	-0.16	-0.12	-0.09	-0.05
D13S153	-∞	0.09	0.26	0.30	0.28	0.24	0.19	0.13	0.08	0.03
D13S156	-∞	-1.8	-1.0	-0.66	-0.4	-0.2	-0.12	-0.05	-0.01	0.01
D13S170	-∞	-2.63	-1.56	-0.99	-0.64	-0.4	-0.24	-0.13	-0.06	-0.01
D13S265	-∞	-0.9	-0.52	-0.32	-0.2	-0.13	-0.08	-0.05	-0.03	-0.01
D13S159	-∞	-3.49	-2.39	-1.69	-1.17	-0.79	-0.51	-0.29	-0.14	-0.05
D13S158	-∞	-1.23	-0.80	-0.56	-0.39	-0.28	-0.19	-0.12	-0.07	-0.03
D13S173	-∞	-3.35	-2.11	-1.44	-0.99	-0.68	-0.45	-0.28	-0.15	-0.06
D13S1265	-∞	-1.19	-0.74	-0.48	-0.31	-0.19	-0.11	-0.06	-0.02	0
D13S285	-∞	-1.69	-0.84	-0.41	-0.15	-0.01	0.05	0.06	0.04	0.01

Table 36. Pedigree 2: Chromosome 14 markers

Marker	Theta=0	0.05	0.1	0.15	0.2	0.25	0.300	0.35	0.4	0.45
D14S261	-∞	-0.59	-0.13	0.08	0.19	0.23	0.23	0.20	0.15	0.08
D14S283	-∞	-2.98	-1.83	-1.2	-0.79	-0.51	-0.31	-0.17	-0.08	-0.02
D14S275	-∞	-0.53	-0.19	-0.05	0.01	0.03	0.02	0.01	0	0
D14S70	-∞	-1.24	-0.69	-0.41	-0.23	-0.13	-0.06	-0.02	0	0.01
D14S288	-∞	-0.96	-0.52	-0.27	-0.11	-0.01	0.04	0.07	0.07	0.04
D14S276	-∞	-2.58	-1.81	-1.31	-0.94	-0.66	-0.43	-0.26	-0.13	-0.05
D14S63	-∞	-3.31	-2.05	-1.35	-0.89	-0.57	-0.34	-0.18	-0.07	-0.02
D14S258	-0.61	-0.36	-0.24	-0.16	-0.11	-0.08	-0.05	-0.04	-0.02	-0.01
D14S74	-∞	-2.01	-1.28	-0.85	-0.57	-0.37	-0.23	-0.13	-0.06	-0.02
D14S68	-∞	-1.36	-0.78	-0.49	-0.31	-0.21	-0.14	-0.10	-0.07	-0.04
D14S280	-∞	-1.26	-0.61	-0.29	-0.11	-0.01	0.03	0.05	0.04	0.02
D14S65	-∞	-3.47	-2.17	-1.44	-0.95	-0.62	-0.38	-0.21	-0.10	-0.03
D14S985		-∞	-1.96	-1.29	-0.91	-0.65	-0.46	-0.32	-0.21	-0.12
D14S292	-∞	-1.64	-1.03	-0.68	-0.46	-0.30	-0.19	-0.11	-0.05	-0.01

Table 37. Pedigree 2: Chromosome 15 markers

Marker	Theta=0	0.05	0.1	0.15	0.2	0.25	0.300	0.35	0.4	0.45
D15S128	-∞	-1.58	-1.07	-0.75	-0.53	-0.37	-0.25	-0.15	-0.08	-0.03
D15S1002	-∞	-1.54	-0.73	-0.32	-0.08	0.05	0.12	0.13	0.11	0.06
D15S165	0.209	0.160	0.126	0.096	0.072	0.053	0.038	0.025	0.015	0.007
D15S1007	-∞	-2.9	-1.69	-1.02	-0.6	-0.32	-0.14	-0.03	0.03	0.03
D15S1012	-∞	-2.74	-1.61	-1.0	-0.62	-0.36	-0.18	-0.07	-0.01	0.01
D15S994	0.556	0.49	0.42	0.36	0.29	0.23	0.17	0.11	0.07	0.03
D15S978	-∞	-2.02	-1.17	-0.72	-0.44	-0.25	-0.13	-0.05	-0.01	0.01
D15S117	-∞	-0.68	-0.35	-0.18	-0.08	-0.02	0.01	0.02	0.02	0.01
D15S153	-∞	-0.78	-0.53	-0.40	-0.31	-0.23	-0.17	-0.12	-0.07	-0.03
D15S131	-∞	0.11	0.28	0.32	0.30	0.25	0.20	0.15	0.09	0.04
D15S205	-∞	-1.82	-1.02	-0.62	-0.37	-0.22	-0.12	-0.05	-0.01	0.01
D15S127	-∞	-1.7	-0.9	-0.57	-0.32	-0.16	-0.06	-0.01	0.02	0.02
D15S130	-∞	-2.35	-1.4	-0.9	-0.7	-0.5	-0.35	-0.24	-0.15	-0.07
D15S120	-∞	-0.92	-0.28	0	0.13	0.18	0.18	0.15	0.10	0.05

Table 38. Pedigree 2: Chromosome 16 markers

Marker	Theta=0	0.05	0.1	0.15	0.2	0.25	0.300	0.35	0.4	0.45
D16S423	-∞	-3.87	-2.50	-1.70	-1.17	-0.78	-0.49	-0.28	-0.13	-0.04
D16S404	-∞	-2.67	-1.5	-0.9	-0.6	-0.4	-0.2	-0.12	-0.06	-0.02
D16S3075	-∞	-2.40	-1.50	-1.0	-0.67	-0.44	-0.27	-0.15	-0.07	-0.02
D16S3103	-0.25	-0.14	-0.08	-0.04	-0.02	-0.01	0	0	0	0
D16S3046	-∞	-1.26	-0.83	-0.57	-0.38	-0.26	-0.16	-0.10	-0.05	-0.02
D16S3068	-∞	-1.66	-0.98	-0.67	-0.51	-0.40	-0.33	-0.25	-0.17	-0.08
D16S3136	-∞	-0.68	-0.33	-0.15	-0.05	0	0.03	0.04	0.03	0.02
D16S415	-∞	-1.36	-0.76	-0.44	-0.25	-0.13	-0.06	-0.03	-0.01	-0.01
D16S503	-1.02	-0.68	-0.45	-0.30	-0.19	-0.11	-0.05	-0.02	0	0.01
D16S515	-∞	-1.53	-0.87	-0.50	-0.26	-0.11	-0.02	0.03	0.05	0.04
D16S516	-1.7	-0.7	-0.4	-0.25	-0.15	-0.09	-0.06	-0.04	-0.02	-0.01
D16S3091	-0.75	-0.51	-0.36	-0.26	-0.19	-0.14	-0.09	-0.06	-0.04	-0.02
D16S520	-∞	-2.7	-1.4	-0.8	-0.4	-0.2	-0.1	-0.02	-0.02	0.02

Table 39. Pedigree 2: Chromosome 17 markers

Marker	Theta=0	0.05	0.1	0.15	0.2	0.25	0.300	0.35	0.4	0.45
D17S849	-1.44	-0.72	-0.43	-0.26	-0.15	-0.07	-0.02	0.01	0.02	0.01
D17S831	-∞	-0.99	-0.45	-0.15	0.02	0.11	0.15	0.14	0.11	0.06
D17S938	-∞	-1.56	-1.13	-0.81	-0.56	-0.37	-0.23	-0.12	-0.06	-0.01
D17S1852	0.54	0.52	0.47	0.42	0.37	0.3	0.24	0.17	0.11	0.05
D17S799	-∞	-1.20	-0.59	-0.28	-0.11	-0.01	0.03	0.04	0.03	0.02
D17S921	1.36	1.26	1.14	0.99	0.82	0.65	0.48	0.32	0.18	0.07
D17S1857	-∞	-1.36	-0.77	-0.46	-0.26	-0.13	-0.05	-0.01	0.02	0.02
D17S798	-∞	-2.53	-1.65	-1.14	-0.78	-0.51	-0.32	-0.18	-0.08	-0.02
D17S1868	-∞	0.47	0.66	0.68	0.63	0.53	0.4	0.26	0.13	0.03
D17S787	-∞	0.38	0.63	0.7	0.69	0.63	0.53	0.41	0.27	0.13
D17S944	-0.11	-0.11	-0.11	-0.10	-0.08	-0.07	-0.06	-0.04	-0.03	-0.01
D17S949	-∞	0.83	0.87	0.80	0.69	0.56	0.43	0.31	0.19	0.08
D17S785	-∞	0.1	0.33	0.39	0.38	0.31	0.22	0.13	0.04	-0.01
D17S784	-0.47	-0.35	-0.23	-0.14	-0.08	-0.04	-0.01	0	0	0.01
D17S928	-∞	-0.11	0.13	0.21	0.21	0.18	0.13	0.08	0.05	0.02

Table 40. Pedigree 2: Chromosome 18 markers

Marker	Theta=0	0.05	0.1	0.15	0.2	0.25	0.300	0.35	0.4	0.45
D18S59	-∞	-2.95	-1.94	-1.35	-0.94	-0.64	-0.41	-0.25	-0.13	-0.04
D18S63	-∞	-1.43	-0.85	-0.55	-0.36	-0.23	-0.15	-0.09	-0.04	-0.02
D18S452	-∞	-1.3	-0.76	-0.47	-0.28	-0.15	-0.07	-0.02	-0.01	0.01
D18S464	-∞	-2.56	-1.63	-1.10	-0.74	-0.48	-0.30	-0.16	-0.08	-0.03
D18S53	-∞	-2.16	-1.28	-0.79	-0.48	-0.28	-0.14	-0.05	0	0.01
D18S478	-∞	-1.25	-0.7	-0.47	-0.3	-0.2	-0.13	-0.07	-0.04	-0.01
D18S1102	-∞	-1.4	-0.69	-0.36	-0.18	-0.07	-0.02	0	0.01	0.01
D18S474	-∞	-0.69	-0.37	-0.2	-0.1	-0.04	0	0.02	0.02	0.01
D18S64	-1.99	-1.19	-0.71	-0.44	-0.28	-0.17	-0.1	-0.05	-0.02	-0.01
D18S68	-2.46	-0.32	-0.07	0.03	0.08	0.09	0.07	0.05	0.03	0.01
D18S61	-∞	-0.81	-0.27	-0.03	0.06	0.09	0.07	0.03	0	-0.02
D18S1161	-∞	-0.54	-0.16	0.05	0.16	0.21	0.22	0.19	0.13	0.07
D18S462	-∞	-0.97	-0.63	-0.44	-0.32	-0.23	-0.16	-0.11	-0.07	-0.03
D18S70	-0.52	-0.23	-0.07	0.02	0.07	0.08	0.08	0.06	0.04	0.02

Table 41. Pedigree 2: Chromosome 19 markers

Marker	Theta=0	0.05	0.1	0.15	0.2	0.25	0.300	0.35	0.4	0.45
D19S209	-∞	-2.30	-1.29	-0.71	-0.39	-0.19	-0.07	-0.01	0.02	0.02
D19S216	0.44	0.35	0.27	0.2	0.14	0.10	0.06	0.03	0.01	0
D19S884	-∞	-2.37	-1.43	-0.93	-0.6	-0.38	-0.24	-0.13	-0.06	-0.02
D19S221	-∞	0.02	0.19	0.23	0.22	0.18	0.14	0.10	0.06	0.03
D19S226	-∞	-0.91	-0.45	-0.24	-0.12	-0.05	-0.02	0	0.01	0.01
D19S414	-∞	-3.5	-2.17	-1.44	-0.9	-0.6	-0.39	-0.22	-0.01	-0.03
D19S220	-∞	-4	-2.4	-1.6	-1.0	-0.66	-0.39	-0.2	-0.08	-0.01
D19S420	-∞	-2.36	-1.45	-0.95	-0.62	-0.38	-0.22	-0.11	-0.04	-0.01
D19S902	-∞	-2.33	-1.44	-0.96	-0.65	-0.44	-0.28	-0.16	-0.08	-0.03
D19S571	-∞	-1.27	-0.87	-0.63	-0.46	-0.34	-0.24	-0.16	-0.10	-0.05
D19S418	1.43	1.40	1.32	1.21	1.08	0.93	0.76	0.58	0.38	0.18
D19S210	-0.8	-0.003	0.226	0.313	0.331	0.308	0.26	0.2	0.129	0.06

Table 42. Pedigree 2: Chromosome 20 markers

Marker	Theta=0	0.05	0.1	0.15	0.2	0.25	0.300	0.35	0.4	0.45
D20S117	-∞	-1.33	-0.4	-0.01	0.188	0.268	0.273	0.23	0.159	0.08
D20S889	-∞	-2.97	-1.74	-1.10	-0.71	-0.44	-0.27	-0.15	-0.06	-0.02
D20S115	-∞	-2.07	-1.24	-0.79	-0.50	-0.31	-0.18	-0.09	-0.03	0
D20S186	-∞	-3.11	-1.98	-1.37	-0.97	-0.68	-0.46	-0.29	-0.16	-0.06
D20S112	-∞	-0.94	-0.59	-0.39	-0.26	-0.17	-0.11	-0.06	-0.03	-0.01
D20S195	-∞	-2.82	-1.68	-1.07	-0.68	-0.42	-0.23	-0.11	-0.04	0
D20S107	0.34	0.30	0.27	0.23	0.19	0.15	0.11	0.08	0.05	0.02
D20S119	-∞	-2.12	-1.22	-0.69	-0.37	-0.17	-0.04	0.02	0.04	0.03
D20S178	-∞	-1.73	-0.92	-0.5	-0.25	-0.09	0	0.05	0.07	0.05
D20S196	-∞	0.04	0.37	0.44	0.42	0.35	0.27	0.18	0.10	0.04
D20S100	0.89	0.77	0.65	0.53	0.42	0.32	0.22	0.14	0.07	0.03
D20S173	-∞	-1.96	-1.18	-0.76	-0.49	-0.31	-0.18	-0.10	-0.04	-0.01
D20S171	-∞	-1.32	-0.62	-0.28	-0.10	0.01	0.04	0.05	0.04	0.02

Table 43. Pedigree 2: Chromosome 21 markers

Marker	Theta=0	0.05	0.1	0.15	0.2	0.25	0.300	0.35	0.4	0.45
D21S1256	-∞	-3.58	-2.22	-1.49	-1.01	-0.69	-0.45	-0.28	-0.15	-0.06
D21S1914	-∞	-2.06	-1.3	-0.9	-0.65	-0.48	-0.35	-0.25	-0.15	-0.07
D21S263	-0.14	0.11	0.22	0.25	0.23	0.19	0.12	0.05	-0.01	-0.03
D21S1252	-∞	-2.46	-1.72	-1.25	-0.91	-0.66	-0.46	-0.30	-0.18	-0.08
D21S266	-∞	0.27	0.43	0.42	0.34	0.21	0.06	-0.08	-0.15	-0.13

Table 44. Pedigree 2: Chromosome 22 markers

Marker	Theta=0	0.05	0.1	0.15	0.2	0.25	0.300	0.35	0.4	0.45
D22S420	-∞	-1.73	-0.87	-0.46	-0.25	-0.14	-0.10	-0.08	-0.07	-0.04
D22S539	-∞	-1.95	-1.25	-0.85	-0.58	-0.38	-0.23	-0.12	-0.05	-0.01
D22S315	-∞	-2.67	-1.55	-0.95	-0.57	-0.32	-0.16	-0.06	0	0.02
D22S280	-∞	-2.8	-1.86	-1.28	-0.87	-0.56	-0.34	-0.18	-0.07	-0.02
D22S283	-∞	-1.25	-0.87	-0.65	-0.5	-0.39	-0.29	-0.21	-0.13	-0.06
D22S423	-∞	-3.14	-1.93	-1.26	-0.81	-0.51	-0.29	-0.14	-0.05	0
D22S274	-0.69	0.096	0.229	0.254	0.233	0.19	0.137	0.082	0.036	0.006

The End